Liquid crystal engineering – new complex mesophase structures and their relations to polymer morphologies, nanoscale patterning and crystal engineering†

Carsten Tschierske

Received 26th June 2007
First published as an Advance Article on the web 30th August 2007
DOI: 10.1039/b615517k

This *critical review* focuses on recent progress in the field of T-shaped ternary amphiphiles. These molecules can self-assemble into a series of new liquid crystalline (LC) phases with polygonal cylinder structures, new lamellar phases and LC phases combining columns and layers. These structures are analyzed on the basis of symmetry, net topology and tiling pattern (Laves and Archimedean tilings) and discussed in relation to morphologies of multiblock copolymers, self organized DNA super-lattices, metal–organic frameworks, crystal-engineering and self-assembled periodic superstructures on surfaces (210 references).

1 Introduction

Supramolecular chemistry aims at the programmed self-assembly of highly complex functional systems from simple molecules interacting by non-covalent intermolecular forces. A prime topic in this field concerns the investigation of the fundamental mechanism involved in the translation of the information imprinted in the molecular structure into well defined complex systems.[1] Among these self assembling systems rod-like molecules are of prime interest. Defined assemblies of molecular rods incorporating π-conjugated aromatic systems are important as building blocks for functional devices for molecular electronics, *e.g.* field effect transistors, photovoltaic devices, light emitting diodes and logic gates.[2,3] Rod-like molecules are also useful building blocks for nanoscale machines,[4] nanocars[5] and self assembled membrane channels.[6]

However, the broadest industrial application of such systems is their use in liquid crystal (LC) devices, dominating the today's market of displays for computers and telecommunication devices, which is presently a hundred billion dollar market.[7] The success of these LC materials, influencing our daily life, is based on the unique combination of order and mobility on a microscopic and macroscopic level.[8–12] The mobility enables these supramolecular systems to respond to different types of external stimuli (*e.g.* electric fields in displays) by changing their configuration. The order in these systems, which gives rise to important application properties, as anisotropic optical, electrical and magnetic properties, is provided by the desire of anisometric rigid units, to adopt a long range orientational order by maximizing the interaction energy and minimizing the excluded volume, which is a powerful general organization principle of matter. The designing principles of these thermotropic LC materials,[13] forming their LC phases in a certain temperature range between the crystalline solid and the disordered liquid state, are quite simple and based on molecules combining mostly rod-like rigid anisometric units, providing order, with flexible terminal chains, responsible for mobility.[8] As shown in Fig. 1, this leads to the classical types of LC phases, namely nematic LC phases with exclusively orientational order and to smectic LC phases, which are fluid layer structures combining long-range orientational order and 1D positional order (layer periodicity).[8]

In such mesogenic materials based on rod-like anisometric units, the complexity of the self assembled structures can be increased (i) by introduction of chirality which leads to helical superstructures,[14] (ii) by a restriction of the rotational disorder of the anisometric segments around their long axes, leading to polar ordered LC phases and spontaneous achiral symmetry breaking (bent-core mesogens, "banana-shaped" mesogens),[15] (iii) by interconnecting identical or different mesogens in dimesigens, oligomesogens, dendrimers and polymers[8,16,17] and (iv) by incorporating these rigid anisometric units into an amphiphilic molecular structure.[9–11]

Carsten Tschierske

Carsten Tschierske received his PhD in Organic Chemistry in 1985 at the University of Halle. After habilitation and several visitor professorships he was appointed in 1994 as Professor of Organic Chemistry/Supramolecular Chemistry at the Martin-Luther-University Halle-Wittenberg, Halle, Germany. His primary research interest is focussed on the design of new materials forming complex self organised soft-matter structures.

Martin-Luther-University Halle-Wittenberg, Naturwissenschaftliche Fakultät II – Chemie und Physik, Institut für Chemie, Organische Chemie, Kurt-Mothes Str. 2, 06120 Halle, Germany.
E-mail: Carsten.Tschierske@chemie.uni-halle.de

† In memory of Dr Michi Nakata.

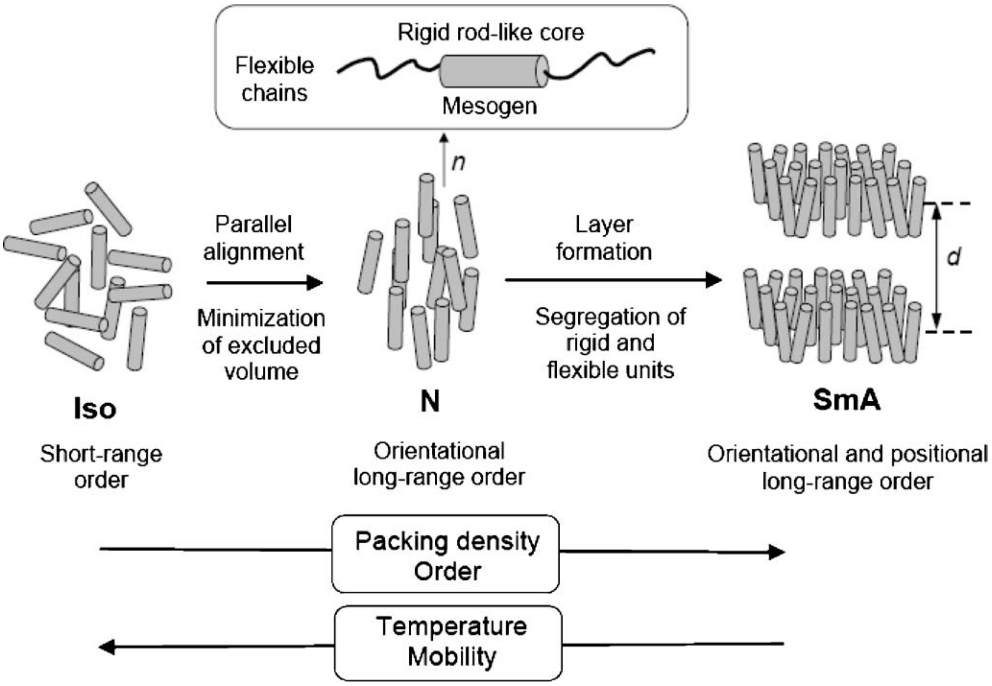

Fig. 1 Organisation of rod-like molecules in LC phases (for clarity the alkyl chains are not shown in the models of the phase structures). Abbreviations: Iso = isotropic liquid state; N = nematic LC phase; SmA = smectic A phase; *n* = nematic director; *d* = layer periodicity.

Self assembly in amphiphilic systems is based on the segregation of incompatible molecular segments into distinct subspaces. Binary amphiphiles organize into a series of mesophases with positional order in one (smectic LC phases), two (columnar LC phases) and three dimensions (cubic mesophases) as shown in Fig. 2 for a series of thermotropic LC phases formed by polyhydroxy amphiphiles.[18–21] In binary amphiphiles composed of two incompatible segments, without anisometric units, the mesophase type is determined by the relative volume of the two incompatible segments. Smectic phases (layer structures) with flat interfaces between the micro-segregated regions of the two incompatible units result only for molecules where the incompatible segments have comparable cross section area. If the size of one segment is increased, then a curvature of these interfaces arises, which leads to columnar and cubic mesophases.[9–11,18–20,22]

The phase sequence shown in Fig. 2[19] for a series of amphiphilic molecules by increasing the size of either the polar or the non-polar units is general and can be found in the phase sequences of other amphiphilic mesogens,[23–26] in lyotropic systems of surfactants with water or other solvents depending on the concentration,[27] as well as for binary block copolymers depending on the size of the two interconnected incompatible polymer chains.[28,29]

Also the mode of organization of rod-like molecules is affected by amphiphilicity and interface curvature. LC materials are intrinsically amphiphilic, as they are usually composed of rigid and flexible segments.[9] Segregation of these distinct segments is a main contribution to formation of positionally ordered LC phases (smectic for rod-like molecules and columnar for disc-like molecules).[9–11] As in the case of flexible amphiphiles also for rod-like molecules the relative size of the incompatible segments, determining the interface curvature, can influence the mesophase morphology, leading to a series of complex mesophases with periodic order in two or three dimensions, as shown in Fig. 3 for so-called rod-coil molecules composed of a rod-like aromatic core and flexible (coiled) poly(oxyethylene) or poly(oxypropylene) terminal chains of different length.[30–32] Related phase sequences can also be observed for rod-like molecules with other bulky chains (*e.g.* oligo(siloxane) groups,[33] perfluorinated chains[34,35]), with branched alky chains (swallow-tail molecules) or with two or more alkyl chains at each end of the rod (polycatenar mesogens).[36]

As first shown for block copolymers, the complexity of the self organized structures and also the diversity of the phase structures can be significantly enhanced by going from binary amphiphiles (AB-diblock copolymers) composed of only two different and incompatible segments to ternary amphiphiles (ABC triblock copolymers) combining three distinct segments, which are all incompatible with each other.[28,29]

As shown in Fig. 4, there is only one possible structure for binary amphiphiles, whereas there are several different topologies and block-sequences in triblock copolymers, with the linear and star-shaped topologies being the most important.[37] The topology, the block size and the block sequence have a huge impact on the phase structures.[29]

A characteristic feature of conventional rod-like LC materials is a molecular structure, in which rigid cores and flexible chains are connected in a linear manner, that the parallel organization of the rigid segments and the segregation of the incompatible molecular parts enhance each other. This leads to the dominance of smectic phases for such materials.[8] Though there have been several attempts to modify the phase structure of these smectic phases by attachment of lateral substituents to the rigid cores, this lead to nematic material in

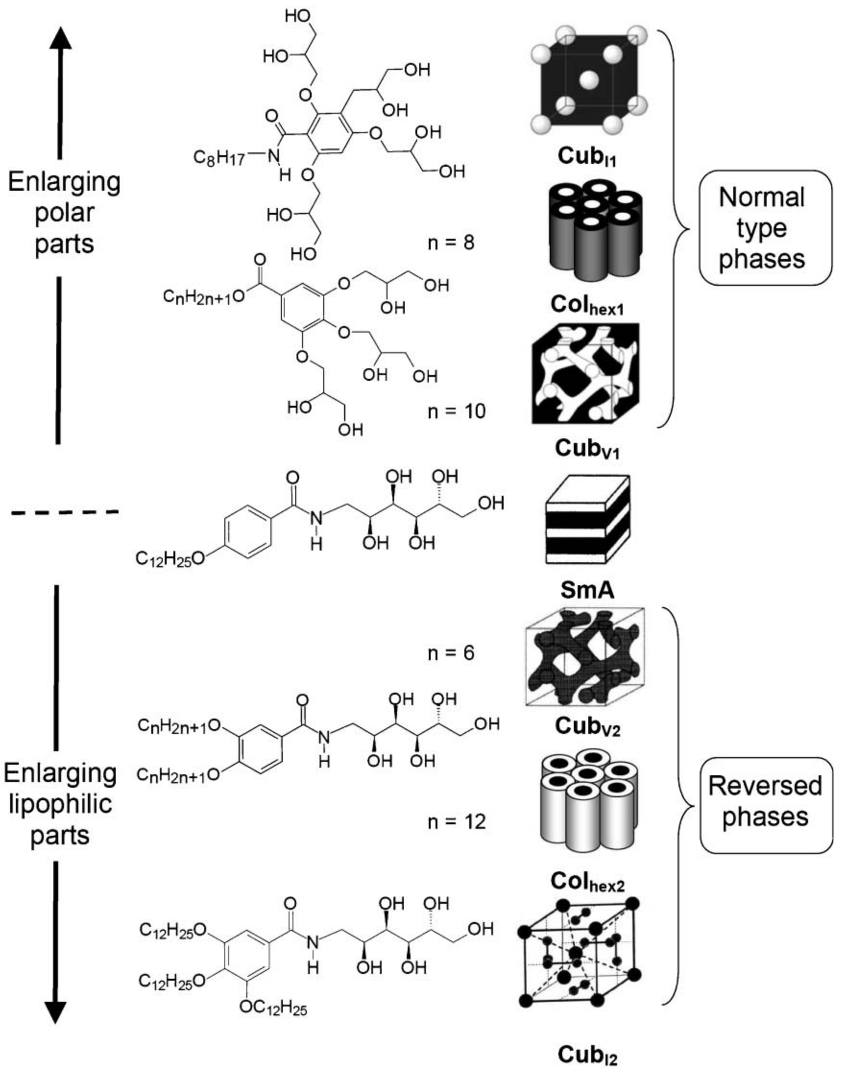

Fig. 2 The general phase sequence of flexible binary amphiphiles as obtained by changing the volume fraction of the incompatible molecular segments[19] (in the models the polar parts are shown in black, lipophilic parts in white); abbreviations: Col$_{hex}$ = hexagonal columnar phase; Cub$_V$ = bicontinuous cubic mesophase formed by interpenetrating networks of branched columns, Cub$_I$ = discontinuous cubic mesophase built up by spheroidic aggregates; the subscript "1" indicates "normal type" phases where the stronger attractive forces (hydrogen bonding) are located in the continuum outside the aggregates, the subscript "2" is assigned to "reversed type" phases where the strongest attractive forces are located inside the aggregates.

most cases, *i.e.* to a loss of the organization in layers.[38,39] The loss of positional long range order is due to a steric distortion as well as to a mixing of the lateral chains with the terminal chains if there is no strong incompatibly between lateral and terminal chains. If the lateral chains are incompatible with the terminal chains, then smectic phases can be maintained, as demonstrated with rod-like molecules having terminal fluorinated chains and lateral alkyl groups[40] or terminal alkyl chains and polar lateral groups.[41,42]

The fundamental design principle for new mesophase morphologies reported herein is based on the functionalization of rod-like molecules by terminal and spacious lateral substituents which are strongly incompatible with each other and also with the rods.[43] In these T-shaped ternary amphiphiles each of the building blocks, the rigid core, the terminal chains and the lateral chain(s) have a tendency to segregate into their distinct own subspace.[44–49] Moreover, this molecular architecture provides a well defined molecular geometry, which leads to a strong competition between the tendency of the rods to align parallel to each other (maximizing the interaction energy and minimizing the excluded volume effect) and the desire of the lateral chains to organize into their own subspaces (nanoscale segregation). The result is that the organization in layers (smectic phases) is distorted and destabilized, and replaced by other modes of organization. With these materials a whole series of new thermotropic LC phases has been obtained in recent years, among them honeycomb-like cylinder structures, where the columns are cells with walls containing the rod-like aromatic cores,[44–46,48,49] a new type of lamellar phases where rod-like units are organized parallel to the layers[50–52] and several mesophases combining columns and layers in a uniform overall structure.[53]

In this *critical review* the progress in this field is described. The new mesophase structures are analyzed on the basis of

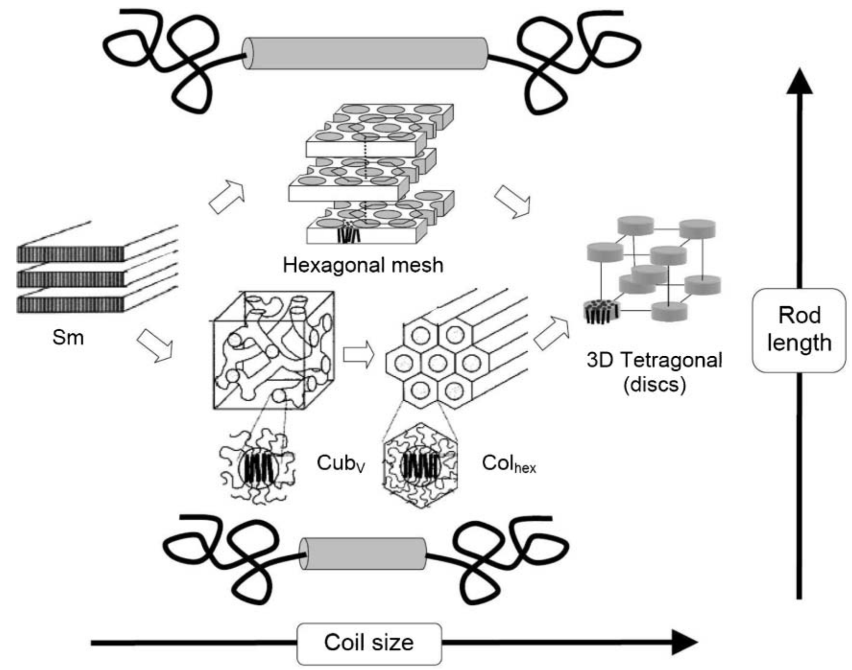

Fig. 3 Modes of self organization of rod–coil molecules; only one representative for each of the fundamental modes of organization in 2D and 3D ordered mesophases is shown.[30]

nets and tiling pattern and their relation to complex morphologies of star shaped ABC triblock copolymers, to self organized DNA super-lattices, metal–organic frameworks and other self-assembled superstructures with 2D periodicity is discussed.

2 Polygonal cylinder phases

2.1 General phase sequences and definitions

The largest group of compounds forming these new mesophases are T-shaped facial amphiphiles, which are rod-like mesogens with alkyl chains at both termini and a polar group in the lateral position,[41–46,53–55] and T-shaped bolaamphiphiles[47–52,56,57] where the positions of non-polar and polar chains is exchanged compared to the facial amphiphiles (see Fig. 5). Chart 1 gives an overview over typical structures of such molecules.

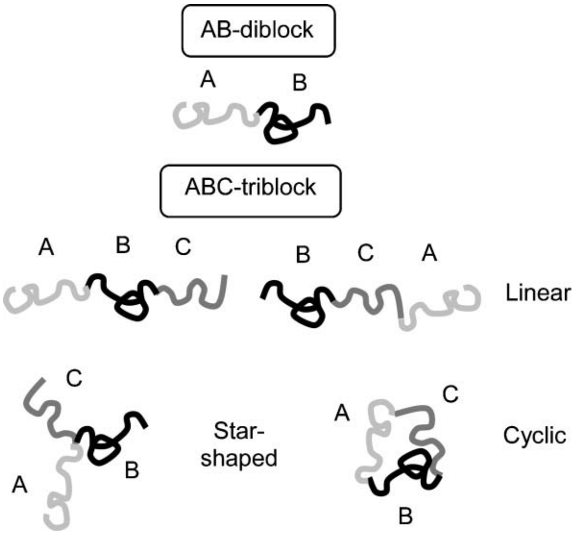

Fig. 4 Comparison of diblock-copolymers and different types of triblock copolymers; only two of the in total three possible sequences for linear triblock copolymers are shown.

As shown in Fig. 6 for the alkyl-substituted bolaamphiphilic molecules, increasing the length of the lateral chain gives rise to a transition from layer structures (smectic phases, SmA) *via* distorted layers (SmA$^+$) to a series of columnar phases (Col$_{rec}$, Col$_{hex}$).[47] In all these columnar phases the lateral chains are organized in columns which are surrounded by shells formed by the aromatic cores.

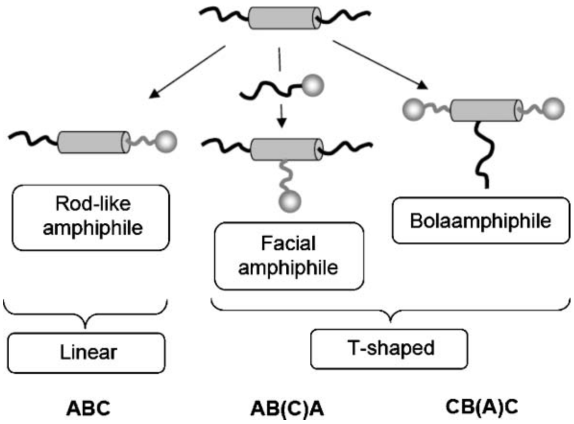

Fig. 5 Distinct molecular topologies and block sequences of ternary amphiphilic molecules incorporating rigid rod-like segments (ternary block-molecules). The facial amphiphiles and bolaamphiphiles discussed here can be regarded as ternary AB(C)A and CB(A)C four-block molecules, respectively, where A, denotes the non-polar chain(s), B the aromatic core and C the polar group(s).

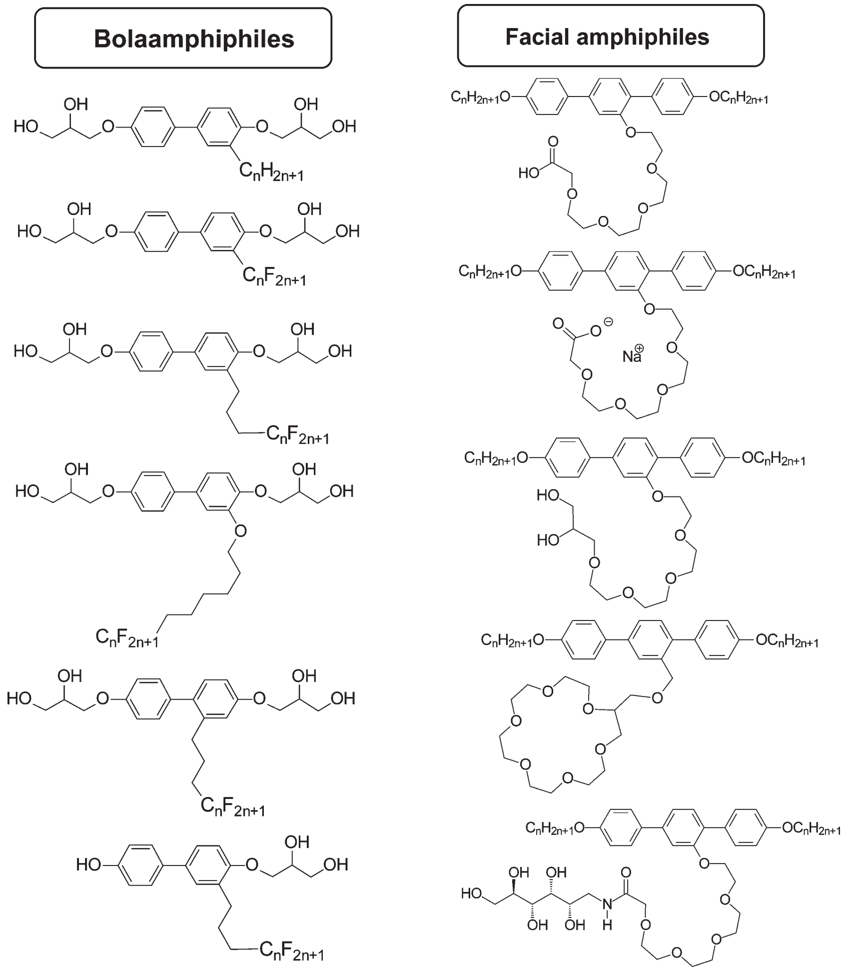

Chart 1 Examples for the chemical structures of T-shaped bolaamphiphiles and facial amphiphiles.[41–57]

In a mathematical sense these shells can be described as *closed generalized cylinders*, *i.e.* as cylindrical surfaces, which represent closed plane surfaces without top and bottom faces[58] with a convex polygonal cross-section (herein also assigned as cylinder shells or cylinder frames).[59] Depending on the size of the lateral chains the shape of the cylinders changes from tetragonal *via* pentagonal to hexagonal (but also trigonal cylinders were observed).[60] These hollow cylinders are aligned parallel and fused side-by-side and edge-to-edge to give a close 2D periodic packing of cylinder shells. This arrangement is assigned as *polygonal honeycomb*. It must be considered that in mathematics honeycomb is uses with different sense. In general it refers to a regular tessellation in three dimensions, *i.e.* a tessellation of 3D-space by polyhedra (sponges, foams), but it is also used for a regular tessellation consisting of regular hexagons, *i.e.* a hexagonal grid in only two dimensions. Herein we use *polygonal honeycomb* more in this second sense, but not restricted to a hexagonal grid, rather than for any *2D periodic packing of parallel aligned generalized cylinders with polygonal cross section*, independent on their shape. Though, the polygonal honeycombs can be described by 2D-nets (see Section 2.7), they do not represent discrete grids (2D objects). As other columnar LC phases these are 2D-periodic structures extended into the third dimension.[61] The interiors of these cylinders forming the honeycomb are assigned as columns. These columns have a polygonal cross section similar to prismatic solids.[62] Though for this reason these new LC phases might be assigned as prismatic phases, they represent a special subtype of columnar phases and therefore the assignment to columnar phases ($\mathrm{Col_{ob}}$, $\mathrm{Col_{rec}}$, $\mathrm{Col_{squ}}$, $\mathrm{Col_{hex}}$) is maintained.[63] In order to specify these phases more precisely the term *polygonal cylinder phase* is suggested where according to the shape of the cylinders forming the honeycomb structure *triangular* (*trigonal*, n = 3), *square*, *rhombic* (*tetragonal*, n = 4), *pentagonal* (n = 5) and *hexagonal cylinder phases* (n = 6) can be distinguished. In the subscript "(n)cyl-m", the number of faces of the polygonal cylinder n (equal to the number of sides of the polygon describing the cross section) is given in brackets and the last number m gives the total number of molecules in the circumference around one cylinder to distinguish the simple cylinder phases with all side length corresponding to the single molecular length from the giant cylinder phases where some or all sides are formed by dimers. The plane group symmetry is added to distinguish mesophases formed by polygonal cylinders with the same number of sides, but with a distinct shape. For example, the deformation of the square cylinder phase ($p4mm$), formed by regular square cylinders, to rectangular or rhombic cylinders would lead to LC phases with $c2mm$ symmetry (see Section 2.7.).

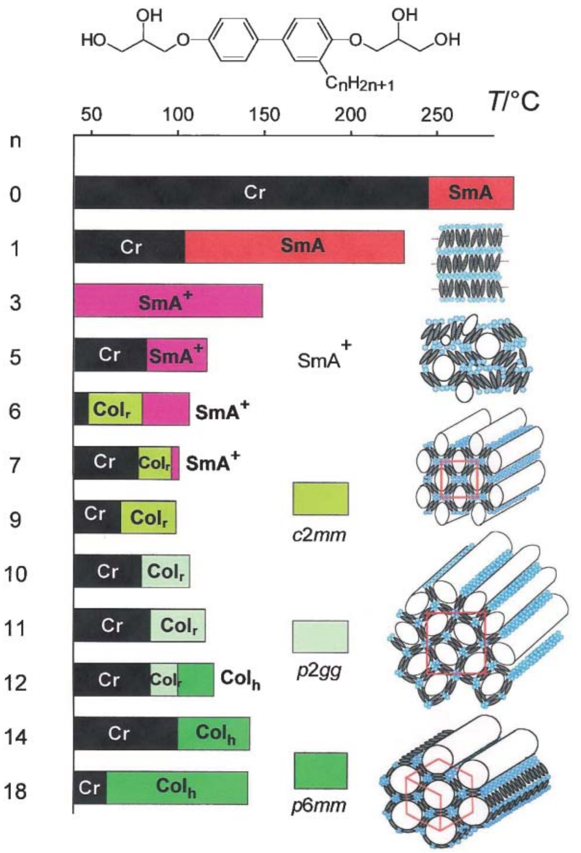

Fig. 6 Dependence of the liquid crystalline phases of boalaamphiphiles with respect to the length of the lateral alkyl chains (Cr = crystalline solid, Col$_r$/*c2mm* = Col$_{rec1(4)cyl-4}$/*c2mm*, Col$_r$/*p2gg* = Col$_{rec1(5)cyl-5}$/*p2gg*, Col$_h$ = Col$_{hex1(6)cyl-6}$/*p6mm*) and models of the organization of the molecules in the polygonal cylinder phases: white = areas of the non-polar chains; blue = H-bonding networks of the terminal diol groups and gray = rod-like biphenyl cores.[47,48] Reprinted with permission from *J. Am. Chem. Soc.*, 2003, **125**, 10977–10997. Copyright 2003, American Chemical Society.

A sequence of related polygonal cylinder phases was also found for facial amphiphiles, where upon increasing the size of the polar lateral group the SmA phase is at first replaced by a perforated layer structure, assigned as ChL$_{hex}$ (see Section 4.4)[53] and on further elongation of the polar lateral chain it is replaced by a square cylinder phase with *p4mm* plane group symmetry, as shown in Fig. 7.[44–46] Depending on the precise structure of the lateral substituent also LC phases composed of smaller and larger cylinder have been observed.[45,46,60] The mesophase morphology of the facial amphiphiles can also be tailored by variation of the length of the terminal alkyl chains, as shown in Fig. 8.[46]

The mesophases formed by these two groups of T-shaped ternary amphiphiles will be discussed in the following sections. Thereby attention is at first focussed on the polygonal cylinder structures.

2.2 Square cylinder phases

As an illustrative example for these LC cylinder phases the square cylinder phase (Col$_{squ}$/*p4mm*) is discussed first. This

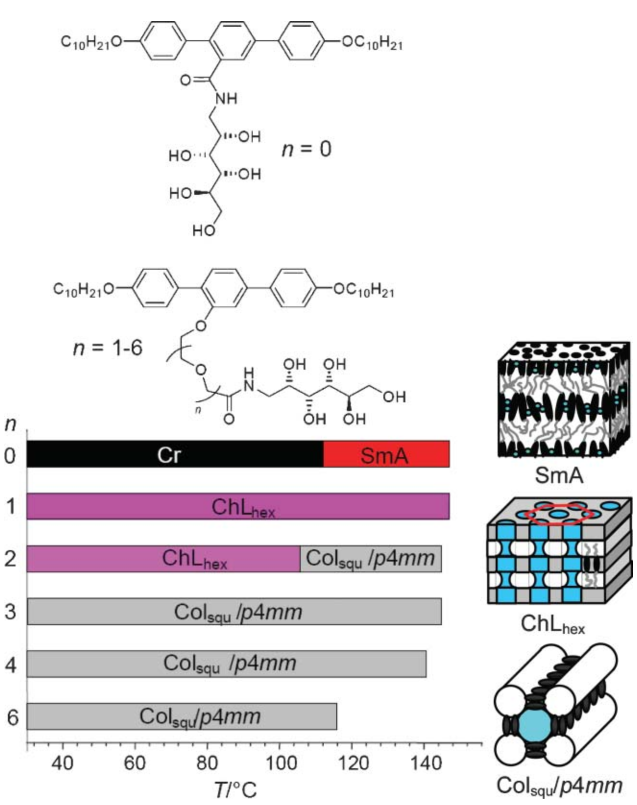

Fig. 7 Mesophase types and transition temperatures (*T*/°C) of the facial amphiphiles depending on the number of oxyethylene units *n* (ChL$_{hex}$ = hexagonal channeled layer phase; Col$_{squ}$/*p4mm* = Col$_{squ2(4)cyl-4}$/*p4mm*) and models of the organization of the molecules in these mesophases, colour code as in Fig. 6.[46] Reprinted with permission from *J. Am. Chem. Soc.*, 2005, **127**, 16578–16591. Copyright 2005, American Chemical Society.

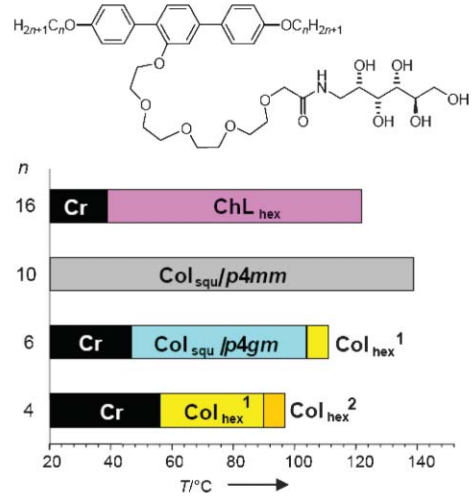

Fig. 8 Mesophase types and transition temperatures (*T*/°C) of the facial amphiphiles as a function of the length of terminal alkyl chains *n* (Col$_{squ}$/*p4gm* = Col$_{squ2(5)cyl-5}$/*p4mm*, Col$_{hex}{}^1$ and Col$_{hex}{}^2$ are non-honeycomb hexagonal columnar phases as explained in Section 4.2 and shown in Fig. 52(i) and (k), respectively), for the other abbreviations, see Fig. 7.[46] Reprinted with permission from *J. Am. Chem. Soc.*, 2005, **127**, 16578–16591. Copyright 2005, American Chemical Society.

mesophase is formed as a predominating phase in the series of facial amphiphiles (Fig. 1, n = 3–6)[44,46] but it can also be observed for some bolaamphiphiles.[48]

Elucidation of the phase structure is mainly based on optical investigations, X-ray diffraction and modelling. For the $\mathrm{Col_{squ}}$/*p*4*mm* phase, under a polarizing microscope a birefringent texture with pseudoisotropic areas can be observed which indicates an optically uniaxial LC phase (see Fig. 9(b)). X-Ray scattering with aligned samples provide the typical diffraction pattern of a non-centred square lattice (*p*4*mm*, Fig. 9(b)). The lattice parameter of this square lattice is limited to the length of the molecule in the most stretched conformation between the ends of the terminal alkyl chains. This is a very typical feature of all *p*4*mm* square cylinder phases, as in these cylinder structures the molecular length between the ends of the terminal groups determines the size of the cylinders. Final confirmation of the phase structure comes from electron-density calculations based on precise scattering data.[44,45] As an example, the reconstructed electron density map of the $\mathrm{Col_{squ}}$/*p*4*mm* phase of a facial amphiphile with a COOH group attached to the end of the lateral chain is shown in Fig. 10(b).[45] It clearly indicates the square arrangement of the alkyl columns (low electron density, yellow and red regions) and the polar columns (high electron density, pink regions). In this structure each of the building blocks of these ternary amphiphiles, the aromatic cores, the terminal alkyl chains and the polar lateral groups is organized in its own distinct region. The aromatic cores (shown as black lines in the electron density map in Fig. 10(b)) form cylinder shells with a square-shaped cross-section, enclosing columns containing the lateral polar chains, whereas the non-polar alkyl chains form separate columns located at the corners of the square cylinders, running along the edges. In this way these alkyl chains interconnect the cylinder sides, which leads to the formation of a square cell honeycomb.[44,45] The walls of this square honeycomb are in average two molecules thick. This square

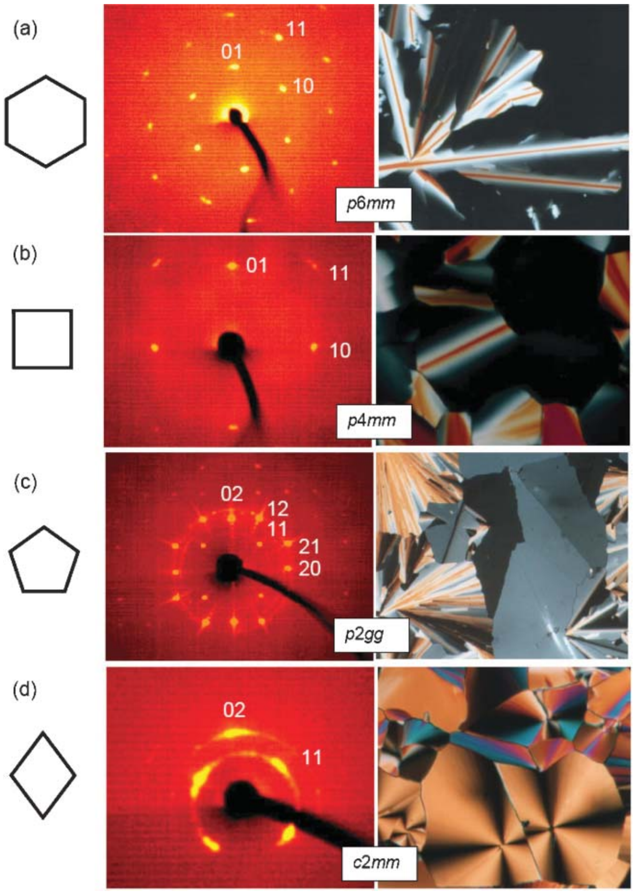

Fig. 9 Typical X-ray diffraction pattern (left, small angle regions of aligned samples) and textures (right, observed between crossed polarizers) of the LC cylinder phases with different plane group symmetries (shape of the cylinders is shown at the left) formed by T-shaped bolaamphiphiles; in (a) and (b) the dark areas are homeotropically aligned regions which indicate optically uniaxial mesophases ($\mathrm{Col_{squ}}$, $\mathrm{Col_{hex}}$).[47,48]

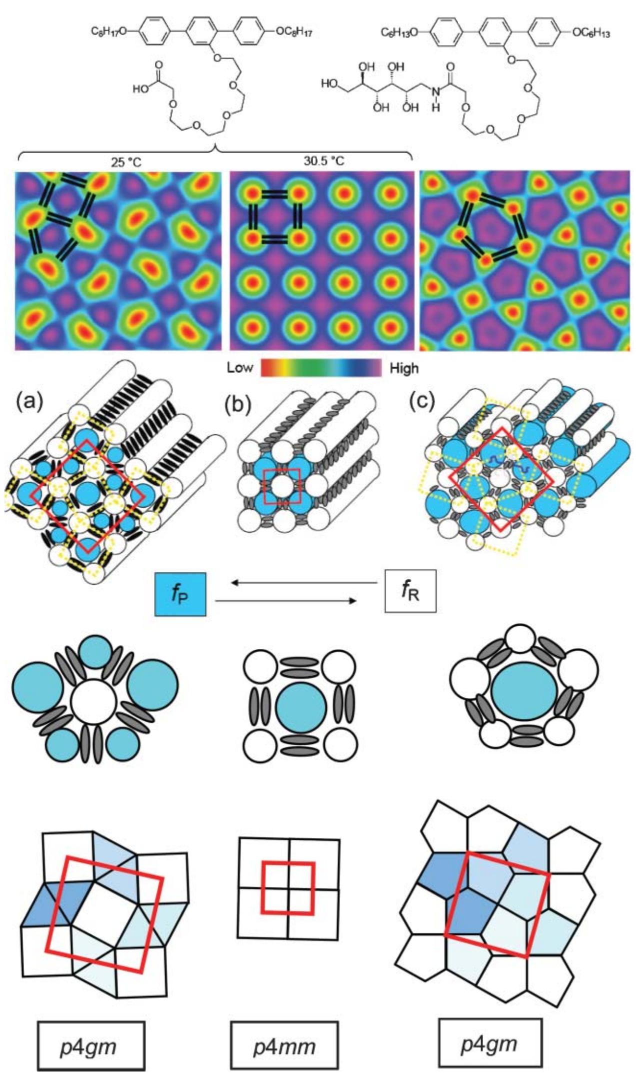

Fig. 10 LC phases of T-shaped facial amphiphiles and their dependence upon the volume fractions of the polar lateral chains (f_P) and non-polar terminal chains (f_R); experimentally determined electron density maps are shown in the top line below the formula (the organization of the rigid cores forming the cylinder frames is indicated as dark lines), models of molecular organization (colour code as in Fig. 6) and tiling patterns are shown in the bottom lines: (a) $\mathrm{Col_{squ2(3,4)cyl\text{-}3,4}}$/*p*4*gm*; (b) $\mathrm{Col_{squ2(4)cyl\text{-}4}}$/*p*4*mm*; (c) $\mathrm{Col_{squ2(5)cyl\text{-}5}}$/*p*4*gm* square cylinder phase.[45]

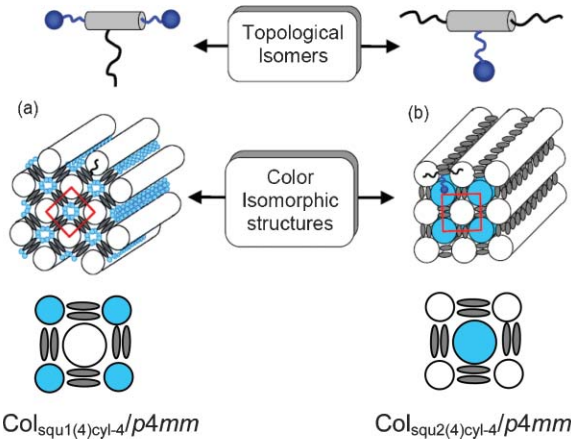

Fig. 11 Color-isomorphic square cylinder phases with *p*4*mm* lattice formed (a) by bolaamphiphiles with non-polar lateral chains and (b) by facial amphiphiles, colour code as in Fig. 6.

cylinder phase is assigned as "$Col_{squ2(4)cyl-4}/p4mm$" where Col_{squ} stands for a columnar phase with *squ*are lattice[64] and the subscript "2" indicates that the strongest cohesive forces (hydrogen bonding) are located inside the cylinders, which is similar to inverse phases (type 2 phases) in lyotropic systems.[27] The subscript "(*n*)cyl-*m*" indicates that the honeycomb has square cells (*n*-gons) formed by four molecules ($m = 4$) in the circumference.

The same type of square lattice as observed for the facial amphiphiles, but with an inverted structure was also found for bolaamphiphiles.[48] Here, the non-polar lateral chains fill the interior of the cylinders whereas the hydrogen bonding networks of the terminal diol groups are organized within the columns interconnecting the cylinder walls (see Fig. 11(a)). A subscript "1" in the phase assignment ($Col_{squ1(4)cyl-4}/p4mm$) indicates that in this structure the strongest cohesive forces (hydrogen bonding) are located within the cylinder frames, which is similar to the "normal" (type 1) LC phases of binary amphiphiles.[27] These two distinct square cylinder structures, having an inverted position of polar and nonpolar columns with respect to the cylinder walls (see Fig. 11) represent inverted structures. As there are three distinct compartments, each of them is arbitrarily assigned to a color and hence these are color isomorphic structures.

Remarkably, there are only few bolaamphiphiles showing the *p*4*mm* square phase and it occurs only in a very narrow temperature range beside other cylinder phases (see for example Fig. 12, $n' = 7$), whereas for the facial amphiphiles this square lattice is the dominating type of organization, as can be seen in Fig. 7.[46] The main reason for this difference is the distinct molecular structure of these two classes of T-shaped ternary amphiphiles. In the bolaamphiphiles the strongest attractive forces (hydrogen bonding) are provided at both ends of the rigid core and, in addition, there is a strong incompatibility of the diol groups with the aromatic cores, *i.e.* there is a strong stabilization of the polygonal cylinder structure. As a consequence relatively short rigid rods (biphenyls) are sufficient to obtain these cylinder structures. Furthermore, the terminal propane-2,3-diol groups are also

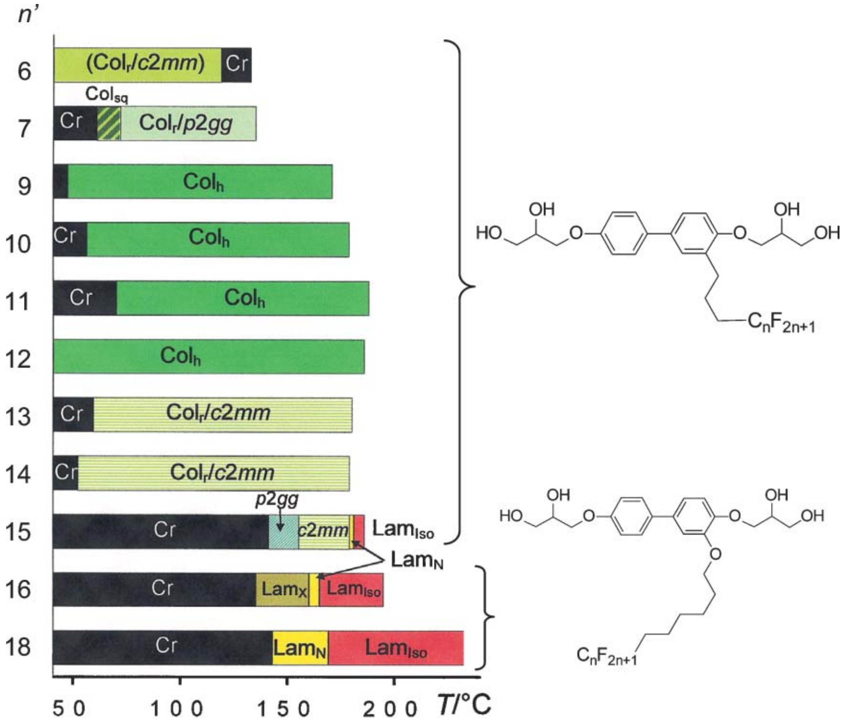

Fig. 12 Dependence of the liquid crystalline phases of the bolaamphiphiles with respect to the length of the semiperfluorinated lateral chain; the number n' means the total length of the lateral chain including the aliphatic spacers (C_3 or C_6) and the perfluorinated segments (*n*); ($Col_r/c2mm$ phase for $n' = 6$: $Col_{rec1(4)cyl-4}/c2mm$, for $n' = 13$–15: $Col_{rec1(6)cyl-8}/c2mm$, $Col_r/p2gg$ phases for $n' = 7$: $Col_{rec1(5)cyl-5}/p2gg$, for $n' = 15$: $Col_{rec1(5)cyl-10}/p2gg$, $Col_{squ} = Col_{squ1(4)cyl-4}/p4mm$, $Lam_X = Lam_{Sm}$, other abbreviations as in Fig. 6).[48] Reprinted with permission from *J. Am. Chem. Soc.*, 2003, **125**, 10977–10997. Copyright 2003, American Chemical Society.

comparatively small and cannot be expanded significantly. Hence, for the bolaamphiphiles there are quite strong restrictions for the size of the lateral chains which have to fill the interior of the cylinders properly. In contrast, in the mesophases formed by facial amphiphiles only the lateral group provides strong cohesive forces (H-bonding, Coulomb forces) and therefore longer terphenyl cores are required to allow self-assembly into LC phases. In addition, the terminal alkyl groups must be relatively long to enable their segregation from the aromatic cores. As a consequence, the cylinders of the facial amphiphiles have a much larger diameter and therefore, the square cylinders of the facial amphiphiles can accommodate much larger polar chains, compared to the square cylinders formed by bolaamphiphiles. As the columns incorporating alkyl chains are much softer than those formed by the diol groups, these columns can expand to a significant extend and therefore these polygonal cylinder structures are less sensitive to changes of the size of the lateral substituent. Therefore, simple square lattices can easily be formed by a wide range of facial amphiphiles with relatively long lateral chains.

2.3 Mesophases incorporating rhombic and triangular cylinders

The shape of the cylinders is determined by the volume required by the lateral chains inside the cylinders with respect to the circumference provided by the cylinder shells. As the rod-like aromatic cores have a quite well defined length, the cross-section of the polygonal cylinders can only change in a stepwise manner. This leads to a series of distinct phase structures. In the case of the bolaamphiphiles reduction of the volume of the lateral chains by replacing perfluorinated chains by alkyl chains with a smaller overall volume leads to a deformation of the square cylinders to cylinders with rhombic cross section ($\mathrm{Col}_{\mathrm{rec1(4)cyl\text{-}4}}/c2mm$ phase). As a consequence the phase symmetry is changed from *p*4*mm* to *c*2*mm* (see Fig. 6, $n = 6$–9).[47] In this way the number of rod-like cores arranged in the circumference around the lipophilic columns can be retained, though the volume inside the cylinders is reduced.

The situation is completely different for the facial amphiphiles. As shown in Fig. 10(a) and (b) the mesophase structure is changed by reducing the temperature. As the lateral oligo(oxyethylene) chains have the largest thermal expansion coefficient, their volume is most strongly reduced with decreasing temperature. In this way[45] the simple square phase (*p*4*mm*), of the carboxylic acid shown in Fig. 10(b), occurring at high temperature ($T = 30.5$ °C, see Fig. 10(b)) is replaced by a square phase with the plane group *p*4*gm* at low temperature ($T = 25$ °C), shown in Fig. 10(a). The electron density map of this $\mathrm{Col}_{\mathrm{squ}}/p4gm$ phase (see Fig. 10(a)) indicates a complex structure composed of triangular and square cylinders in a ratio 2 : 1. The polar chains (high electron density) fill the narrow triangular and square columns, whereas the alkyl chains (low electron density) represent the larger columns interconnecting five cylinder walls. Hence, the $\mathrm{Col}_{\mathrm{squ}}/p4gm$ phase of this facial amphiphile is a unique and new liquid crystalline phase formed by a periodic array of two different types of cylinders ($\mathrm{Col}_{\mathrm{squ2(3,4)cyl\text{-}3,4}}/p4gm$ phase).[45] This periodic packing of regular triangles and squares represents one of the Archimedean tilings (see Fig. 21 in Section 2.7). This tiling pattern seems to be a new fundamental and also general mode of organization in soft matter systems as it was also found as a motif in the organization of spheroidic supramolecular dendrimers in a complex tetragonal 3D mesophase with $P4_2/mnm$ symmetry[65] and more recently it was reported as a new morphology of star shaped triblock copolymers (see Section 3.1).[66] Also in the first quasicrystalline 3D mesophase with 12-fold symmetry a packing of triangles and squares is found, but these are tiled in a quasi-periodic manner.[67,68]

Polygonal honeycomb structures composed exclusively of triangular cylinders ($\mathrm{Col}_{\mathrm{hex2(3)cyl\text{-}3}}/p6mm$, also abbreviated as $\mathrm{Col}_{\mathrm{hex}\Delta}$) were recently proven for the $\mathrm{Col}_{\mathrm{hex}}$ phases of facial amphiphiles with longer terminal or shorter lateral chains.[60] It is remarkable that the reduction of the size of the lateral chains with respect to the length of the rod-like segments leads to very different phase structures for the two distinct series of T-shaped amphiphiles; rhombic cylinders ($\mathrm{Col}_{\mathrm{rec1(4)cyl\text{-}4}}/c2mm$) for bolaamphiphiles and triangular cylinders ($\mathrm{Col}_{\mathrm{hex2(3)cyl\text{-}3}}/p6mm$) or mixed organizations of triangular and square cylinders ($\mathrm{Col}_{\mathrm{squ2(3,4)cyl\text{-}3,4}}/p4gm$) for facial amphiphiles. The flexibility of the lateral chains, filling the interior of the cylinders, seems to be of significant importance for this difference. The relatively short lateral alkyl and semiperfluoroalkyl chains, used as lateral substituents in the series of bolaamphiphiles, preferably adopt a linear conformation, whereas the longer lateral oligo(oxyethylene) chains of the facial amphiphiles are much more flexible (gauche effect leads to a predominance of non-linear conformations). These flexible chains can easily fill the smaller triangular cylinders. In the *c*2*mm* lattice of the bolaamphiphiles the cylinders adopt a slightly elliptical shape upon reduction of the side-chain volume. This is advantageous for the organization of the more rigid (but still fluid!) lateral alkyl chains of these compounds, because the organization within elliptic cylinders requires less deviation from linearity and allows a more parallel packing of these chains than it would be possible within triangular cylinders. Moreover, the positions of the lateral chains are in the middle of the aromatic core for the facial amphiphiles and in most cases closer to the periphery for the T-shaped bolaamphiphiles (see Chart 1). The peripheral position of the chains should additionally contribute to the preference of rhombic cylinders for the bolaamphiphiles.

2.4 Pentagonal cylinder phases

Even more exciting new phase structures were observed by increasing the size of the lateral chains. In the series of facial amphiphiles, increasing the volume inside the cylinders either by elongation of the lateral chain (*e.g.* by replacement of the COOH group by a larger carbohydrate unit as shown in Fig. 10 at the right), leads to a transition from a simple square phase (*p*4*mm*) to another square lattice with plane group *p*4*gm*, shown in Fig. 10(c).[45,46]

This $\mathrm{Col}_{\mathrm{squ}}/p4gm$ phase, formed by a carbohydrate terminated facial amphiphile is distinct from that one formed by the related carboxylic acid with a much smaller size of the lateral chain, shown in Fig. 10(a) and (b). As can be seen in the reconstructed electron density map in Fig. 10(c) the polar

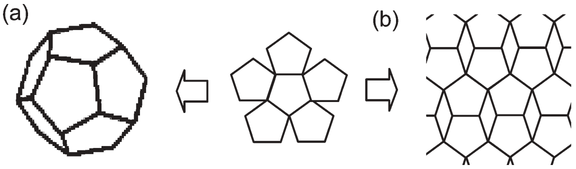

Fig. 13 Packings of regular pentagons (a) by curvature of the plane with formation of a pentagon-dodecahedron, (b) by tiling a plane in conjunction with rhombuses.

chains (high electron density regions, shown in pink) form pentagons which are separated by squares and triangles of low electron density (yellow to red) containing the alkyl chains. Hence, also this mesophase is a cylinder structure, but in this case with a pentagonal cross sectional shape of the cylinders. In this structure, the columns formed by the terminal alkyl chains interconnect either three or four cylinder walls formed by the terphenyl units (see black lines in the electron density maps in Fig. 10(c)).

The formation of a periodic self-organized pentagonal cylinder structure is surprising as it is known that regular pentagons cannot tile a Euclidean plane (Fig. 13). However, they can adopt a close edge-to-edge packing by escape from planarity, leading to pentagon-dodecahedra (Fig. 13(a)). Alternatively, the regular pentagons can be combined with rhombuses (Fig. 13(b)) or other polyhedra to tile the flat plane. Tessellation of a plane can also be achieved by a deformation of regular pentagons to nonregular pentagons (bottom line in Fig. 14). Consequently, pentagonal cylinders can only organize in a periodic 2D-lattice if there would be additional cylinders with a rhombic cross section (or with other shapes) which can fill the void space, or if they adopt a non-regular shape, *i.e.* if not all angles and side length of the pentagonal cylinders are identical (Fig. 14). Such non-regular pentagonal cylinders form cylinder pairs and these pairs have a higher symmetry than the individual cylinders. In the *p*4*gm* phase these pairs adopt a 90° turn herringbone-like packing, leading to the *p*4*gm* lattice with four cylinders per unit cell ($\mathrm{Col}_{\mathrm{squ2(5)cyl\text{-}5}}$/*p*4*gm*), as shown in Fig. 10(c). It is the unique combination of order and mobility in the liquid crystalline state of matter which allows this deformation of the pentagonal cylinders as required for a periodic packing of these cylinders. Hence, a periodic organization of pentagonal cylinders is a unique feature of soft matter systems, such as liquid crystals.

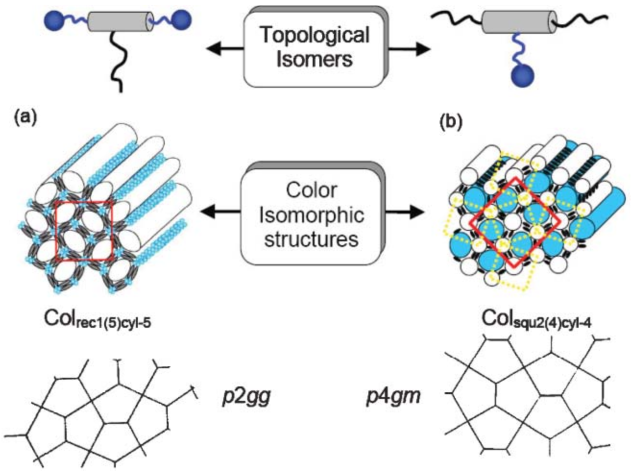

Fig. 14 Color isomorphic pentagonal cylinder phases formed (a) by bolaamphiphiles (*p*2*gg*) and (b) by facial amphiphiles (*p*4*gm*); the *p*2*gg* lattice is a slightly distorted *p*4*gm* lattice.

Pentagonal cylinder phases can also be observed for the T-shaped bolaamphiphiles by increasing the size of the lateral chains (Fig. 6 and Fig. 12).[48] In these cylinder phases the interior of the pentagonal cylinders is filled by the lateral alkyl chains or semiperfluorinated alkyl chains and the cylinder walls are interconnected by columns of hydrogen bonding networks running parallel to the edges ($\mathrm{Col}_{\mathrm{rec1(5)cyl\text{-}5}}$/*p*2*gg* phase). Hence, this organization can be considered as a color isomorphic structure to the related pentagonal cylinder phase formed by the facial amphiphiles (Fig. 14). An additional difference between the pentagonal cylinder phases formed by bolaamphiphiles and facial amphiphiles is the reduced symmetry (*p*2*gg* instead of *p*4*gm*, see Fig. 14(a) and (b)) which is due to an additional deformation of the cylinders in the *p*2*gg* phases. The reason is related to that causing the $\mathrm{Col}_{\mathrm{squ}}$/*p*4*gm* (squares + triangles) to $\mathrm{Col}_{\mathrm{rec}}$/*c*2*mm* (rhombuses) transition; *i.e.* the more rigid alkyl chains used as lateral chains for bolaamphiphiles give rise to a stronger distortion of the pentagons which in turn allows a more dense parallel packing of these chains.[69]

2.5 Hexagonal cylinder phases

Up to now the pentagonal cylinder phase is the largest polygonal cylinder structure which has been achieved for the facial amphiphiles.[46] For bolaamphiphiles, with shorter biphenyl units and stronger attractive forces at the edges, cylinder structures with a larger number of sides were obtained by further increasing the size of the lateral chains (Fig. 6 and Fig. 12).[48] Lateral alkyl chains with perfluorinated segments are especially efficient, because these fluorinated segments provide a significantly larger volume than alkyl chains with the same length. The stronger incompatibility of the fluorinated chains with the aromatic and polar units also increases the incompatibility which in addition leads to a significant stabilization of the LC phases. Hexagonal cylinder phases were observed for both series of bolaamphiphiles (with fluorinated or non-fluorinated lateral chains), shown in Fig. 6 and Fig. 12.[47,48] Here the regular hexagonal cylinder frames are formed by six molecules organized in the circumference. In the series of the bolaamphiphiles this is the most favored structure, found for the broadest range of lateral chain lengths (see Fig. 12, $n' = 9$–12). More generally, as the hexagonal honeycomb provides the least perimeter-to-area ratio this is the most favored periodic network structure, found in numerous self organized systems at different length scales. Though this appears to be obvious, it is interesting to note that rigorous mathematical proof came only recently.[70,71]

2.6 Giant cylinder phases

As the lateral chains of the bolaamphiphiles are further elongated, the hexagonal cylinders become too small to accommodate these chains; the shells expand further, which leads to giant cylinder phases (see Fig. 12, $n' = 13$–15 and

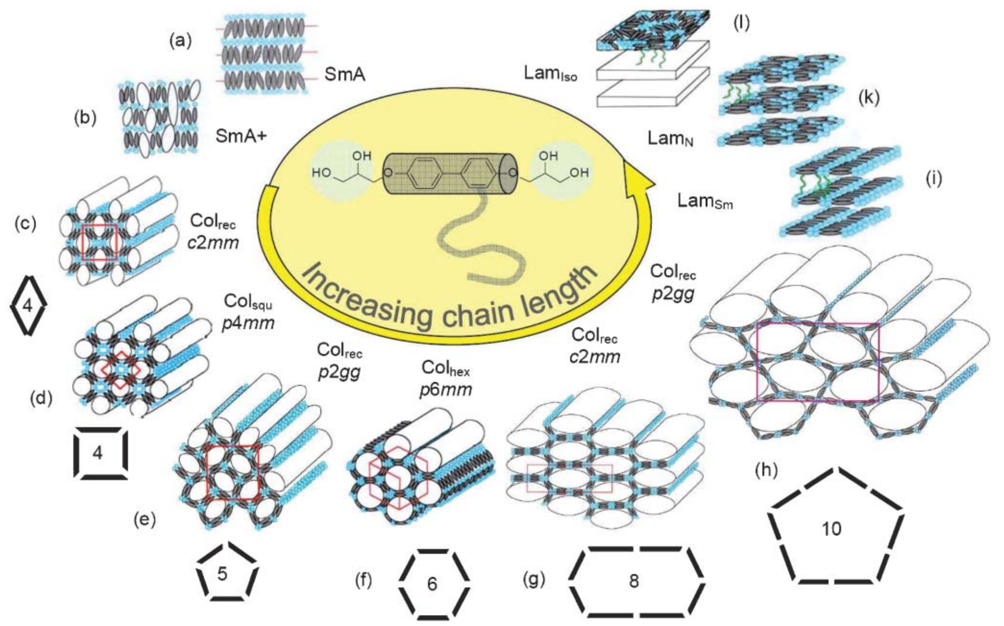

Fig. 15 Sequence of polygonal LC cylinder structures (c–h), smectic phases (a, b) and lamellar phases (i–l) formed by self-organization of T-shaped bolaamphiphiles, depending on the size of the lateral chain, colour code as in Fig. 6.[48]

Fig. 15(g) and (h)).[48] One of them has a centered rectangular lattice (*c*2*mm*) with huge lattice parameters. The organization of the molecules involved in this columnar mesophase is shown in Fig. 15(g).[48] In this phase the cylinder shells are formed by eight bolaamphiphilic units in the circumference instead of only six as found for the Col$_{hex}$ phases. Because regular octagons cannot periodically pack into a 2D lattice without leaving void space, the shells adopt a hexagonal shape instead. Within these hexagons two opposite sides are stretched, *i.e.* two sides of these hexagons are formed by side-by-side pairs of end-to-end dimer (see Fig. 15(g)). This causes a reduction of the symmetry, leading to a change of the lattice type from *p*6*mm* to *c*2*mm* (Col$_{rec1(6)cyl\text{-}8}$/*c*2*mm* phase). For one of the bolaamphiphiles shown in Fig. 12 ($n' = 15$) another mesophase was found below the *c*2*mm* giant hexagonal cylinder phase. The diffraction pattern of this mesophase, which is shown in Fig. 16, is unique for a LC phase as more than hundred spots-like reflections can bee seen in the small angle region, indicating a nearly perfect long range order. The diffuse and nearly circular wide angle scattering indicates a local disorder and confirms the LC state of the system.[48] It can be assigned to a non-centered rectangular lattice with the plane group *p*2*gg* and lattice parameters a = 11.5 nm and b = 7.7 nm. These lattice parameters are much larger than those found for all other mesophases of these bolaamphiphiles. This *p*2*gg* lattice represents a periodic packing of four cylinders per unit cell, each cylinder having a pentagonal cross sectional shape and made up of ten molecules in the circumference, *i.e.* each side of the pentagon is formed by end-do-end dimers as shown in Fig. 15(h) (Col$_{rec1(5)cyl\text{-}10}$/*p*2*gg* phase).[48] This shows that further elongation of the lateral chains allows a further expansion of the cylinders which gives rise to a series of giant cylinder phases with the giant pentagonal cylinder structure as the largest of these structures found so far. These giant cylinder phases are really unique, as they contain three distinct types of H-bonding networks in a single superstructure, two of them are located at the edges and interconnect either three or four cylinder walls and another type is located in the middle of the elongated cylinder walls.

The complexity of these structures is further increased if relatively large fluorinated segments are combined with long non-fluorinated alkyl spacers. The segregation of these segments from each other can give rise to the formation of *core–shell* columns inside the honeycomb cells, composed of R_F cores with R_H shells around them.[72] These *core–shell* columns are embedded in a polygonal honeycomb formed by the walls of aromatic cores and the polar columns interconnecting these walls at the edges, as shown in Fig. 17(b).

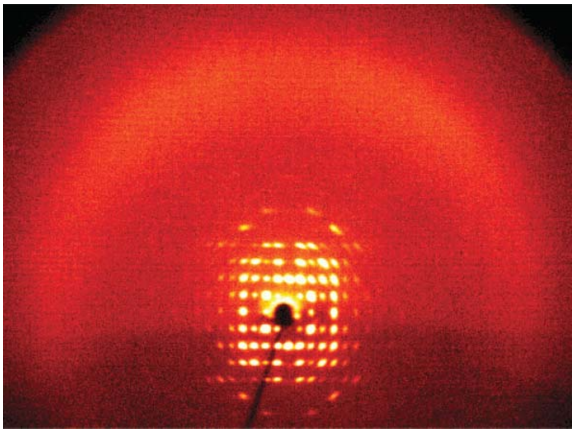

Fig. 16 X-Ray diffraction pattern of an aligned sample of the *p*2*gg* phase with giant pentagonal cylinder structure (Col$_{rec1(5)cyl\text{-}10}$/*p*2*gg*); the diffuse wide angle scattering indicates the fluid liquid crystalline state of this mesophase.[48] Reprinted with permission from *J. Am. Chem. Soc.*, 2003, **125**, 10977–10997. Copyright 2003, American Chemical Society.

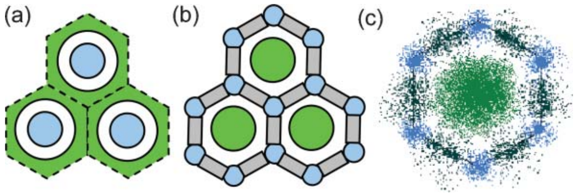

Fig. 17 Core–shell morphologies: (a) simple core–shell morphology of semiperfluorinated amphiphiles and dendrimers; (b) *core–shell-in-cylinder* morphology of bolaamphiphiles with perfluorinated lateral chains connected by a relatively long alkyl spacer unit to the bolaamphiphilic core; (c) shows a more realistic picture of the *core–shell-in-cylinder* structure, showing the diffuse character of the interfaces between the micro-segregated regions in this LC phase (blue = polar regions of H-bonding networks, white = R_H, green R_F, gray = aromatic cores); these *core–shell-in-cylinder* structures are possible for all polygonal cylinder phases, the simple hexagonal honeycomb is chosen as an example for illustration.

Simple *core–shell* morphologies without these polygonal cylinder frames were previously reported for the $\mathrm{Col_{hex}}$ phases of other amphiphilic molecules with perfluorinated segments (see Fig. 17(a)),[73] and for dendrimers composed of aromatic and aliphatic segments.[74] Core shell morphologies are also common for linear or star shaped ABC triblock copolymers.[28,29,75] However, the *core–shell-in-cylinder* morphologies formed by the T-shaped bolaamphiphiles are distinct from these simple structures, as they are located in a polygonal honeycomb which is composed of two distinct compartments (Fig. 17(b)). This further enhances the complexity of these mesophases, as there are in total four distinct compartments arranged in a periodic array.

Though these structures are highly complex, they represent ordered fluids, as indicated by the diffuse character of the wide angle scattering seen in the XRD pattern of all reported LC phases (see for example Fig. 16). This means that there is a long range periodic order (sharp small angle reflections) though the local structure is disordered (fluid). In these fluid superstructures the individual molecules do not have fixed positions as might be suggested by the shown models. There is a high degree of mobility in these ordered structures, where the molecules rapidly rotate and exchange their positions. Hence, the structures can be described as composed of regions with enhanced local concentrations of the distinct molecular parts with diffuse interfaces between them, as illustrated in Fig. 17(c). The sharpness of these interfaces is determined by the degree of incompatibility between adjacent compartments. Also the rheological properties of the materials are characterized by a soft grease-like consistence.

Fig. 15 summarizes the sequence of LC structures achieved with the bolaamphiphiles by increasing the size of the lateral chain. It can be seen that at first a transition from smectic phases to polygonal cylinder phases takes place. Further enlargement of the lateral chains leads to giant cylinder phases and finally to a novel type of lamellar phases (Lam phases) which will be discussed in Section 4.1. Before focusing on these non-cylinder structures, the polygonal cylinder phases will be analyzed in more detail based on symmetry, topology and tiling pattern.

2.7 Nets, nodes and tilings

The polygonal cylinder phases can be classified according to the symmetry of the 2D-lattice.[76] Fig. 18 shows the 17 different plane groups resulting from the combination of the symmetry elements (translation, rotation, glide and mirror-planes) that fill the 2D space. For classical columnar LC phases formed by binary amphiphiles or disc-like molecules the columns are rotational disordered and therefore the *p*6*mm* plane group with highest symmetry and the slightly distorted versions of this lattice ($\mathrm{Col_{ob}}$: *p*2 and $\mathrm{Col_{rec}}$: *c*2*mm*) are dominating, whereas square lattices (*p*4*mm*) are rare or never observed (*p*4*gm*). The polygonal cylinder phases have a broader variety of different plane groups, including the *p*4*mm* and *p*4*gm* square

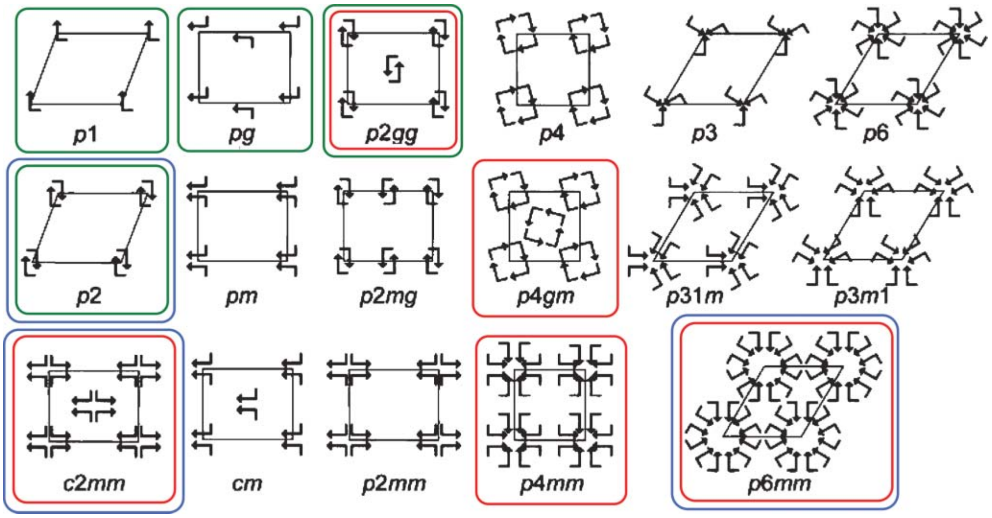

Fig. 18 Schematic representation of the 17 plane groups used to describe the symmetry of columnar LC phases.[77] An arrow indicates each asymmetric unit, and unit cells are denoted with gray lines. Reprinted with permission from *Acc. Chem. Res.*, 2007, **40**, 287–293. Copyright 2007, American Chemical Society. The frames indicate the plane groups dominating in the polygonal LC cylinder structures (red), the columnar LC phases of disc-like and amphiphilic molecules (blue) and crystalline monolayer 2D packings (green).

lattices, which are determined by the specific shape of the individual cylinders ranging from triangular *via* square and pentagonal to hexagonal. In a recent analysis of the crystalline 2D packing at surfaces a clear dominance of plane groups with low symmetry, namely *p*1, *p*2, *pg* and *p*2*gg* was found. Obviously, in the crystalline phases these packing motifs allow a maximization of the contacts between the molecules.[77] Hence, starting from classical columnar LC phases *via* the LC cylinder phases to crystalline lattices the rotational disorder is decreased, the importance of specific interactions increases, and hence, lattices with reduced symmetry become more important.

However, for a given symmetry, the shape of the polygonal cylinder can be quite different as shown in Fig. 19 for periodic structures with a centered rectangular *c*2*mm* lattice, which can be formed by triangular, rectangular, rhombic, pentagonal or hexagonal cylinders. Hence the plane group alone cannot satisfactorily describe the structures of the polygonal cylinder phases.

The polygonal cylinder phases can also be described with plane nets if the extension of the cylinder in *c*-direction (along the cylinder long axis) is disregarded.[78,79] The resulting nets can be systematized according to the net topology which is given as a general symbol (*n*,*p*) where *p* is the number of connections to neighboring nods that radiate from any nod (connectivity) and *n* is the number of nods in the smallest closed circuits in the net.[78] Thus the number 6 in the symbol (6,3) indicates that the smallest complete circuits in the net are hexagons and the number 3 indicates that each node is connected to three other nodes, which describes the hexagonal honeycomb structure of the LC cylinder phases composed of regular (*p*6*mm*) or stretched (*c*2*mm*) hexagonal cylinders (see Fig. 19(a)). However, the net topology only distinguishes geometrical properties that remain unchanged upon continuous deformation as can be seen in Fig. 19(a), (b) and (d) showing three different shapes of the cylinders for networks with (6,3) net-topology. Similarly, the pentagonal cylinder phase $\mathrm{Col_{rec}}$/*p*2*gg* is a slightly deformed version of the $\mathrm{Col_{squ}}$/*p*4*gm* pentagonal cylinder phase (see Fig. 14) and hence, both mesophases have the same topology.

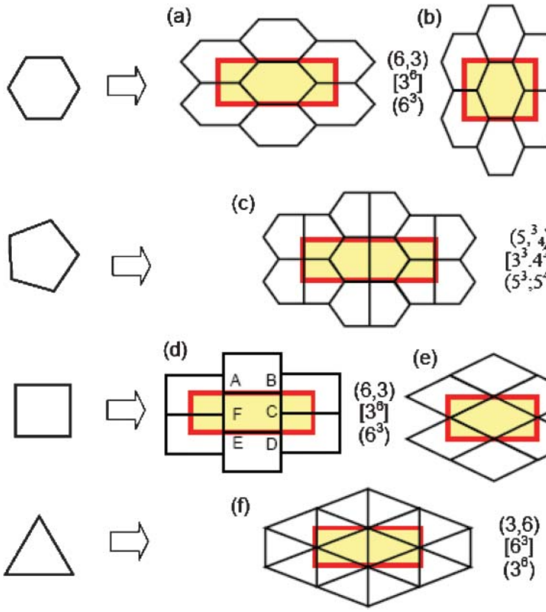

Fig. 19 Periodic tilings by non-regular polygons into 2D lattices with *c*2*mm* plane group symmetry, together with three distinct assignments of the topology. In the net topology (*n*,*p*) *p* is the number of connections to neighboring nodes and *n* is the number of nodes in the smallest circuit; in [v^n] and (n^v) the letter *v* denotes the valence of the vertex, *i.e.* the number of tiles meeting at the vertex, whereas *n* provides the number of vertices belonging to one tile (number of sides of the polygon; *n*-gon). Note that (a), (b) and (d) have the same topology (all three results from the deformation of the hexagonal honeycomb) and therefore cannot be distinguished from a topological point of view. The meaning of A–F in (d) is explained in the Appendix.

Because a net corresponds to a surface tessellation, a plane net is a way to divide a plane into polygons, where the polygons (*n*-gons) correspond to the circuits of the net and the vertices correspond to the points (nodes) of the net. Hence, cylinder phases can also be described in terms of a tiling of a plane.[79] This describes not only the topology of the cylinder network, but in addition it considers the interior of the cylinders, which can be described by the shape, the sequence and the color of the tiles, *i.e.* the materials inside the cylinders. In the general expression (n^v) the letter *v* denotes the number of vertices meeting at a node. The number *n* provides information about the number of vertices of one tile, which in plane nets corresponds to the number of sides *n* of the polygon (*n*-gon). For example, the number 6 in the symbol (6^3) (given in round brackets) indicates that the tiles are hexagons and the number 3 indicates that three of them meet at each vertex which indicates a tessellation composed of hexagons (see Fig. 19(a)). These symbols allow a classification of tessellations composed of different types of polygons (*e.g.* Archimedean tilings). For example, the expression (3^2.4.3.4) which describes the topology of the *p*4*gm* cylinder phase composed of triangular and square cylinders, means that each vertex in the tiling joins, in a circular sequence, two triangles, a square, a triangle and a square (see Fig. 20, left).

The expression [v^n] is advantageous for tiling patterns composed of identical polygons and incorporating different vertices (*e.g.* Laves tilings). Also in this description *n* gives the number of sides (edges) of the polygon and *v* is the valence of the vertex. The number 6 in the symbol [3^6] (in square brackets) indicates that the tiles are hexagons and the number 3 means that three of them meet at each node (see Fig. 21). For tessellations incorporating different types of vertices each vertex is described separately and the sequence is given. For example, the expression [3^2.4.3.4] for the *p*4*gm* or *p*2*gg* pentagonal cylinder phases means that there is a sequence of two 3-fold vertices, a 4-fold, a 3-fold and a 4-fold vertex around a pentagon ($\sum n = 5$; see Fig. 20, right).

From a topological point of view, the two apparently very different cylinder networks with *p*4*gm* lattice, the pentagonal cylinder phase and the cylinder phase composed of triangular and square cylinders represent duals of the same topological class (3^2.4.3.4). This means that in both tessellations the nodes and tiles are exchanged as illustrated in Fig. 20. Intersection of each side of the pentagons in the [3^2.4.3.4] tiling * (red lines) leads to a tessellation , composed of square and triangular tiles in the ratio 1 : 2 (black lines), corresponding to the

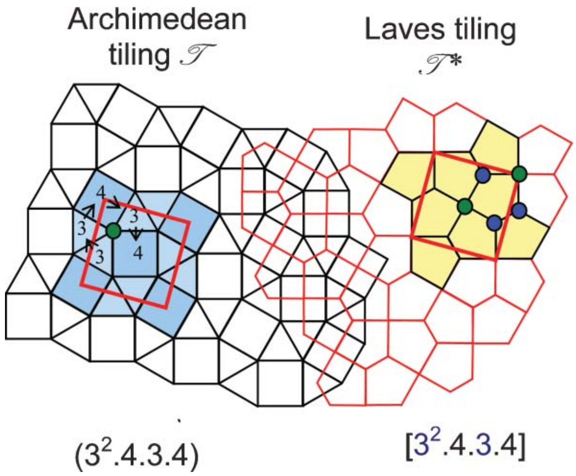

Fig. 20 The pair of tiling duals with *p*4*gm* lattice. The Laves tiling [3^2.4.3.4] composed of pentagonal tiles (red lines) is superimposed on the dual uniform tiling composed of squares and regular triangles (Archimedean tiling (3^2.4.3.4), black lines). Note that each vertex of the Laves tiling is the centre of one of the tiles of the Archimedean tiling, and vice versa; [3^2.4.3.4] gives the sequence of vertices around a tile, whereas (3^2.4.3.4) describes the sequence of tile around a vertex.[45]

(3^2.4.3.4)-tiling. In the resulting tessellation there are exclusively 5-fold vertices exactly at the positions of the pentagonal tiles in the dual, and the triangles and squares develop from the 3-fold and 4-fold vertices, respectively. Hence, the dual tilings and * are topologically equivalent. Topological duals can be constructed for any periodic edge-to-edge tiling, except for the (4^4) tiling which is its own dual.

The simplest (most "uniform") modes of tessellations by regular polygons are collated in Fig. 21. These are the tree *regular* tilings (3^6, 4^4 and 6^6) composed of identical tiles and vertices, tessellations composed of identical tiles (monohedral tilings, Laves tilings) and tessellations by regular polygons interconnected by only one type of vertices. (Archimedean tilings). Each of the 11 Laves tilings, shown at the left has exactly one topological dual, shown in the same line at the right, which is one of the 11 Archimedean tilings. Remarkably all the LC cylinder structures, but also most morphologies formed by ABC star triblock copolymers and regular pattern described in Section 3 are derived from the tiling topologies shown in Fig. 21, Only the patterns with a high valence of the vertices ($n > 6$, see Fig. 21(b–d), left) are unlikely for self-organized systems.

The description of the LC cylinder networks as nets or as tessellations of a plane represent simplifications where the cylinder walls are regarded as infinitely thin lines and the columns at the vertices are regarded as points (see Fig. 22(a) and (e)). However, in reality the cylinder walls have a certain thickness as they are formed by in average two aromatic cores arranged side by side. Moreover, the nodes are composed of a different material than the connections between the nodes and these nodes represent columns with a significant diameter, incorporating either the hydrogen bonding networks of the diol groups or the relatively long alkyl chains.

Therefore, in an alternative description each of the three distinct micro-segregated regions, the columns at the edges, the columns inside the cylinders and the cylinder walls, could be

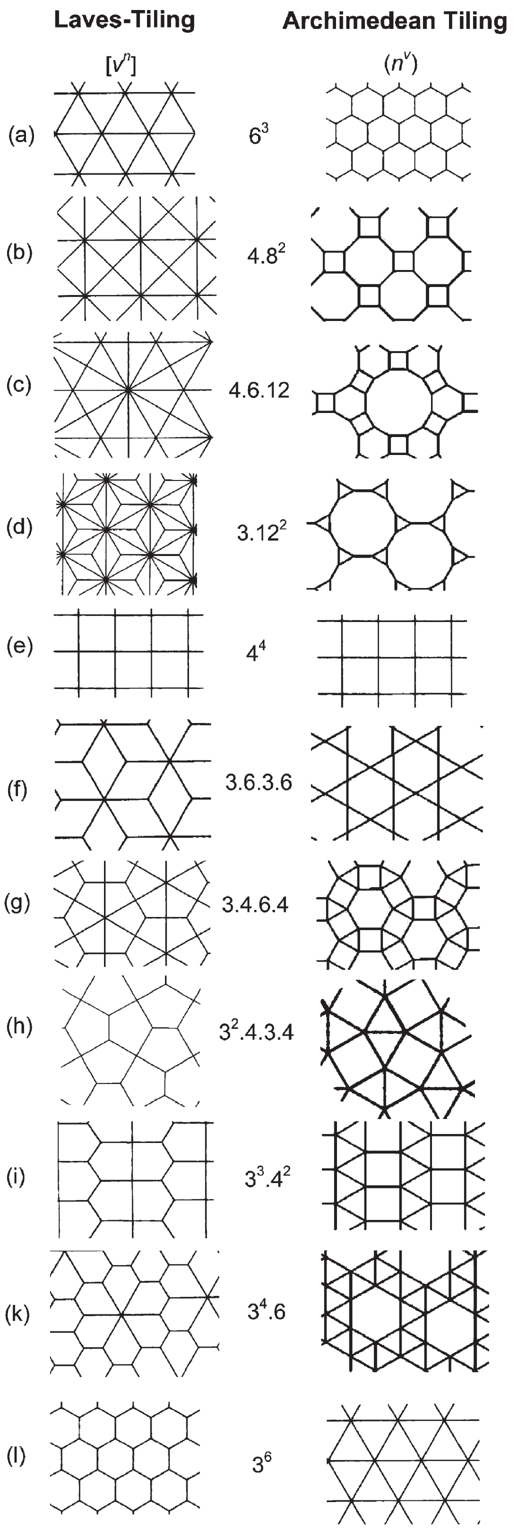

Fig. 21 The 11 Laves tilings [v^n] and their duals, the Archimedean tilings (n^v). Note that the three regular tilings (3^6), (4^4) and (6^3) belong to both series, whereby the (4^4) tiling is its own dual. Tilings with a valence of $n > 6$ (*e.g.*: [4.8^2], [4.6.12] and [3.12^2]) are unlikely in soft matter systems, whereas their duals describe three-color tilings in block copolymer morphologies (see Fig. 23). In each line the Laves tilings at the left is the topological dual of the Archimedian tiling at the right and *vice versa*.[79]

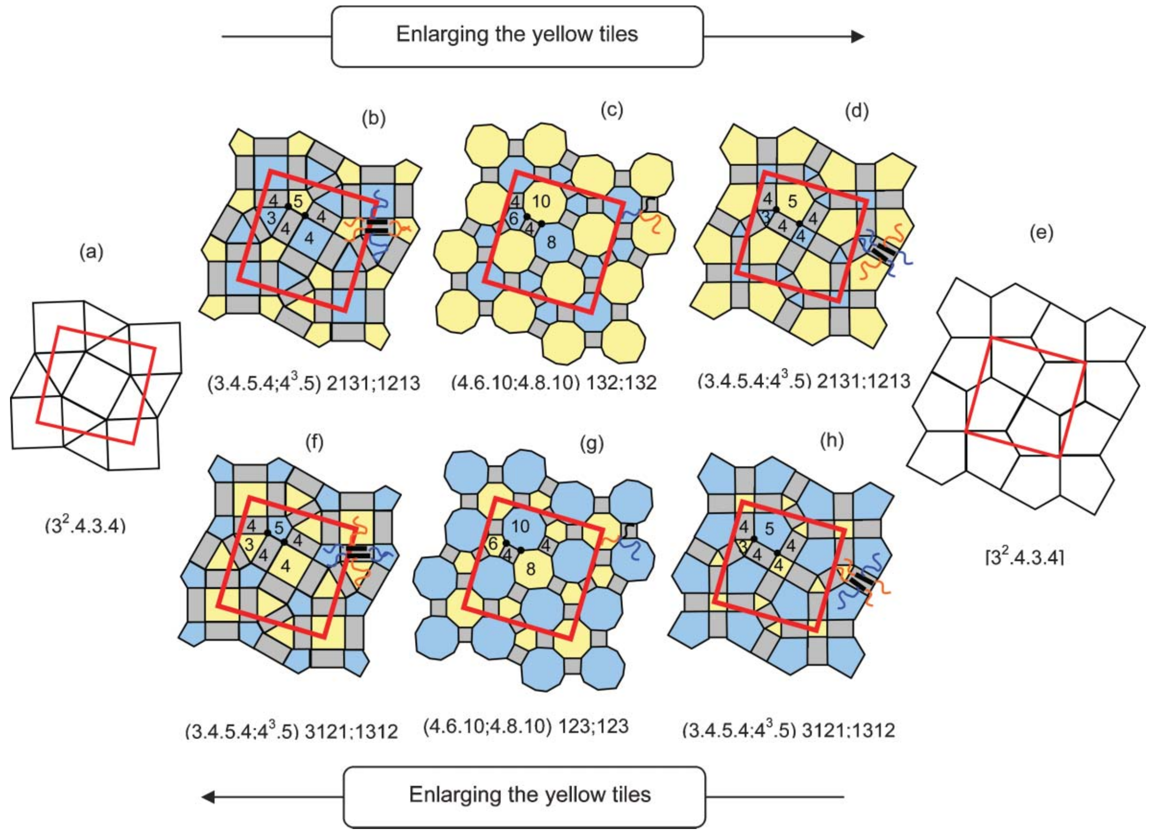

Fig. 22 Three-color tiling patterns which describe the *p*4*gm* cylinder phases composed of triangular and square cylinders (a, b, f) and pentagonal cylinders (d, e, h), formed by facial amphiphiles (b, h), or bolaamphiphile with non-polar lateral chains (f, d); color-code: grey (1) = aromatics, blue (2) = polar regions, yellow (3) = non-polar parts. Pattern (c, g) are of relevance for morphologies formed by ABC star triblock copolymers. Structures (b, c, d) in the upper row represent color isomorphs of the structures (f, g, h) in the lower row. In each structure there are two types of nodes assigned separately; the color sequence is given as a sequence of numbers following the tiling pattern. In (a) and (e) the walls of the polygonal honeycombs form the net, whereas in (b–d) and (f–h) the interfaces between the micro-segregated compartments represent the nets.

assigned to a set of distinct tiles with different color (see Fig. 22(b), (d), (f) and (h)). Here the interfaces between the distinct micro-segregated regions form the net. As shown in Fig. 22(b), the *p*4*gm* lattice of the $\mathrm{Col}_{\mathrm{squ2(3,4)cyl\text{-}3,4}}$/*p*4*gm* phase of the facial amphiphiles can be regarded as a three-color-tiling composed of blue squares and triangles (polar columns inside the cylinder frame), yellow pentagons (columns of the alkyl chains interconnecting the cylinder walls) and grey rectangles (cylinder walls). However, this tiling requires that the polygonal columns at the corners have a side length corresponding exactly to the thickness of the cylinder walls, so that all three materials are only in contact with each other at the vertices. By increasing the size of the columns located at the corners at the expense of the columns within the cylinder frames additional interfaces arise. The additional contacts between these columns give rise to a cylinder structure which can be described by a tiling pattern (see Fig. 22(c)), where only the grey tiles (representing the cylinder walls) retain a rectangular shape whereas the number of sides forming the blue and yellow tiles (representing the columns) are doubled. This tessellation is composed of tetragonal, hexagonal, octagonal and decagonal tiles. Further increasing the size of the yellow tiles leads to the same type of tiling as shown in Fig. 22(b), but with a reversed size of yellow and blue tiles (see Fig. 22(d)). In this organization the position of the blue and yellow tiles with respect to the rod-like cores forming the cylinder walls is exchanged. This three color tiling represents the structure of the pentagonal cylinder phase formed by the bolaamphiphiles. The corresponding simplified description as non-colored tessellation of a plane by pentagons is shown in Fig. 22(e).

Similar sequences can be seen for the color-isomorphic tilings shown in Fig. 22(f–h), where the structure shown in Fig. 22(h) corresponds to the *p*4*gm* pentagonal cylinder phase of the facial amphiphiles. The structure in Fig. 22(f) could be expected for bolaamphiphiles with short lateral chains, but these molecules prefer an organization in cylinders with rhombic shape (see Section 2.3). This detailed analysis of the phase structures indicates additional complex pattern where the number of sides of the polygons located at the corners and within the cylinders is doubled (Fig. 22(c) and (g)). Related three-color tilings can be derived from any other tiling pattern. Remarkably, the structures derived from the *regular* tilings (3^6, 4^4 and 6^3), shown in Fig. 23 represent Archimedean tilings (see Fig. 21).

Though this three-color tiling describes the structure most precisely it must be considered that in the LC phases the micro-segregated domains are only small and the interfaces are

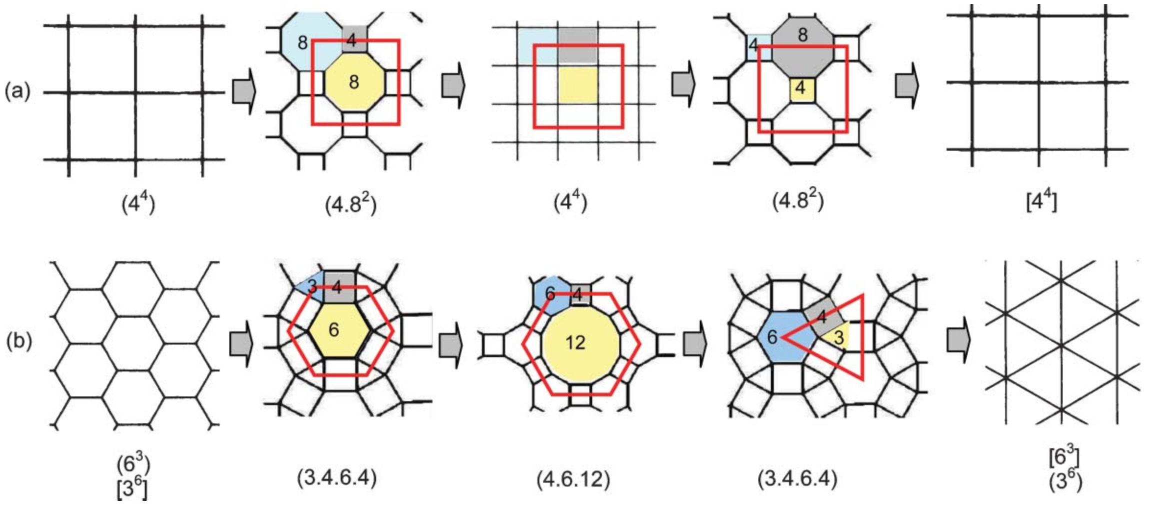

Fig. 23 Topological duals and three-color tiling patterns which describe (a) the *p*4*mm* square cylinder phases and (b) the *p*6*mm* hexagonal cylinder phases (note that all tilings represent Archimedean tilings, see Fig. 21, and that these pattern are often found as morphologies of ABC triblock star polymers, see Fig. 24 and Fig. 26); red triangles, squares and hexagons indicate the shape of the cylinders.

quite diffuse and it is questionable if it is in this case justified to assign a discrete polygonal shape to the individual micro-segregated regions. Therefore, for polygonal LC cylinder phases the description as simple nets (where the cylinder walls and the interconnecting columns are regarded as nets) is preferred. The descriptions as three-color-tilings becomes of increasing relevance as the contribution of the anisometry of the rigid unit in these T-shaped molecules is reduced and as the size of the molecules is increased. Hence, these three-color tilings are more appropriate for the description of morphologies of flexible ABC star triblock copolymers as discussed in the next Section 3.1.

Hence, there is the possibility of a huge number of highly complex tiling patterns available for self organization in soft matter systems, which is general, as shown in the following sections. However, only a small fraction of the possible structures has been explored up to now.

3 Periodic tiling pattern in other self-organized systems

In the following paragraphs the LC cylinder structures will be discussed in relation to other self organized periodic structures formed in block copolymers, in solid state structures and at surfaces.

3.1 Block copolymers

As the molecules under discussion are composed of three incompatible molecular parts they can be regarded as low molecular weight analogs of ternary block copolymers. Due to the non-linear T-shaped molecular geometry there is some similarity to star shaped triblock copolymers.[29,80] In these star copolymers composed of three incompatible arms, connected at discrete junction points the requirements of minimizing the interfacial area and optimizing chain stretching at a given volume fraction determine the tiling pattern.[81–84]

The broadest variety of morphologies was obtained for star shaped triblock copolymers composed of three strongly incompatible polymer chains, namely polybutadiene (B), polystyrene (S) and poly(2-vinylpyridine) (P)[83,84] or composed of polyisoprene (I), polystyrene and poly(2-vinylpyridine).[66,85–87] Because the process of preparation of these ABC star polymers with exact compositions is difficult and time consuming, methods of blending these triblock copolymers with homopolymers or diblock copolymers have also been used for precise control of composition.[75,84,87,88]

The morphologies obtained with these polymers and polymer blends are very similar to the morphologies realized with the ternary block molecules, namely the LC square cylinder phase and the hexagonal cylinder phase (see Fig. 15(d) and (f)) are analogous to morphologies obtained for BSP star polymers shown in Fig. 24.[66,84] Even the duals with (3^2.4.3.4) topology composed of square and triangular, or pentagonal cylinders, respectively (Fig. 10), were reported for ABC star polymers[66] after the first description of these morphologies in LC systems.[45] As shown in Fig. 25, not only the transition electron microscopy (TEM) image of a stained sample indicates this tiling, also the small angle X-ray diffraction pattern obtained by microbeam SAXS of this polymer morphology is identical to XRD pattern observed for the LC systems and indicates a *p*4*gm* lattice.[87]

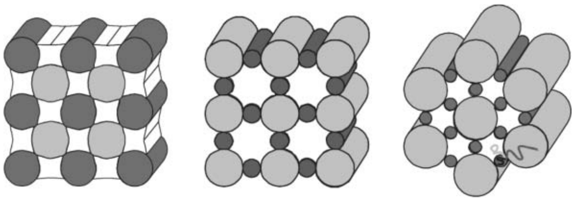

Fig. 24 Morphologies of BSP triblock star block copolymers representing square and hexagonal arrangements of three distinct sets of columns (B = polybutadiene = black, S = polystyrene = white, P = polyvinylpyridine = gray).[84]

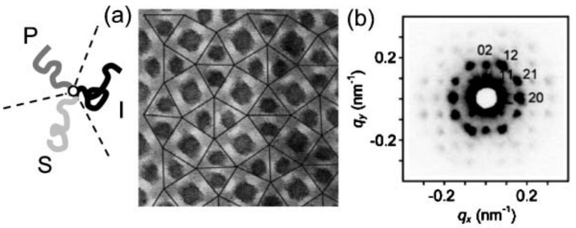

Fig. 25 ISP triblock star polymer consisting of a junction point and three arms of different chemical species. (a) TEM image of the polymer morphology corresponding to the $(3^2.4.3.4)$ Archimedean tiling; (b) micro-beam SAXS pattern.[87] Reprinted with permission from *Macromolecules*, 2006, **39**, 9402–9408. Copyright 2006, American Chemical Society.

The morphologies shown in Fig. 26 were obtained for ISP star polymers depending on the composition. In analogy to the LC phases of the T-shaped amphiphiles, these morphologies can be regarded as composed of columns of one component inside a cylinder framework formed by the other two components (the cylinders are indicated by red doted lines). In a similar fashion as observed for the T-shaped amphiphiles, the polymer morphologies are governed by the relative volume fraction of the incompatible components. This is seen in Fig. 26 for the series of morphologies obtained by increasing either the volume fraction of P or S, respectively. For example, in the series of Fig. 26(a)–(e) the shape of the cylinder frames changes from hexagons *via* pentagons to squares with increasing volume fraction of the white S-block, which reduces the relative volume fraction of the gray P blocks inside the cylinder frames. However, there are also differences to the LC cylinder morphologies, which mainly result from the absence of restrictions provided by the rod-like segments (rigidity, geometry, length). For example, in T-shaped amphiphiles the rod-like cores can only act as cylinder walls and not as nodes interconnecting the walls, *i.e.* these segments have specific functions which cannot be exchanged. In contrast, in the ABC star polymers the junction points between the polymer segments are fixed to the vertices, and no junction points are permitted to stay on the microdomain interfaces, but any of the components can be placed either in the cylinder walls, in the interior of the cylinders or in the columns at the vertices. For example, in the morphology shown in Fig. 26(a), all I-blocks (black) are located at the vertices whereas in the morphology shown in Fig. 26(c) these blocks form the cylinder walls.

Interestingly, for these block copolymers there are additional morphologies, where within a uniform periodic structure the microdomains of the same chemical composition have distinct positions and functions. For example, in the morphology shown in Fig. 26(b), in each hexagonal cylinder the I-blocks are located at the vertices (black hexagons) as well as in the cylinder walls (black rectangles), which reduces the overall symmetry of the hexagonal cylinder structure.

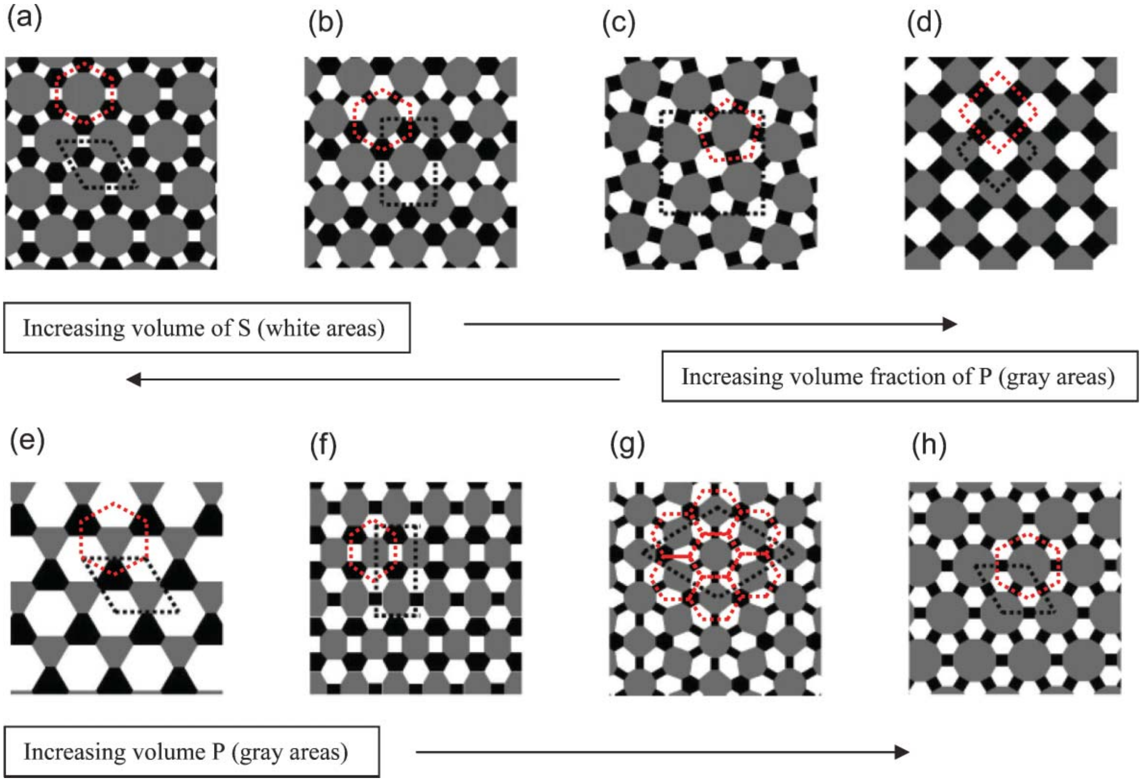

Fig. 26 Tiling pattern (cross sections through the cylinder structures) of ISP star terpolymers with different composition based on TEM images (I = black, S = white, P = gray): (a–d) $I_{1.0}S_YP_{2.0}$ series with increasing S-content: (a) Y = 1.3, (b) Y = 1.6; (c) Y = 2.3 and (d) Y = 2.7; (e–h) $I_{1.0}S_{1.8}P_X$ series with increasing P-content: (e) X = 1.0, (f) X = 1.6; (g) X = 2.0 and (h) X = 2.9; the dotted black lines indicate the unit cells, whereas the dotted red lines indicate the shape of the cylinders in the network.[87] Reprinted with permission from *Macromolecules*, 2006, **39**, 9402–9408. Copyright 2006, American Chemical Society.

Similarly, also the S-blocks (white) can be found in both positions. It seems that this complex morphology allows a change of the enclosed P-columns (gray) from larger dodecagons (Fig. 26(a)) to smaller decagons by retaining the hexagonal structure of the cylinder frames, before in a next step, after further enlarging the S-blocks, a pentagonal cylinder frame (see Fig. 26(c)) is formed around these decagonal columns. In this pentagonal net (Fig. 26(c)) the position of I-blocks (white) and S-Blocks (white) is uniform, but exchanged with respect to the hexagonal net in Fig. 26(a). Two additional types of such "mixed" morphologies (Fig. 26(f) and (g)) were observed in the series shown in Fig. 26(e–h) by increasing the P-block size (gray) at constant I : S ratio. It is also interesting to note that most of the complex structures shown in Fig. 25 and 26 have been first predicted by Monte Carlo simulations[89–91] before they were experimentally detected.[87]

Presently, block copolymers with attractive interactions between selected polymer blocks arise increasing interest as a tool to achieve new hierarchically ordered structures.[92] Bolaamphiphilic block copolymers having hydrogen bonding acceptor sites at both ends of a lipophilic polymer chain, as for example PIP, composed of a lipophilic polyisoprene chain (I), terminated at both ends by polar poly(2-vinylpyridine) blocks (P), can form "closed-loop" structures (Fig. 27) with a triangular or square shape after blending with complimentary hydrogen bond donor functionalized amphiphilic SH diblock polymers (S = polystyrene, H = 4-hydroxystyrene) which provide the third incompatible segment S.[93] It was proposed that in the morphology shown in Fig. 27 the positions of the hydrogen bonding sites (dark columns containing the phenol-pyridine complexes PH) are fixed by the I-polymer chains interconnecting these columns. Though this concept has some similarities to that of low molecular weight bolaamphiphiles, in this case the coiling of the flexible and non-polar I-polymer chains can self-fill the space inside the triangular and square loops, giving rise to uniform and non-interrupted I-cylinders around the hexagonal S-columns and hydrogen bonding networks located at the edges of the hexagonal cylinders.[94]

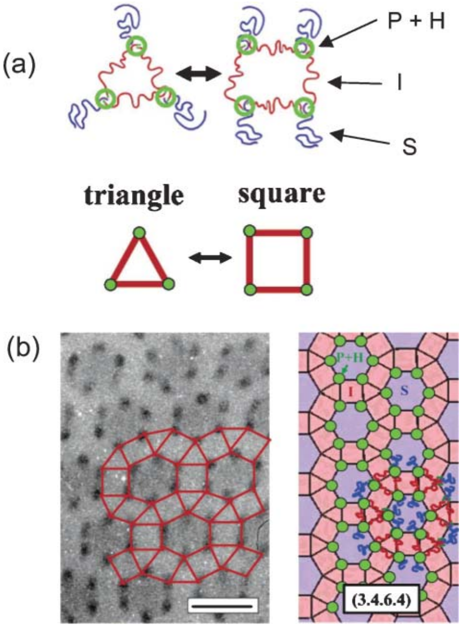

Fig. 27 (a) Schematic drawing of self-assembled closed-loop structures formed by a PIP/SH = 2/1 blends; (b) TEM image and schematic drawing of the polymer morphology. Auxiliary lines are drawn to make clear the domain packing manner.[93] Reprinted with permission from *Macromolecules*, 2006, **39**, 2232–2237. Copyright 2006, American Chemical Society.

Major differences between polymers and low molecular weight amphiphiles are associated with the difference in molecular size. In both systems, in polymers, as well as in low molecular weight systems, micro-segregation (nano-segregation) is a main driving force for structure formation. It requires a sufficiently strong positive mixing enthalpy between different segments, which compensates the entropy of mixing, disfavouring the segregation.[95] For low molecular weight amphiphiles the contribution of the entropy of mixing is more important, because the number of molecules per volume unit is much larger than for polymers. Therefore, highly incompatible units and relatively strong attractive forces, such as hydrogen bonding or Coulomb forces are required for low molecular weight amphiphiles to increase the enthalpic contribution to segregation which compensates the entropic penalty and enables self organization of these materials.[9,10] The rigid rod-like cores significantly contribute to the mesophase stabilization due to the strong rigid-flexible incompatibility provided by these units. In addition, due to the excluded volume effect, favoring a parallel organization of these rods, and due to the restrictions provided by these rigid segments (fixed distances, molecular geometry) new morphologies could be obtained which are not achievable with flexible molecules or polymers. Among them tilings by pentagons and giant lattices are the most remarkable structures (see Section 2.4 and 2.6).

In addition to volume fractions and interfacial energies also crystallization of distinct polymer segments can modify the polymer morphologies.[96,97] Crystallization can drive micro-segregation, due to the stronger incompatibility of the crystalline (*i.e.* rigid) segments with fluid segments. As linear polymer segments crystallize more easily than branched segments, which stay in the fluid (or glassy) state, these chains organize preferably parallel to each other. This leads to a dominance of lamellar morphologies if crystallization takes place from the disordered state or from weakly segregated polymer morphologies. In contrast, in strongly segregated systems crystallization occurring below the order-disorder transition temperature is confined in the morphology provided by micro-segregation. Here the fundamental structure is retained, but additional order occurs within the crystallized domains. Hence, the effect of crystallization is similar to the effect of introduction of rigid segments. In low molecular weight systems, due to the smaller molecular size of the molecules there is a stronger coupling between the incompatible segments and hence changing the order in one of the compartments influences the others more strongly. Therefore, crystallization of only one of the micro-segregated domains is usually not observed for low molecular mass liquid crystals. However, if there are relative large rigid units combined with highly flexible parts (*i.e.* if there is a large difference between rigid and flexible units), then structures composed of crystalline and fluid or conformationaly disordered compartments are possible. More importantly, in LC systems containing rigid segments there is usually a different degree of local order in the distinct compartments. For example, in the polygonal cylinder phases of the T-shaped ternary amphiphiles there is an additional orientational order of the rod-like units in the cylinder walls providing a preferred alignment of these units parallel to the cylinder walls and perpendicular to the long axis of the inner columns, whereas the lateral chains in the inner columns are more disordered.

In general, due to the high molecular weight, polymers are highly viscous and well developed polymer morphologies can only be obtained by solution casting during evaporation of a solvent in a very slow self organization process (several days). Due to this inherent viscosity the obtained lattices are only local and often deformed. Hence, it is not always clear if the obtained polymer morphologies represent thermodynamic equilibrium structures or if these are metastable structures.[98] In the liquid crystalline phases of the low molecular weight triblock molecules, the morphologies develop in a much faster self-assembly process ($\ll 1$ s) under thermodynamic control. These morphologies are spontaneously formed from the isotropic liquid state by changing the thermodynamic parameters, mostly temperature. The transitions from the disordered isotropic liquid state and between different cylinders morphologies take place without significant hysteresis, *i.e.* these are fast and reversible first order phase transitions. This allows the easy preparation of uniformly aligned domains of larger size by slow cooling from the isotropic liquid state. Moreover, due to the low viscosity, these superstructures can quickly respond to external stimuli. In addition, the self organized LC structures are about one magnitude smaller in size (2–15 nm), than the morphologies of the related polymers (50–100 nm) which is important for the further miniaturization of periodic arrays.

3.2 DNA superstructures

DNA is not only the blue print containing the information that encodes instructions for life; it is nowadays also a nanoscale construction tool.[99–101] This field, called "structural DNA nanotechnology" is based on the fact that the double helix can be regarded as a rigid rod-like nanoscale object with a persistence length of $\sim$150 base pairs. This implies that up to a length of $\sim$50 nm the DNA double helix behaves as a rigid rod. The rules of base pairing allow specific and predictable recognitions, facilitating the organization of the double helix strands in space.

To construct frameworks, the base pairing logic is used to make specific contacts between DNA strands, which is achieved by single stranded segments or overhangs that have complimentary base sequences. Hence, oligonucleotides can fuse at specific points into different regular pattern. Depending on the connectivity of the junction points distinct types of 2D grids can be constructed in a directed manner as shown in Fig. 28 and Fig. 29, but also 3D nets representing platonic solids have been obtained.[102]

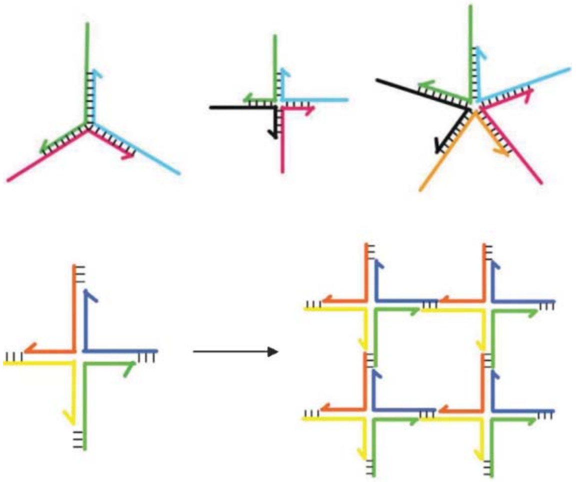

Fig. 28 Selected examples of DNA junctions and formation of a square grid.[101] Reprinted with permission from *Chem. Soc. Rev.*, 2006, **35**, 1111–1121. Copyright 2006, The Royal Society of Chemistry.

DNA nets composed of triangular, square, rhombic and hexagonal tiles have already been realized.[103] In contrast to the LC cylinder phases which represent polygonal honeycombs of infinite cylinders, these DNA superstructures represent 2D nets. Only recently Seeman and co-workers reported a regular continuous 3D DNA lattice with a Kagome motif (Archimedean 3.6.3.6 tiling, see Fig. 21(f)), where adjacent grids are fixed on top of each other, giving rise to a porous cylinder structure with channels running perpendicular, as well as parallel to the DNA grids.[104] In this structure the recognition motif is provided by hydrogen bonding due to specific and nonspecific base pairing and the stability mainly results from π-stacking of the nucleobases. This shows that honeycomb cylinder structures are also possible with DNA strands and due to the relatively large size of the building blocks the dimensions of the cylinders are significantly larger than those of LC systems, but in the same range as the length scale of the periodicities in block copolymers. It was suggested to use these cylinders to organize non-crystallizable proteins in a periodic way in order to be able to analyze their structure by X-ray diffraction.[105] This potential application should also be considered for the giant lattices formed in the LC phases of some T-shaped ternary block molecules. The advantage of LC systems would be that these arrays could be grown with a much larger uniform domain size than presently achievable with related DNA arrays and that these arrays could be more easily addressed by external fields.

Recently, also five-point-star motifs (Fig. 28)[106] and six-point-star motifs (Fig. 29(c)) became available.[107] So it can be expected that the pentagonal grid incorporating 3-fold and 4-fold junctions and DNA nets composed of triangular and square tiles incorporating 5-fold junctions should also become available by appropriate design of the DNA strands and junctions. In an attempt to organize a mixture of two DNA motifs, a four-point-star motif and a three-point-star motif (see Fig. 29(b) and (c)) forming square[108] and hexagonal 2D-arrays, respectively, a self sorting behavior was observed, where each motif associates only with like motifs and excludes unlike motifs.[109] In this case a hetero-assembly is unlikely to occur, because a mixed organization of hexagons and squares

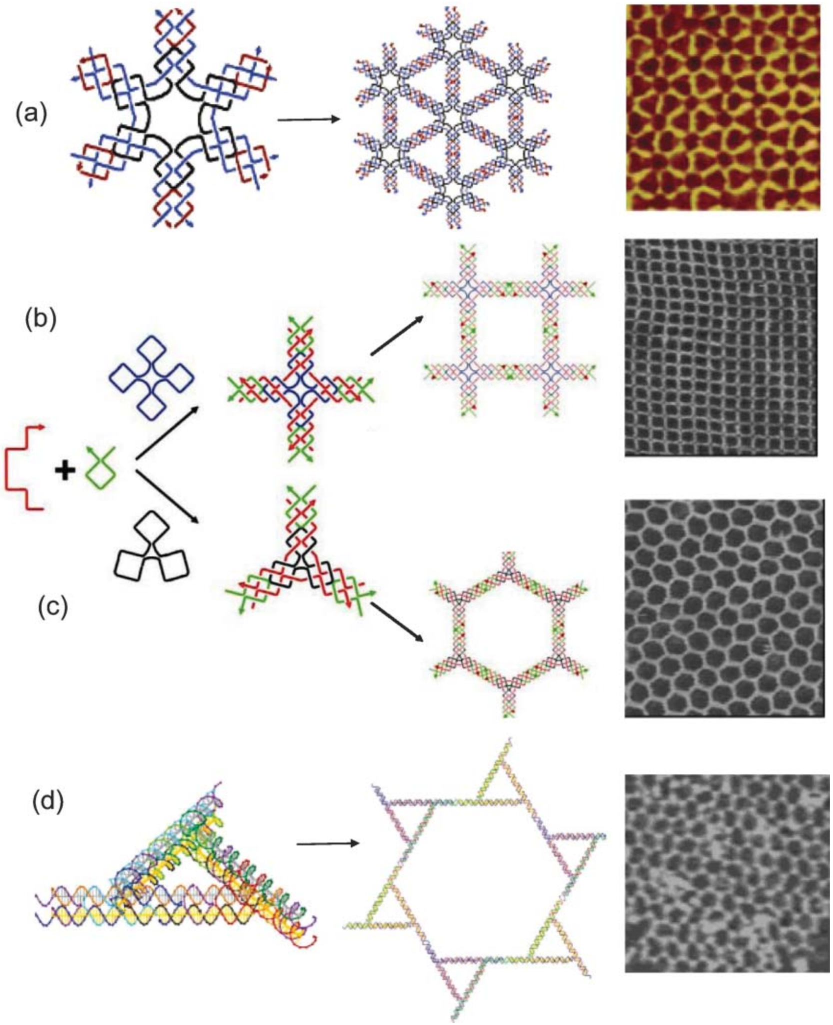

Fig. 29 Different 2D-net structures formed by self assembly of DNA strands: (a–c) periodic tiling patterns by triangles, squares and hexagons, respectively[107,109] (d) combination of hexagons and triangles.[111] (b) and (c) reprinted with permission from *Chem. Commun.*, 2007, 165–167. Copyright 2007, The Royal Society of Chemistry; (a) and (d) reprinted with permission from *J. Am. Chem. Soc.*, 2006, **128**, 15978–15979 and *J. Am. Chem. Soc.*, 2004, **126**, 10230–10231. Copyright 2006, 2004, respectively, American Chemical Society.

cannot give rise to a periodic tiling. In contrast, the Kagome grid, which is a periodic tiling (3.6.3.6 Archimedean tiling, see Fig. 21(f)) composed of triangular and hexagonal tiles in a ratio 2 : 1 and containing only one type of nodes, was already achieved.[110] Another tiling composed of triangular and hexagonal tiles is shown in Fig. 29(d).[111]

3.3 Crystal engineering and coordination polymers

Also crystal engineering has rapidly advanced over the recent years. The vast majority makes use of relatively strong intermolecular interactions, either hydrogen bonding[112] or ligand-to-metal coordinative bonding to link individual components in a defined way (Fig. 30). Self-assembly of transition metals and rigid or semi-rigid multifunctional organic ligands turned out to be a successful paradigm for synthesis of either discrete[113–117] or infinite structures (coordination polymers, metal–organic frameworks) extended in one, two or three dimensions.[118,119]

In the context of this review two-dimensional nets composed of polygons are of special interest and the discussion is limited to these structures. Nets composed of a regular array of polygons have been reported in the recent years for numerous solid state structures. Especially, the node-and-spacer approach has been remarkably successful in producing predictable network architectures. The role of the organic ligand is to serve as a rigid spacer that links the nodes that are defined by the metal coordination geometry. The coordination geometry of the metal, as well as the shape and topology of the di- or multi-dentate organic ligand, determine the resulting self-assembled structure (Fig. 31). Linear dipyridines[120] and dicarboxylates[121,122] represent the most frequently used ligands to design plane grids, but also divalent bent and tripodal ligands or hydrogen bonding units (see Fig. 32)[123–125] have been used. The square grid is among the most common network structures in metal–organic frameworks, because many metals have octahedral or square coordination geometries, which combined with linear bifunctional ligands give rise to this net topology. However, also hexagonal and more complex grids, as for example the Kagome lattice (see Fig. 33(a)) have been obtained.[126–128]

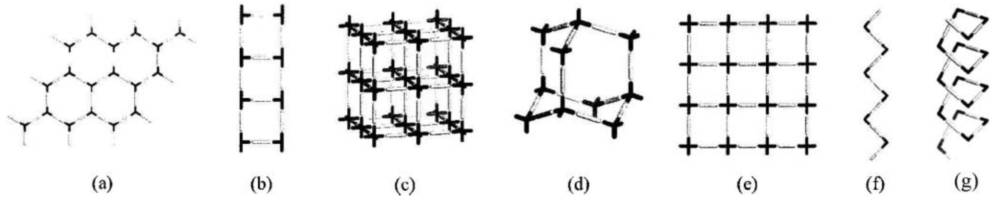

Fig. 30 Schematic representation of some simple network architectures of metal–organic frameworks: (a) 2D-hexagonal grid; (b) 1D-ladder; (c), (d) 3D-nets; (e) 2D-square grid, (f) 1D-zigzag chain and (g) helix.[118] Reprinted with permission from *Chem. Rev.*, 2001, **101**, 1629–1658. Copyright 2001, American Chemical Society.

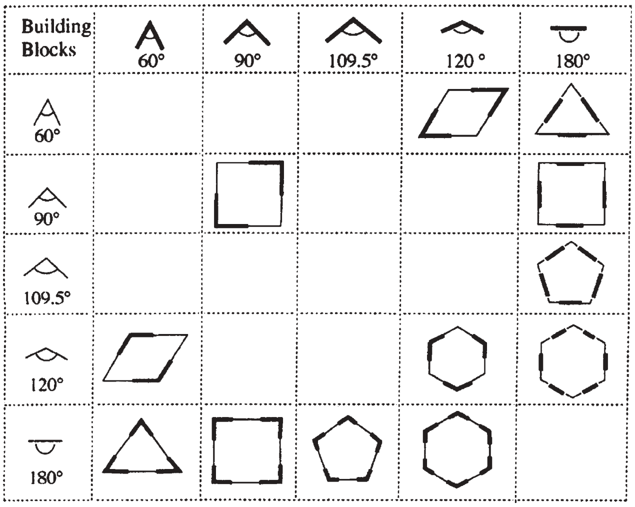

Fig. 31 Selective formation of different discrete polygons by appropriate choice of coordination geometries provided by the corners and the geometry of the ditopic bridging units (bidentate ligands); only discrete polygons are shown, but this scheme is also applicable to infinite 2D nets, with exception of the regular pentagons which cannot tile a plane (in addition, the tetrahedral angle slightly deviates from the angle of 108° required for a regular pentagon).[113] Reprinted with permission from *Chem. Rev.*, 2000, **100**, 853–908. Copyright 2000, American Chemical Society.

To the best knowledge there is only one report about a net formed by a periodic organization of exclusively pentagons (see Fig. 33(b)). However, this network does not have a flat topography, because tetrahedral nodes, provided by the donor-sites of the tetradentate ligand hexamethylenetetramine were used to adopt both, the 3-fold and the 4-fold nodes of the (3^2.4.3.4) pentagon net.[129] Escape from planarity reduces strains resulting from this coordination geometry and allows a periodic packing of the pentagons. In general, because bond-length and angles are fixed within relatively narrow limits due to the rather well defined coordination geometries, a flat net, representing a uniform and periodic tiling by pentagons should be difficult to achieve with coordination networks. In contrast, the combination of order and mobility in the LC state is a unique feature which allows an easier organization into pentagonal honeycombs.

A common feature of coordination networks and polygonal honeycomb phases is, that in both cases the attractive forces providing the network structure are positioned at the ends of a rigid linear molecule, and that these ends are interconnected by attractive intermolecular interactions. However, there are also significant differences. One major difference is, that the hydrogen bonding networks are highly dynamic and flexible (fluid). Due to this flexibility, there is no fixed valence and geometry. Therefore, different polygonal honeycombs can be realized and the shape of the polygons is mainly determined by

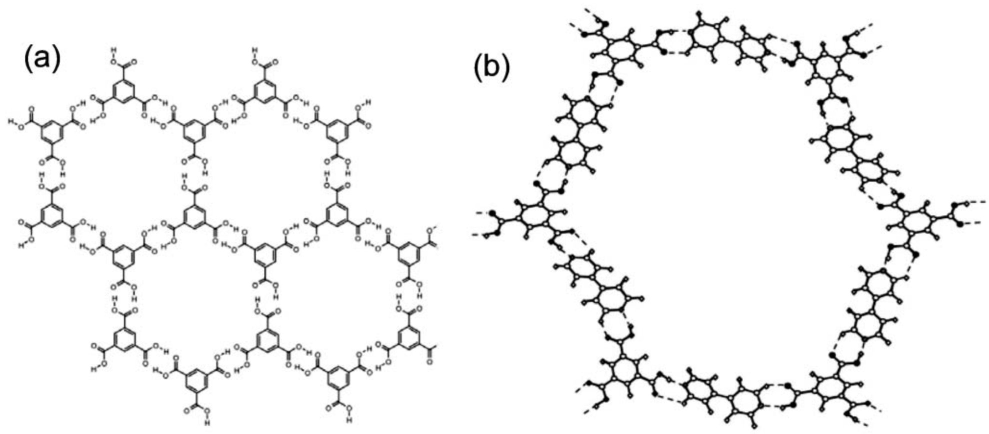

Fig. 32 Hexagonal nets formed by directed hydrogen bonding: (a) 1,3,5-benzenetricarboxylic acid with regular hexagons organized in a flat topography (space filling is achieved by interpenetration); (b) 1 : 1 complex of 1,3,5-benzenetricarboxylic acid with 4,4′-dipyridine, where the hexagons are not regular and the topography of the grid is not flat.[123] Reprinted with permission from *Chem. Commun.*, 2001, 1–9. Copyright 2001, The Royal Society of Chemistry.

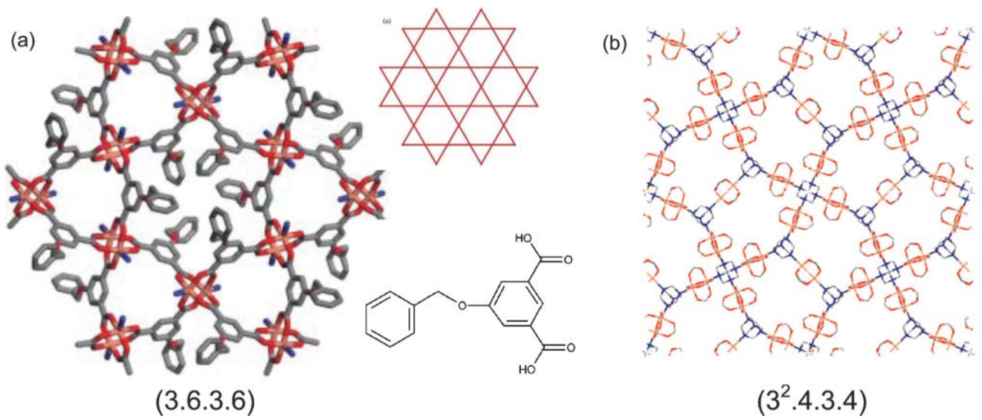

Fig. 33 (a) Kagome-lattice formed by $[\{Cu_2(pyridine)_2(5\text{-benzyloxy-1,3-bdc})_2\}_3]_n$, the pyridine rings have been removed for clarity, except for the nitrogen atoms (blue), the 5-benzyloxy-1,3-bdc ligand is shown at the right.[126] Reprinted with permission from *Chem. Commun.*, 2004, 2534–2535. Copyright 2004, The Royal Society of Chemistry. (b) Pentagonal grid (H-atoms omitted for clarity) as seen in the crystal structure of $[HMTA]_3[Cu_2(\mu\text{-}O_2CEt)_4]_5$ (HMTA = hexamethylenetetramine, blue: N, red: O, gray: C).[129] Reprinted with permission from *J. Am. Chem. Soc.*, 2001, **123**, 9224–9225. Copyright 2001, American Chemical Society.

the ratio of the space required by the lateral chains which fill the interior of the cylinders with respect to the perimeter of the cylinder-frame. For these reasons also structures combining nodes with two or even three distinct valences and with distinct geometries within a uniform structure are possible. This is a prerequisite for the formation of pentagonal cylinders and giant cylinder structures. In the metal–organic nets, however, the valence and coordination geometry are well defined and hence dominate the net topology.

Also the superstructures are different, because the cooperative nature of hydrogen bonding leads to extended hydrogen bonding networks (Fig. 34(b)). Therefore, the interactions do not only lead to the formation of distinct nets, they also provide attractive forces between the nodes of adjacent nets, which immediately gives rise to formation of polygonal honeycombs. Formation of honeycombs is also facilitated by the lateral chains, as these chains completely fill the space inside the cylinders which avoids any sliding or interpenetration. Properties, similar to those described for the H-bonding networks of the bolaamphiphiles are also provided by the van der Waals interactions between the terminal alkyl chains of facial amphiphiles. Though the cohesive force between individual CH_2 groups is smaller than that between two OH groups, the larger number of CH_2 groups incorporated in the alkyl chains gives rise to a significant contribution to the total stabilization energy.

In contrast, in the metal–organic frames and in the networks built up by directed hydrogen bonding (carboxylic acids) there is usually no interconnection between adjacent nets. Often, these nets form interpenetrating structures in which the voids associated with one framework are occupied by one or more independent frameworks (see Fig. 35(a)).[130] Interpenetration can be avoided if the void space is efficiently occupied by solvent molecules, additional guest molecules and in the case of charged frameworks also by counter ions. If there is no interpenetration, then a sliding of adjacent grids is often observed. Therefore, uninterrupted channels running orthogonal to the net-planes are difficult to achieve. Polygonal honeycomb structures can be obtained by anions which act as linkers between adjacent networks if the metals, positioned at the vertices, provide additional coordination sites in the direction perpendicular to the net (see Fig. 35(b)).[131–133] This leads to rather stable three dimensional solid state networks, as for example to the 3D net, shown in Fig. 35(b) where square grids are fixed on top of each other.

Fujita and co-workers used another approach to avoid interpenetration. They designed rod-like and at both ends pyridine-terminated ligands containing lateral ethylene glycol chains. Complexation with Co(II) yielded a square grid network structure, where the grid sheet layers are stacked above each other (Fig. 36(a)).[134] As there is no connection between the metal centers at the vertices there is an offset of both edges by ½, leading to an AB-packing, so that four channels per mesh result. Though this mode of organization is very different from

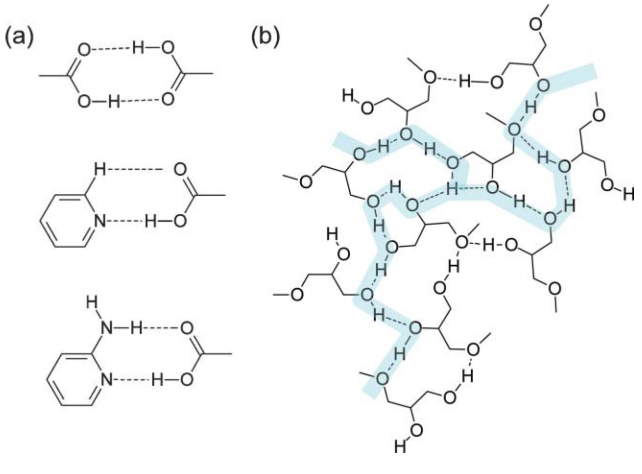

Fig. 34 Hydrogen bonding as attractive interaction for the design of nets and polygonal honeycombs: (a) directed hydrogen bonding between discrete donor and acceptor groups as used for construction of discrete supermolecular structures and nets, (b) dynamic hydrogen bonding network in diols, alcohols and water, where the OH-group acts simultaneously as proton donor and acceptor, this leads to a cooperative behavior which favors polymeric aggregates and this type of hydrogen bonding is used for the design of LC cylinder phases.

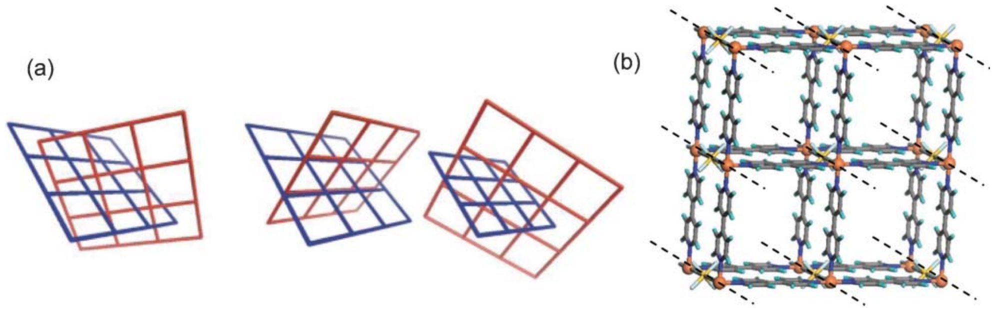

Fig. 35 (a) Different modes of interpenetration of square grid networks. Reprinted with permission from *Chem. Rev.*, 2001, **101**, 1629–1658. Copyright 2001, American Chemical Society. (b) Formation of a 3D-network by linking square grids composed of Zn(II) vertices and 4,4′-bipyridine sides by SiF_6^{2-} anions.[118,132] Reprinted with permission from *Chem. Commun.*, 2006, 4169–4179. Copyright 2006, The Royal Society of Chemistry.)

the organization within the LC square cylinder phases, where there is no offset, similarly to the situation in the LC systems formed by the facial amphiphiles, the lateral ethylene glycol chains play important roles: They fill the hollow channels (together with some H_2O guest molecules), thus avoiding interpenetrations of the grids. Moreover, these chains add considerable stabilization to the channel structure due to the formation of infinite hydrogen bonding arrays that interpenetrate the layers along the cylinder long axis. In addition, these chains introduce flexibility inside the cavity, allowing guest molecules to behave as in solution. Related hexagonal channel structures were prepared by Lee *et al*, but in this case tripodal building blocks were coordinated with linear Ag^+ linkers. Here the influence of different types of lateral chains (poly(oxyethylene) or alkyl) and their position was investigated systematically (Fig. 36(b)).[135–137] Hence, these

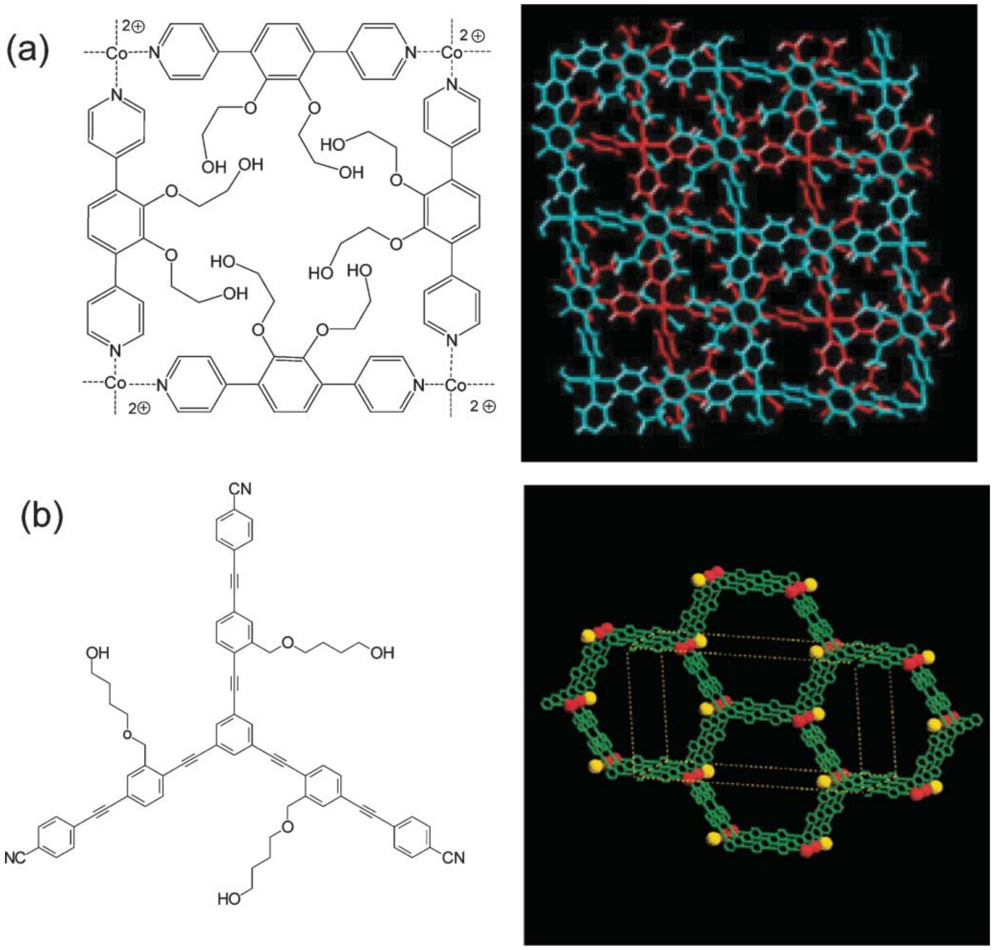

Fig. 36 Examples of coordination networks formed by ligands with space filling lateral substituents: (a) square grid network adopting a two-layer AB stack packing.[134] Reprinted with permission from *Angew. Chem., Int. Ed.*, 2005, **44**, 2151–2154. Copyright 2005, Wiley-VCH. (b) Nearly eclipsed hexagonal grid with channel structure formed by coordination with AgOTf (Tf = trifluoromethanesulfonate, Ag: red, S: yellow).[136] Reprinted with permission from *J. Am. Chem. Soc.*, 2000, 122, 6871–6883. Copyright 2000, American Chemical Society.

coordination networks are solid state structures combining a rigid framework with a fluid or semi-fluid interior whereas the LC polygonal cylinder structures combine a fluid, but ordered cylinder framework with a disordered fluid interior. In addition, the crystal structures are formed by precipitation from solutions and once formed these structures cannot be significantly changed, whereas LC polygonal cylinder structures represent dynamic and stimuli-responsive soft matter systems corresponding to thermodynamic equilibrium states. These structures can easily be modified by temperature changes, solvent molecules (see Section 5) and other external stimuli.

3.4 Periodic 2D-nets on solid surfaces

Individual metal–organic grids were also grown on solid surfaces which is another way to avoid interpenetration and self-filling. In most cases rod-like dicarboxylic acids, divalent phenols, dinitriles and other linear or tripodal bi- or tridentate rigid organic ligands were used. These molecules organize into square and hexagonal grids after coordination with transition metal ions (see for example Fig. 37(a)).[138] However, under 2D conditions the usual coordination geometry can be altered by the presence of a metal substrate. For example, trigonal coordination geometries were observed for Fe and Co, which are uncommon for their coordination chemistry in 3D nets.[138]

Not only the position of the donor sites at the ligands and the coordination geometry of the metal ions, but also the periodicity provided by the substrate lattice (graphite, Au, Ag, *etc.*) influences the resulting self-assembled metal–organic grids. A mismatch between the substrate and network nodal symmetry can reduce the overall symmetry by deformation of the net (shape of the polygons). It can also reduce the size of the single domains and give rise to the occurrence of differently oriented domains. Also the elongation of the building blocks (*e.g.* in rod-like oligophenylene based dicarboxylic acid and their dinitriles[139]) can change the degree of mismatch of the self assembled net with the surface lattice and hence the structure is not simply expanded, but is changed by deformation of the grid[140] or by a complete change of the mode of organization.[139] Different types of organization could also be obtained on different surfaces. Generally, the influence of the surface is more important if the strength of the intermolecular interactions, forming the net (metal coordination > H-bonding > polar interactions > van der Waals interactions) is weak and if the interaction energy between net and surface is strong (*e.g.* Au(111) > graphite(0001)). Thereby, the interaction with the nodes (metals) as well as with the polygon sides (organic ligands) must be considered, which makes predictions more difficult for labile nets.[141]

Polygonal grids were also formed by tripodal molecules capable or hydrogen bonding, as carboxylic acids,[142–144,147] carboxylic acid-pyridine complexes[145] and aromatic amines.[146] For metal–organic frames deposition of the materials to the surface is usually done from the gas phase under ultra high vacuum (UHV) whereas for purely organic materials often self assembly from appropriate solvents is used. In the latter case there is an additional solvent effect due to the competitive interaction with the acceptor and donor sites and the ability of

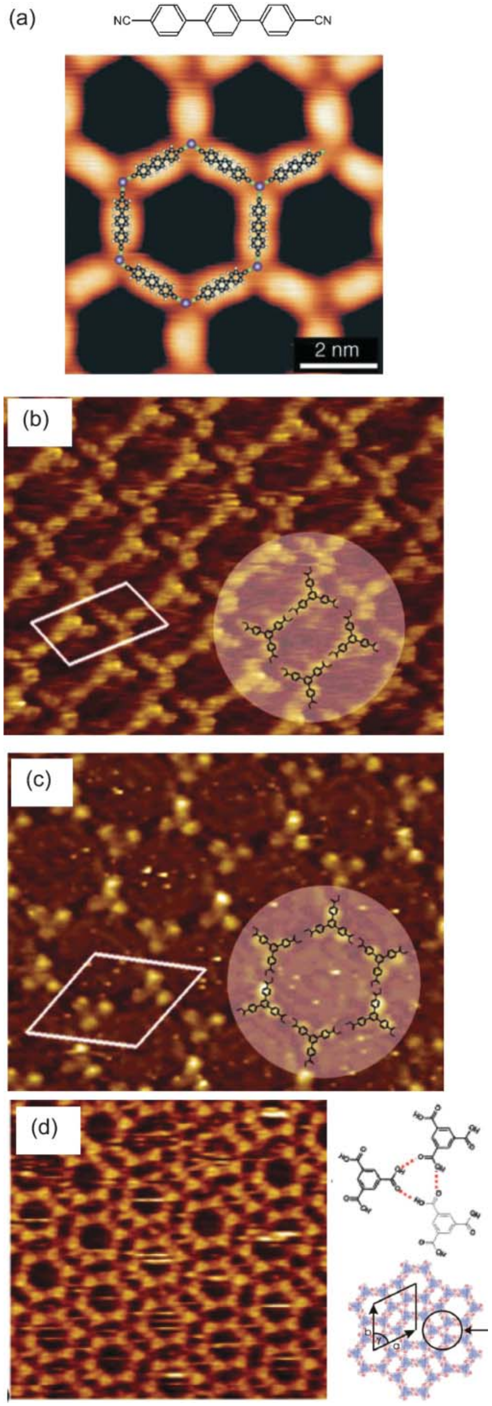

Fig. 37 STM (scanning tunneling microscopy) images of self-assembled monolayers of periodic 2D grids of a metal–organic frame and hydrogen-bonded frames on surfaces: (a) Co–4,4″-dicyano-*p*-terphenyl on Ag(111) deposited under UHV.[138] Reprinted with permission from *Angew. Chem., Int. Ed.*, 2007, **46**, 710–713. Copyright 2007, Wiley-VCH. (b) 1,3,6-Benzenetribenzoic acid on HOPG(0001) with an oblique unit cell as obtained from heptanoic acid and decanol. (c) Honeycomb as obtained from nonanoic acid and 1-phenyloctane as solvents.[147] Reprinted with permission from *J. Phys. Chem. B*, 2006, **110**, 10829–10836. Copyright 2006, American Chemical Society. (d) Flower structure of 1,3,6-benzenetricarboxylic acid on HOPG as obtained from pentanoic acid. Reprinted with permission from *Langmuir* 2005, **21**, 4984–4988. Copyright 2005, American Chemical Society.

these solvents to fill the empty spaces in the nets (but the space filling seems to be less important than in non-supported structures).[147] 1,3,6-Benzenetribenzoic acid, for example, can organize into an array of rectangular cavities with oblique lattice or into a hexagonal honeycomb on highly oriented pyrolytic graphite (HOPT), depending on the used solvent (see Fig. 37(b) and (c)).[147] Similarly, a solvent dependent change from a hexagonal grid to a complex (3.4.6.4) tiling pattern composed of hexagons, rectangles and triangles (flower structure) on increasing the polarity of the solvent was observed for 1,3,6-benzene tricarboxylic acid (trimesic acid, see Fig. 37(d)).[143]

Moreover, similar to the observations made for T-shaped ternary amphiphiles, where formation of LC polygonal cylinder phases is even possible with facial amphiphiles, interconnected by the relatively weak van der Waals forces between alkyl chains, also grids on solid surfaces can be obtained by self assembly mediated by alkyl chains. For example, flat rhombic or triangular aromatic cores, functionalized at the corners by alkyl chains can organize with formation of 2D grids where the aromatic cores are located at the nodes and the interdigitated linear alkyl chains form the nets interconnecting these nodes (see Fig. 38).[148,149] Depending on the shape of the aromatic core, which determines the direction of the alkyl chains, this gives raise to two different structures, the Kagome (rhombic π-system) and the hexagonal honeycomb (triangular π-system). The dense packing of the rhombic nodes of compound **1** represents the [3.6.3.6] Laves tiling and the resulting net structure is the dual of this structure, the Archimedean (3.6.3.6) tiling, representing the Kagome pattern (see Fig. 21(f) and Fig. 38(a)). Similarly, for the triangular π-systems of compound **2** close packing would give the [6^3] Laves tiling of triangles and the observed structure is a hexagonal net corresponding to the (3^6) Archimedean tiling (see Fig. 21(a) and Fig. 38(b)). This dual relationship between node geometry and net-topology is a general feature of all 2D nets and polygonal cylinder structures,[150] provided that there is a sufficient directionality of the interaction between the nodes and that there are no other competing forces, as incommensurate interaction with the substrate. For example, these net structures are lost by elongation of the alkyl chains which gives rise to chain-like superstructures (smectic-like 2D organizations).[149] This is assumed to be due to the increasing dominance of the interactions with the surface lattice of graphite, which for long chains organized in the cyclic structures, would lead to a misalignment of the chains with the main symmetry axis of graphite.

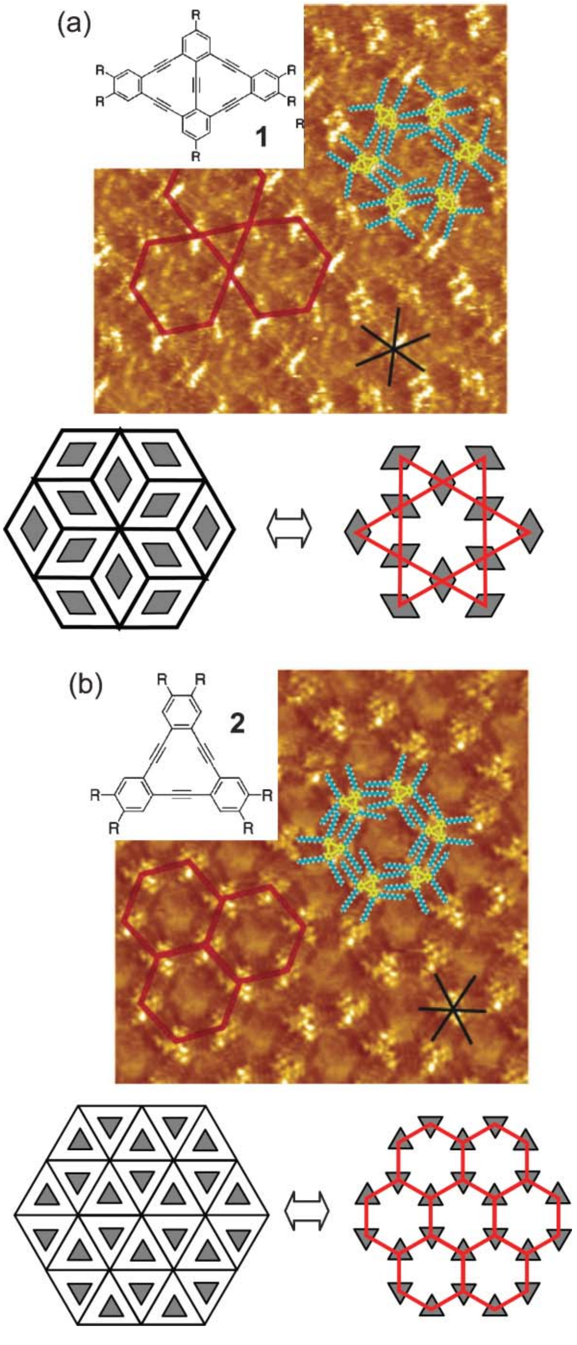

Fig. 38 STM images of self-assembled monolayers of periodic 2D grids formed on pyrolytic graphite by van der Waals interaction between alkyl chains: (a) The rhombic molecule **1** forms a 2D Kagome which is the topological dual of the tiling provided by the close packing of rhombs and. (b) The triangular molecule **2** forms a 2D hexagonal grid which is the dual of the close packing of triangles ($R = n\text{-}C_{10}H_{21}$).[148] Reprinted with permission from *J. Am. Chem. Soc.*, 2006, **128**, 3502–3503. Copyright 2006, American Chemical Society.

3.5 Periodic protein structures

It is known that nanotubes can be formed by self-assembly of cyclic peptides through formation of intermolecular hydrogen bonds between functional groups in the peptide backbones.[6,151] Much larger nanotubes can be formed by amphiphilic surfactant-type peptides and bolamphiphilic peptides. Dipeptides formed by amino acids with hydrophobic residues have recently emerged as an unexpected source of stable microporous solid state materials based on the hydrogen bond formation of the peptide backbone and the aggregation of the hydrophobic entities in the side chains.[152] Depending on the amino acids involved in these dipeptides either the hydrogen bonding network between the peptide or the lipophilic residues form the cylinder walls. The other part forms the inner surface of the hollow cylinders with distinct shapes which are filled by appropriate solvent molecules. Here, the rigidity of the highly directional crystalline hydrogen bonding networks of the peptide backbones and the packing of the hydrophobic residues provide the necessary molecular information for this type of self assembly with formation of well defined hexagonal or square cylinders (see Fig. 39(a–c)). This example clearly shows that segregation of incompatible units and the curvature of the resulting interfaces due to steric factors are also dominating in the self assembly of solid crystals and hence they are of significant importance for crystal engineering.[135,136]

The Kagome motif formed by Leu-Ser (Fig. 39(d)) is especially remarkable, as it represents a complex self-organized two colour tiling built up by hexagonal tiles containing the *iso*-butyl groups of Leu and triangular tiles filled by the CH_2 groups of the serine side chains in a (3.6.3.6)-net formed by the peptide backbones and the OH groups of Ser.[152]

Formation of hollow cylinder structures was also observed for dipeptides functionalized with lipophilic dendrons, leading to columnar LC structures with a regular (mostly hexagonal) organization of the peptide cylinders in the lipophilic continuum formed by the dendrimers shells.[153]

3.6 Periodic arrays of organic frames and covalently connected nets

Also covalently connected 2D-nets and polygonal honeycombs formed by on-top stacking of these nets have been reported. For example, solid state organic materials formed by polycondensation of rod-like difunctional boronic acids and hexahydroxytriphenylene form covalently connected rigid hexagonal grids which stack into non-interpenetrated hollow cylinder networks (see Fig. 40).[154] It was reported that these solid state materials retain their nanoporous structure even after removing the solvent and the resulting materials have a gas storage capacity superior to inorganic zeolites.

Also discrete macrocycles, where rigid units are interconnected by covalent bonds can self-organize into periodic polygonal cylinder structures in solid structures, as for example shown by Stoddart and co-workers for square shaped cyclophanes.[155] In this case charge transfer interactions between donor and acceptor sides of these squares lead to a stacking of these molecular squares into square channels (filled by counter ions and guest molecules) and the packing of these channels into a (slightly distorted) square cylinder network (see Fig. 41). Other self-assembled organic nanotubes were recently reviewed.[151]

Also shape-persistent macrocycles with a hexagonal shape give a variety of highly ordered packing motifs in the solid state.[114] Macrocycles based on a hexagonal frame, functionalized at the corners with OH groups organize in the crystalline state into 2D hexagonal networks by H-bonding between the OH groups and the 2D layered structures stack on top of each other, leading to extended channels, as shown in Fig. 42(a).[156]

There is some relation of these hexagonal honeycombs to the polygonal honeycombs formed by the bolaamphiphiles as the channel walls are formed by π-systems and the structure is held together by hydrogen bonding. However, due to the covalent fixation of the aromatics in the hexagonal frames there is no dynamics in this structure and the type of the channels is fixed by the shape of the cyclic frames. Though some shape persistent macrocycles functionalized with long

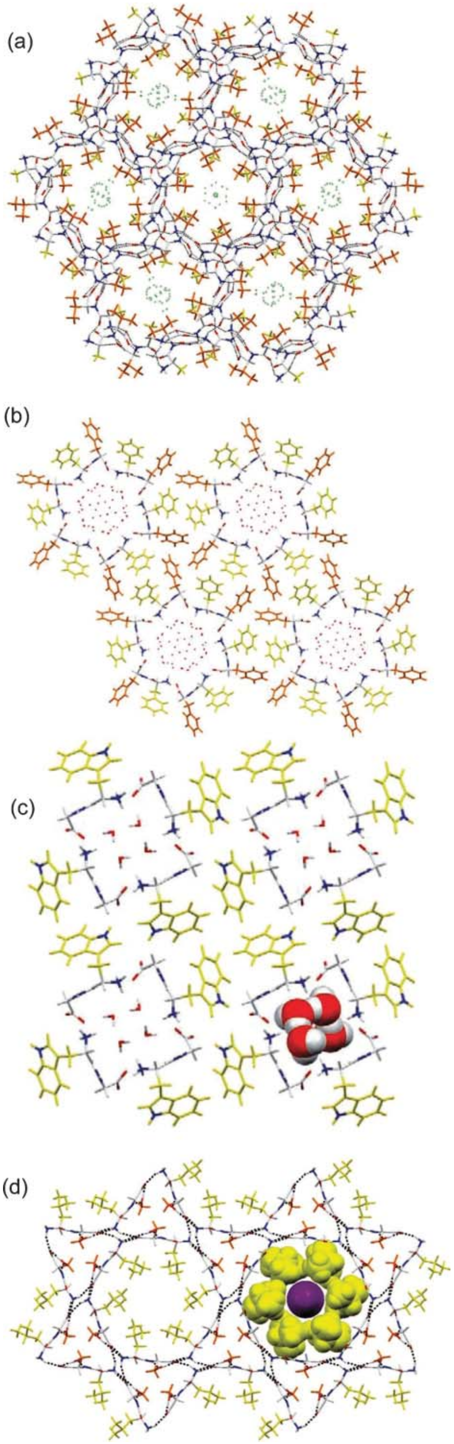

Fig. 39 Crystal packing arrangements of hydrophobic dipeptides (blue: peptide backbones, yellow and red: hydrophobic residues): (a) Ala-Val 2-propanol hydrate (hexagonal structure where the hydrogen bonding of the peptide backbone forms the hexagonal honeycomb); (b) Phe-Phe and (c) Trp-Gly (reversed structures where the aromatic substituents form the cylinder walls of the hexagonal and square honeycombs, respectively); (d) Kagome-like structure of Leu-Ser.[152] Reprinted with permission from *Chem.–Eur. J.*, 2007, **13**, 1022–1031. Copyright 2007, Wiley-VCH.

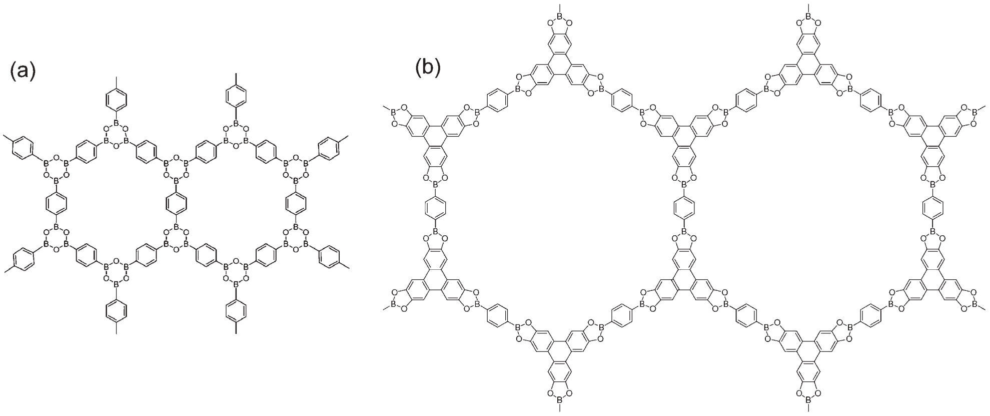

Fig. 40 Covalent hexagonal grids formed (a) by benzene 1,4-diboronic acids anhydride and (b) by reaction of hexahydroxytriphenylene with benzene 1,4-diboronic acid.[154]

alkyl chains can form columnar and nematic LC phases in addition to the crystalline phases (see Fig. 42(b)), none of these LC phases represents a polygonal cylinder structure as observed for the T-shaped polyphiles.[157] This raises the question concerning the general requirements for molecular self assembly into periodic lattices of polygonal cylinder in the LC state.

3.7 Requirements for formation of self-assembled periodic arrays of uniform and structurally persistent structures in soft matter

As shown above, periodic polygonal pattern are quite common in solid state structures where the close packing of the molecules at fixed positions gives rise to numerous strong and weak interactions defining the organization of the molecules. As the molecular mobility is increased by enhancing the temperature the weak interactions break and only the strong interactions remain, which dominate the liquid state superstructures (micelles, LC phases, *etc.*). These remaining strong structure-forming forces, necessary for the self assembly in soft matter structures, are provided by nanoscale segregation of incompatible molecular parts, by parallel alignment of anisometric rigid units and by strong cohesive intermolecular interactions, such as hydrogen bonding and Coulomb forces. Small amphiphiles without rigid segments organize into layer-like, cylindrical or spherical aggregates as shown in Fig. 2. As the size of molecules is small the aggregates contain a rather large number of molecules and the organization of the individual molecules can easily follow the curvature required by the aggregate surfaces. In contrast, larger amphiphiles lead to aggregates with only few molecules organized in the cross section. Though the organization still requires minimization of the interfaces, the shape of the amphiphiles and specific intermolecular interactions between the peripheries of these molecules can in this case give rise to aggregates composed of a well defined number of molecules with a specific shape. For example, the two amphiphiles shown in Fig. 43 form micelles with uniform polyhedral shapes.[158–161]

For the same reasons the organization of the linear aromatic cores of the T-shaped amphiphiles into columnar aggregates leads to cylinders with well defined polygonal cross section. These polygonal cylinders can only assemble into polygonal honeycombs if the rotation around their long axis is frozen, because this rotation would average out the specific shape of

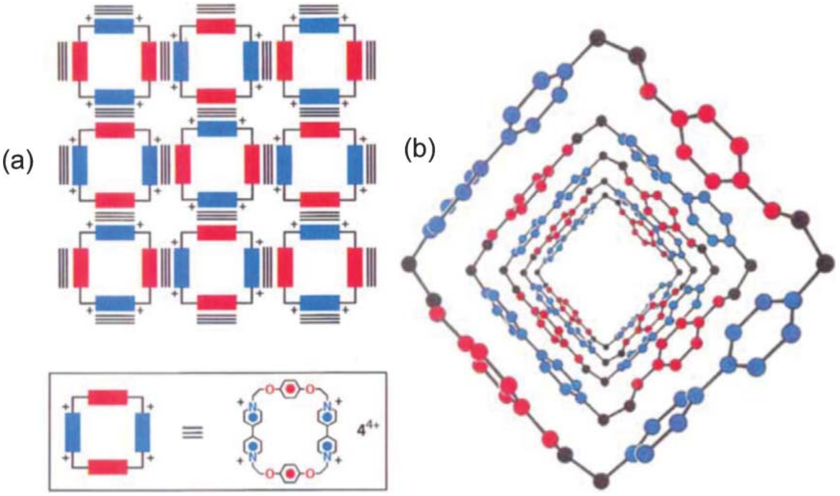

Fig. 41 Cyclophane based square channel solid state structure based on donor–acceptor interactions.[155] Reprinted with permission from *Angew. Chem., Int. Ed. Engl.*, 1995, **34**, 1862–1865. Copyright 1995, Wiley-VCH.

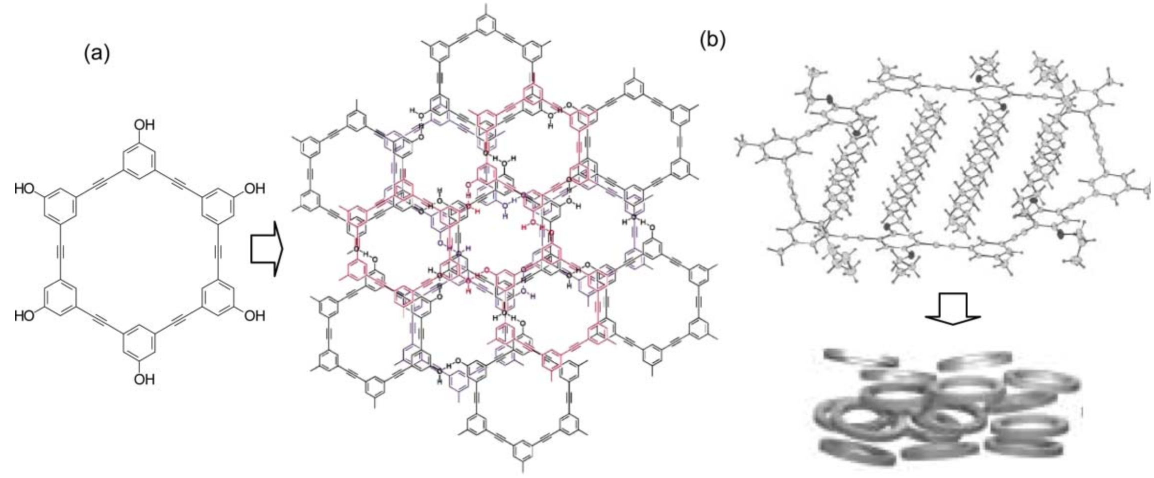

Fig. 42 Selected shape-persistent macrocycles: (a) OH functionalized macrocycle which organizes into a hexagonal 2D grids by hydrogen bonding at the corners (peripheral OH groups are not shown) and stack into a hexagonal honeycomb solid state structure[114,156] Reprinted with permission from *Chem. Commun.*, 2003, 807–818. Copyright 2003, The Royal Society of Chemistry. (b) Hexagonal frame filled by the attached alkyl chains (crystals structure) which organizes into a nematic LC phase.[157] Reprinted with permission from *Angew. Chem., Int. Ed.*, 2000, **39**, 2267–2270. Copyright 2000, Wiley-VCH.

these cylinders (see Fig. 44(b)) and this would lead to a packing in a hexagonal lattice. However, the segmented ABA structure along these aromatic cores gives rise to a sufficiently strong segregation of the aromatic cores (B) and the terminal groups (A) which disfavors any rotational disorder of these cylinders (see Fig. 44(c)). The segregated end-groups (A) fuse the individual cylinders edge-to-edge and side-by-side into periodic polygonal honeycomb structures with symmetries defined by the shape of the individual cylinders. If this segregation is lost, then non-honeycomb Col_{hex} phases are formed (see Section 4.2).

3.8 Nanoparticle arrays

Similar to rod-like molecules, also anisometric nanoparticles can form nematic, smectic and columnar LC phases in solvents, depending on the concentration of these particles and their length to diameter ratio.[162,163] Recently, semiconductor rods were functionalized with gold caps at both ends.[164,165] Such "bolaamphiphilic" nanoparticles could possibly also be able to self assemble into polygonal grids or honeycombs. It should also be mentioned that the pioneering work of Whitesides and co-workers have shown that also macroscopic polygonal objects can self-organize into well defined periodic pattern and into functional devices by means of capillary forces between the edges.[166]

3.9 Quasiperiodic tiling pattern

All tilings found so far in LC polygonal cylinder phases, DNA nanostructures and crystalline nets are periodic. The formation of 2D quasiperiodic pattern (see Fig. 45) was achieved by holographic patterning of mixtures of LC's and polymers with three and more coherent laser beams.[167] However, these structures were only formed under the influence of the external stimuli and once formed they were fixed by photochemical polymerization.

Spontaneous formation of 3D quasiperiodic order has been found in arrays of spherical atoms in few metal alloys.[168] Very recently quasicrystalline organization was also observed in a self-organized soft matter system (liquid quasi crystal = LQC) formed by spherical dendrimer aggregates.[67,68] Interestingly, the organization of these spheroidic aggregates can be described as an array of sparsely and densely populated layers and the sparse layers are made up of a mixture of squares and triangles, but these are tiled in a quasiperiodic rather than truly periodic manner.

Calculations also proposed the possibility of a quasiperiodic organization in the morphology of ABC triblock star polymers[169] with a tiling pattern composed of triangles and squares with the ratio of triangles to squares of 2.309 ($= 4 : \sqrt{3}$). A star-shaped ABC triblock copolymer was recently synthesized which shows a triangle to square ratio of 2.305 which is very close to this theoretical value. The morphology of this polymer is composed of regions with a $(3^2.4.3.4)$ tiling corresponding to a 2/1 ratio of triangular and square tiles (*p*4*gm*) and regions with an 8/3 ratio and 6-fold symmetry (*p*6*mm*) as well as transition regions between them (see Fig. 46). For this polymer a diffraction pattern (microbeam X-ray) was obtained which was interpreted as a kinetically frozen tiling pattern with dodecagonal symmetry and quasicrystalline order of few micrometers.[170]

The Penrose tiling[171] (see Fig. 47), consisting of two different types of rhombic tiles, is another example for a uniform tiling pattern with long range translational and orientational order, but without periodicity. The Fourier transform of the Penrose tiling pattern has pentagonal symmetry. However, quite a lot of molecular design has to be done to obtain a thermodynamically stable 2D-grid or 2D-honeycomb structure with a long range quasiperiodic order.

4 Novel types of liquid crystalline non-cylinder phases

Polygonal cylinder phases represent the majority of new mesophase morphologies formed by T-shaped ternary amphiphiles. However, also several distinct non-cylinder phases can

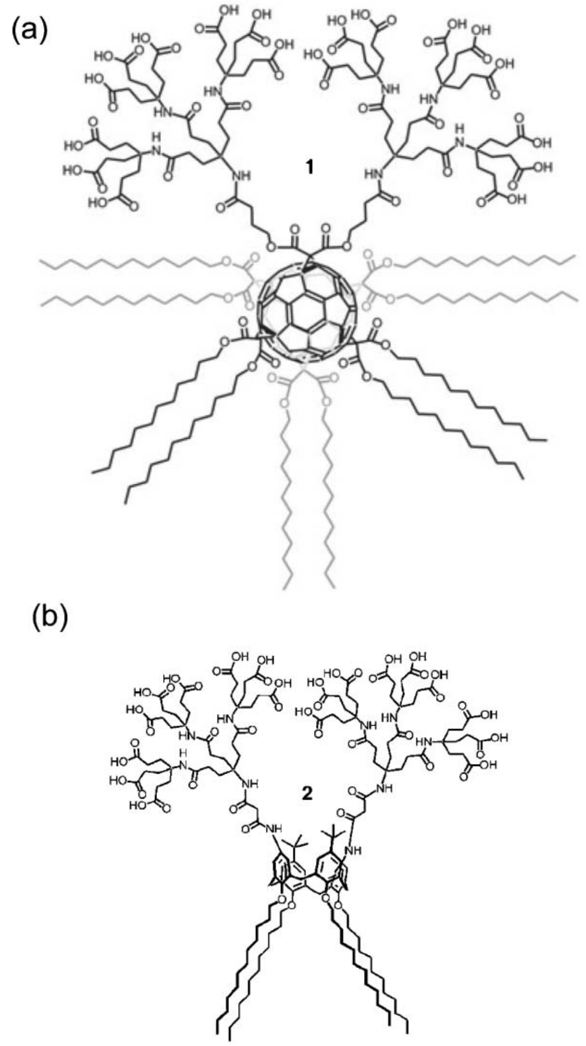

Fig. 43 Amphiphilic fullerene and calixarene derivatives with dendritic branches forming structurally persistent micelles.[158] Reprinted with permission from *Angew. Chem., Int. Ed.*, 2005, **44**, 2976–2979. Copyright 2005, Wiley-VCH.

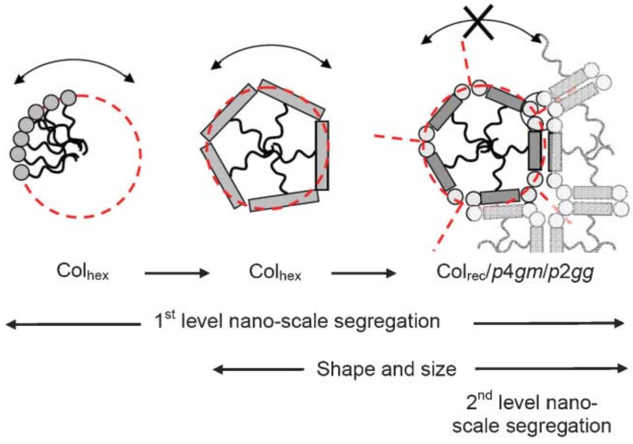

Fig. 44 Development of aggregate shape and regular packing motifs by increasing the molecular complexity, explained for the transition from Col$_{hex}$ phases formed by rotationally disordered columns to LC pentagonal cylinder phases.

be found and the occurrence of these structures can have different reasons. At first, bulky lateral substituents which cannot be accommodated in a cylinder structure give rise to removal of some cylinder walls and to a transition to layer structures (Lam phases, see Fig. 15).[48–52] Polygonal honeycomb structures can also be lost if the segregation between the rods and the terminal groups becomes weak,[46] which leads to a nematic-like organization of the rod-like cores and destroys the distinct polygonal shape of the cylinder frames. In all polygonal cylinder phases of the T-shaped amphiphiles the aromatic cores are arranged perpendicular to the cylinder main axis. Hence, another source of mesophase diversity arises from a change of the direction of the rod-like cores with respect to the nano-segregated columns.[46]

4.1 Lamellar phases

T-shaped ternary bolaamphiphiles with extremely large lateral substituents form a novel type of lamellar phases (Lam).[48–52] In these mesophases the lateral chains are too large to enable the formation of cylinder structures; instead these chains fuse to infinite layers which are separated by layers containing the aromatic cores and the polar groups. Within the layers of the lateral chains these chains are strongly disordered (liquid-like), but with a certain preferred direction either perpendicular (nonbranched chains) or parallel (branched chains) to the layer planes. For bolaamphiphiles with comparatively long alkyl spacers between the laterally attached fluorinated segment and the rigid core triple layer structures composed of aliphatic, aromatic and perfluoroalkyl sublayers are formed. Some bolaamphiphiles (see Fig. 12, $n' = 15$) show a temperature dependent transition from giant cylinder phases at low temperature to these lamellar mesophases at high temperature.[46,48]

Three distinct lamellar phases were observed depending on the temperature and these phases can be distinguished by the order within the aromatic sublayers. In the high temperature Lam$_{Iso}$ phase (Fig. 48(a)) the rod-like cores are organized in hydrogen bonded clusters which are completely disordered within their sublayers. At reduced temperature these clusters grow in size and the rod-like cores adopt a long range orientational order within the layers as well as an organization parallel to the layer planes. In adjacent layers the direction of the rod-like cores is parallel, *i.e.* there is an orientational correlation between adjacent layers (Fig. 48(b)).[48,50,51,172,173] This organization of the rod-like units parallel to the layer planes distinguishes these lamellar phases from conventional smectic phases, where the rod-like units are arranged on average perpendicular (SmA) or uniformly tilted with respect to the layer planes (SmC).[174] It can be regarded as a lamellar phase built up by thin layers with cybotactic nematic order,[175] separated by isotropic layers of the lateral chains and therefore this mesophase is designated as *lam*inated *n*ematic (Lam$_N$) phase.

Upon further cooling, the clusters fuse to infinite stripes and hence, an additional periodicity occurs within the aromatic sublayers (Fig. 48(c)). This lamellar phase is built up of thin layers with SmA-like in-plane order (perpendicular to the layer periodicity), separated by the isotropic layers formed by the lateral chains. In these LC phases there are two distinct

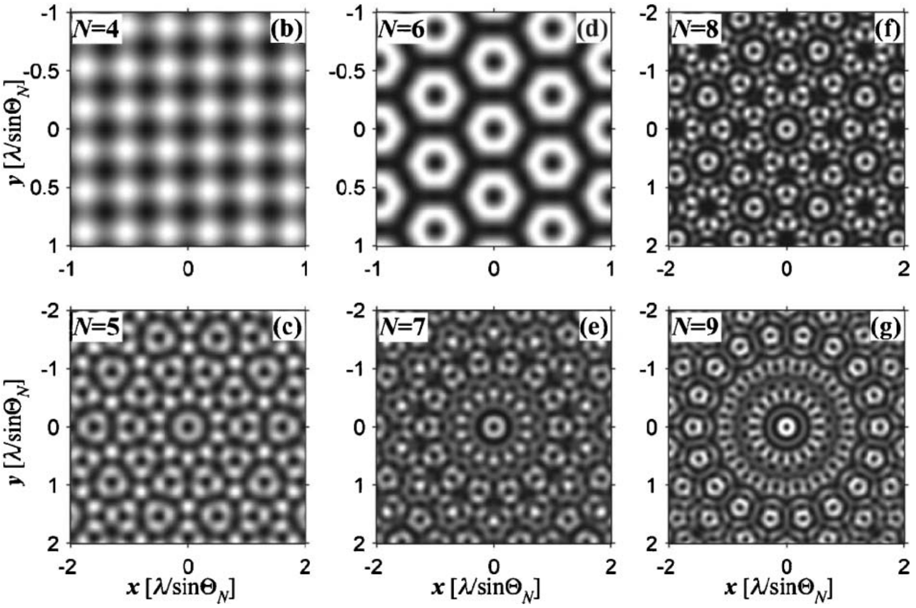

Fig. 45 Periodic ($N = 4, 6$) and aperiodic patterns ($N = 5, 7–9$) as obtained by holographic patterning of a LC/polymer mixture with a number of N coherent laser beams.[167] Reprinted with permission from the article: "*Holographic photonic crystals*", M. J. Ecuti and G. P. Crawford, *Opt. Eng.*, 2004, **43**, 1973–1987. Copyright 2004, International Society for Optical Engineering, SPIE.

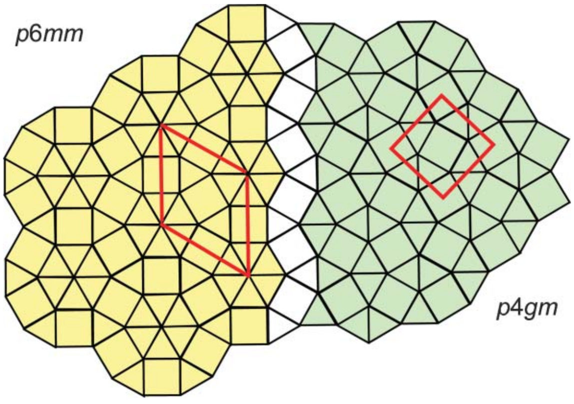

Fig. 46 Two types of triangle/square tiling pattern with different ratio of triangles to squares: yellow = 8/3 tiling (*p*6*mm*); green = 2/1 tiling (*p*4*gm*) with the transition region shown in white as seen for a star-shaped triblock copolymer (in addition there are different orientations of the lattices which are not shown).[170]

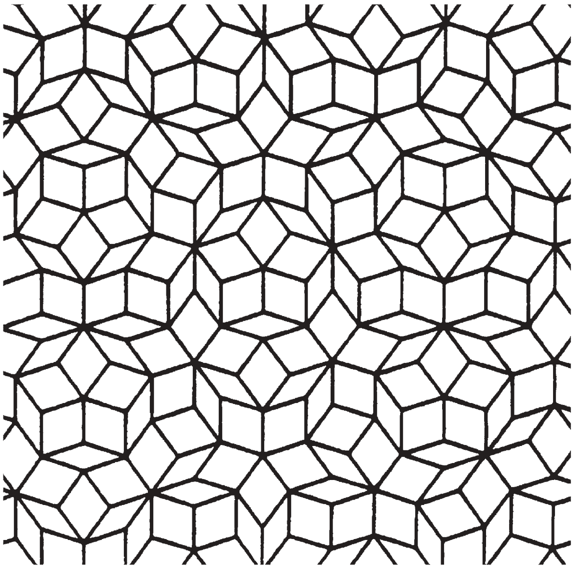

Fig. 47 Penrose tiling pattern.

periodicities, one is provided by the layer distance and is mainly determined by the length of the lateral chains, and the second one is parallel to the layer planes and it is determined by the length of the bolaamphiphilic cores. If there is only an orientational correlation, but no long range positional correlation between adjacent layers, this phase is assigned as $\mathrm{Lam}_{\mathrm{Sm}}$. If in these $\mathrm{Lam}_{\mathrm{Sm}}$ phases a long range correlation of the periodicities in adjacent layers occurs, then lamellar phases with a 2D lattice are obtained.[52] An AA-type correlation of adjacent layers leads to a non-centered rectangular 2D lattice ($\mathrm{Lam}_{\mathrm{Sm\text{-}rec}}$/*p*2*mm*), shown in Fig. 49(c) and (d), whereas an AB stacking would give rise to a centered rectangular 2D-lattice ($\mathrm{Lam}_{\mathrm{Sm\text{-}rec}}$/*c*2*mm*). These mesophases are assigned as correlated lamellar phases and combine features of columnar phases (2-D lattice, optical textures) and lamellar phases (periodic stacking of layers) and therefore these phases can also be regarded as a special type of lamello-columnar phases. The subscript "lam" in the phase assignment distinguishes these mesophases with 2D lattice from other columnar phases and polygonal cylinder phases.

For bolaamphiphiles with branched lateral chains consisting of an alkyl and a perfluoroalkyl branch (see formula in Fig. 49) the occurrence of a non-centered lattice (*p*2*mm*) is assumed to be due to the formation of nano-segregated cylinders containing the fluorinated segments, organized within the aliphatic sublayers (see Fig. 49(c)).[52] Hence, there are similarities to *cylinder-in-lamellae* (Fig. 49(a)) and *cylinder-on-lamellae* morphologies (Fig. 49(b)) found for linear ABC triblock

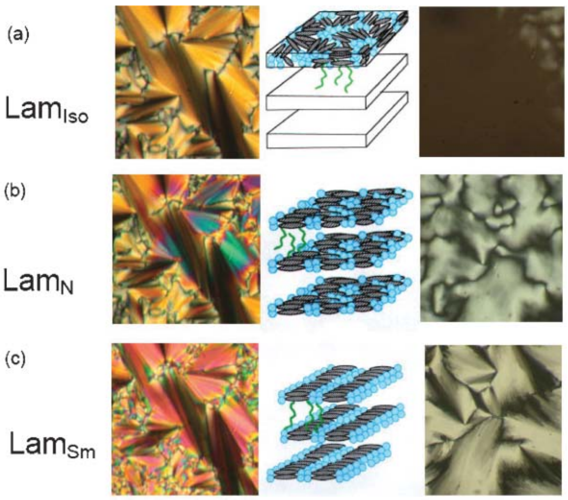

Fig. 48 Textures of the Lam phases as seen between crossed polarizers (left: alignment of the layer is perpendicular to the substrate surfaces, at the right it is parallel, view is perpendicular to the substrate surfaces) and models of the organization of the molecules.[51] Reprinted with permission from *J. Am. Chem. Soc.*, 2002, **124**, 12072–12703. Copyright 2002, American Chemical Society.

copolymers.[29,88,93,176,177] The same sequence of lamellar phases is also observed in the series of bolaamphiphiles shown in Fig. 50 (*n* = 8–12) where one of the propane-2,3-diol groups is replaced by a single phenolic OH group.[49]

In contrast, in the series of facial amphiphiles with longer terphenyl rigid cores, these lamellar phases are more difficult to achieve. In this case very bulky lateral chains would be required which are difficult to obtain by chemical design. For these compounds $\mathrm{Lam_{Iso}}$ and $\mathrm{Lam_N}$ phases were obtained only by addition of polar solvents which swell the lateral chains, as explained in Section 5.[46]

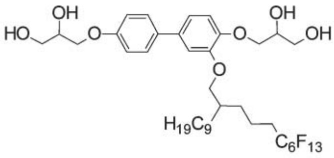

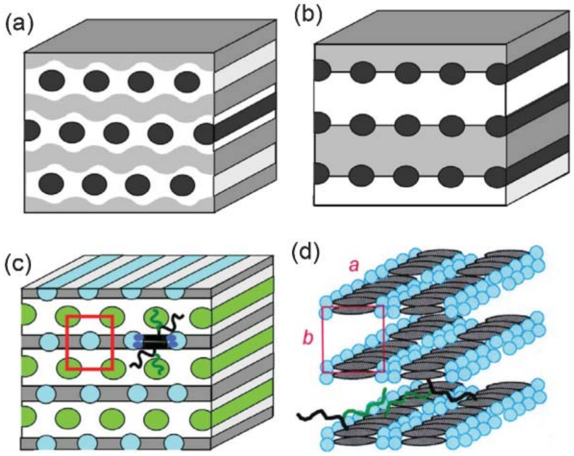

Fig. 49 Soft-matter structures combining lamellar and columnar organizations: (a) *cylinder-in-lamellae* morphology and (b) *cylinder-on-lamellae* morphology of linear ABC triblock copolymers;[29] (c), (d) correlated layer structure with *p*2*mm* lattice ($\mathrm{Lam_{Sm\text{-}rec}}/p2mm$ phase) as formed by bolaamphiphiles with a branched lateral chain (see formula).[52]

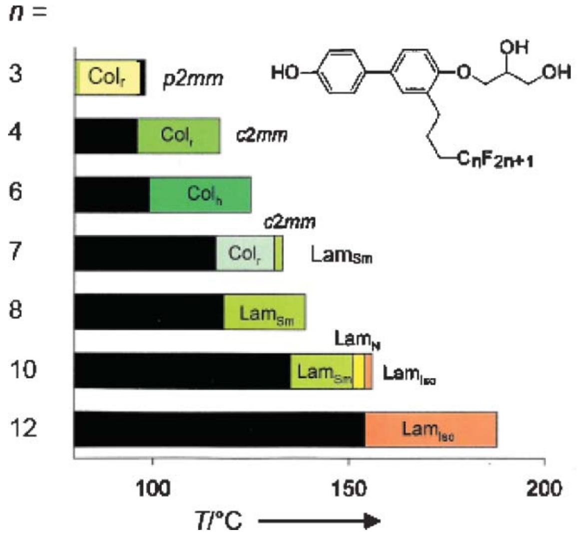

Fig. 50 Dependence of the liquid crystalline phases of the series of bolaamphiphiles with only one diol group, depending on the length of the semiperfluorinated lateral chain. $\mathrm{Col_h} = \mathrm{Col_{hex1(6)cyl\text{-}6}}/p6mm$, $\mathrm{Col_r}/p2mm = \mathrm{Lam_{Sm\text{-}rec}}/p2mm$ phase, the $\mathrm{Col_{rec}}/c2mm$ phases of compounds with *n* = 4 and *n* = 7 are slightly distorted hexagonal honeycombs (see Fig. 51(b) and (d) for the models). The monotropic low temperature phases $\mathrm{Col_{rec1(6)cyl\text{-}8}}/c2mm$ (for *n* = 7) and $\mathrm{Lam_N}$ (for *n* = 12) are not shown.[49] Reprinted with permission from *J. Am. Chem. Soc.*, 2004, **126**, 12930–12940. Copyright 2004, American Chemical Society.

4.2 Slightly deformed hexagonal cylinders and hexagonal arrays of columns in a nematic-like continuum

The strength of segregation of terminal groups and rod-like cores within the cylinder frames has also a significant impact on the mesophase structures. For the bolaamphiphiles with only one diol group and a phenolic OH group at the other end the incompatibility between aromatic cores and polar end groups is reduced and also the attractive hydrogen bonding is weaker (see Fig. 50). In this series of compounds the hexagonal LC cylinder phase is the only stable cylinder structure (*n* = 6).[49] Molecules with longer chains (*n* = 7) form centred rectangular columnar phases (*c*2*mm*) comprised of hexagonal cylinders slightly stretched along a diagonal (see Fig. 51(d)) whereas molecules with shorter chains (*n* = 4) form hexagonal cylinders slightly stretched along the normal to two of the sides (see Fig. 51(b)), *i.e.* the hexagonal lattice is slightly distorted, leading to *c*2*mm* symmetry for both phases. In contrast to the giant cylinder phases, the distortion is only small and there are no cylinder walls formed by discrete dimers. Due to the weaker segregation and strength of the hydrogen bonding the framework structure becomes weaker and the position of the molecules in the cylinder frames is less well defined. Therefore, the desire of the non-polar columns to adopt a dense packing in a hexagonal organization (minimization of

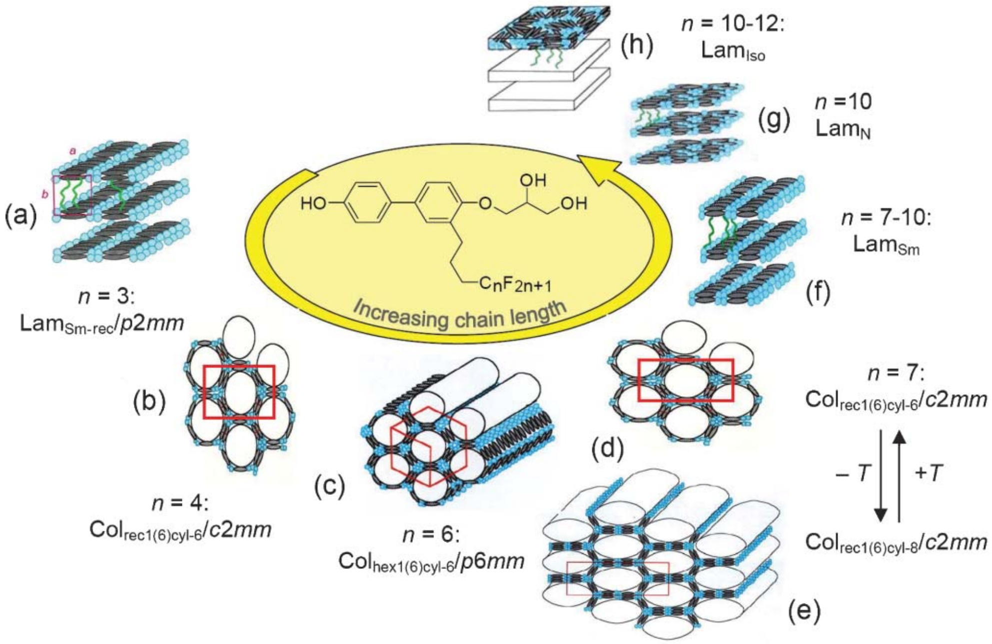

Fig. 51 Phase sequence of the bolaamphiphilic molecules with only one diol group depending on the chain length.[49] Reprinted with permission from *J. Am. Chem. Soc.*, 2004, **126**, 12930–12940. Copyright 2004, American Chemical Society.

the excluded volume) becomes the dominating structure determining force. As a result networks composed of cylinders with a smaller or larger number of sides are suppressed and hexagonal cylinders are maintained, but these cylinders become slightly deformed. For molecules with reduced side chain length the pentagonal cylinder phase is replaced by a hexagonal cylinder phase stretched along the normal to two sides. The square lattice, expected for the shortest chains, is bypassed by adopting a correlated layer structure instead (n = 3, $\mathrm{Lam}_{\text{Sm-rec}}/p2mm$). Therefore, the unique phase sequence, shown in Fig. 51, with regular and slightly deformed hexagonal cylinder phases occurring between lamellar phases is observed.[49] Because the segregation increases with decreasing temperature well defined cylinder structures can appear at low temperature. For example, the giant hexagonal LC cylinder phase with 8 molecules in the circumference ($\mathrm{Col}_{\mathrm{rec1(6)cyl\text{-}10}}/c2mm$) is observed at reduced temperature for the compound with n = 7 (see Fig. 51(e)) below the slightly stretched hexagonal cylinder phase (Fig. 51(d)).

In the series of the facial amphiphiles, the incompatibility between rigid cores and terminal alkyl chains can be tuned in a more systematic way by changing the length of these chains (see Fig. 52). For molecules with relatively short terminal alkyl chain a transition from the pentagonal LC cylinder phase ($\mathrm{Col}_{\mathrm{squ2(5)cyl\text{-}5}}/p4gm$) to a hexagonal columnar phases takes place by rising the temperature. In this $\mathrm{Col}_{\mathrm{hex}}$ phases the segregation of the aromatic cores from the alkyl chains is strongly reduced and the aromatic cores can nearly freely rotate around the polar columns.[178] Hence, the hexagonal organization is not based on a polygonal honeycomb organization, rather then it is due to the dense packing of the polar columns in a continuum. In this continuum, the rod-like cores retain an alignment nearly perpendicular to the column long axis, as indicated by the negative birefringence of this mesophase. This type of hexagonal columnar phase (Fig. 52(i)) is assigned herein as $\mathrm{Col}_{\mathrm{hex}}{}^{1}$. A temperature dependent inversion of the sign of birefringence within the temperature range of the $\mathrm{Col}_{\mathrm{hex}}$ phase can be observed in some cases where upon further increasing the temperature the sign of the birefringence becomes positive, which means that the terphenyl cores become aligned predominately parallel to the polar columns ($\mathrm{Col}_{\mathrm{hex}}{}^{2}$, Fig. 8, n = 4).[46] Hence, in the continuum between the polar cylinders there is a preferred parallel (''nematic-like'') order of the terphenyl cores as shown in Fig. 52(k) ($\mathrm{Col}_{\mathrm{hex}}{}^{2}$ phase). At the $\mathrm{Col}_{\mathrm{hex}}{}^{1}$ to $\mathrm{Col}_{\mathrm{hex}}{}^{2}$ transition a continuous change of the nematic director from perpendicular to parallel to the columns takes place.

The vacillating alignment of terphenyl mesogens in the $\mathrm{Col}_{\mathrm{hex}}$ phase is an indication of the frustration caused by two opposing tendencies: one for the alkyl chains to phase separate in discrete columns, and the other to maximize the interaction between mesogens by allowing them to form a nematic-like continuum with the director parallel to the columns. For facial amphiphiles with short terminal chains the latter tendency prevails at enhanced temperature, *i.e.* microphase separation is abandoned and nematic-like alignment is achieved. This is due to the stepwise loss of segregation between the alkyl chains and aromatic cores. It thus seems that segregation of aromatic and aliphatic parts may not be completely lost at the $\mathrm{Col}_{\mathrm{squ2(5)cyl\text{-}5}}/p4gm$ to $\mathrm{Col}_{\mathrm{hex}}{}^{1}$ transition and locally residues of the cylinder shells remain. These residual pentagonal or hexagonal clusters are rotationally disordered around the polar columns. Upon heating, these clusters decrease in size and the excluded volume effect becomes more dominating, giving rise to an average alignment of the terphenyls closer to parallel to the column axis, leading to positive birefringence ($\mathrm{Col}_{\mathrm{hex}}{}^{2}$ phase).[46]

Considering the arrangement of the micro-segregated columns in these mesophases, there is some relation to the

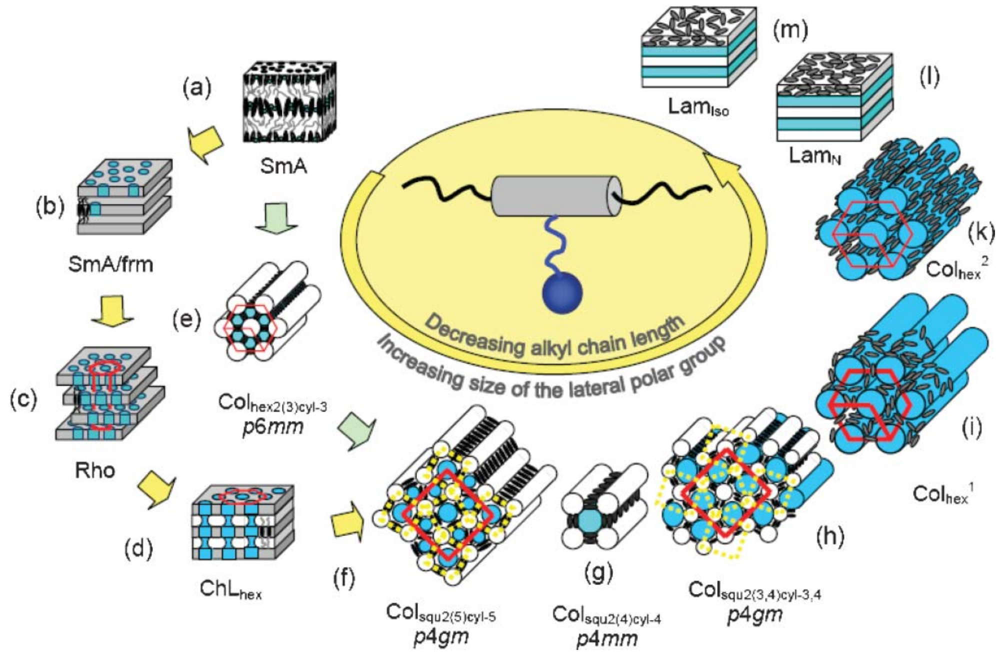

Fig. 52 Phase sequence of the facial amphiphiles with increasing size of the lateral substituent and decreasing length of the terminal alkyl chains.[46]

self organization of rigid main-chain polymers with flexible lateral chains (hairy rods) which is discussed in the next section.

Organizations of columns in a nematic continuum were also reported for oligomesogens in which rod-like units are laterally connected to an oligosiloxane or silsesquioxane branching point (see Fig. 53) which exhibit Col$_{hex}$ and Col$_{rec}$ phases below a nematic or chiral nematic phase.[179,180] These columnar phases are formed due to the segregation of the silyl units into distinct columns and the organization of these columns into a 2D lattice. As the aromatic cores are comparatively long and the terminal alkyl chains are relatively short, the parallel alignment prevails over rigid–flexible segregation. Hence, the aromatic cores are organized in a nematic (or cybotactic nematic) continuum with the nematic director parallel or slightly tilted to the column long axes. Also in the nematic phases of these polypeds the segregated siloxane containing cylinders seems to be present, but without long range positional correlation.

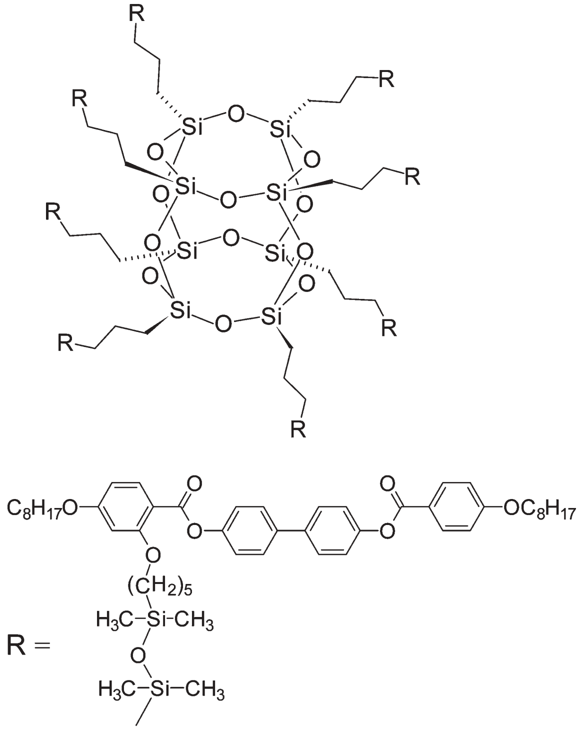

Fig. 53 Example of a LC polyped.[179]

4.3 LC phases of rod-like polymers with lateral chains

Rigid polymers (polyvinylacetylenes, polyphenylenevinylenes, polyfluorenes, polythiophenes, *etc.*) become of increasing interest as semi-conducting, photo-conducting and electroluminescent organic materials.[2,3] These polymers were functionalized with lateral alkyl chains, polyether chains, fluorinated chains or dendritic brushes in order to increase their solubility and processibility and to reduce their melting temperatures. Many of these polymers are capable of forming thermotropic and lyotropic LC phases. The LC states of these polymers are of significant interest, as they can be used to organize these materials in a defined way, as required for their use in functional devices. The mode of self-organization strongly depends on the size and density of the lateral chains along the polymer backbone, as shown in Fig. 54. For polymers with a high density of the lateral chains the rigid backbones are separated by these chains and predominately nematic phases are formed where the polymer backbones adopt only an orientational long range order. Hexagonal columnar phases arise if these rigid backbones adopt a long-range positional correlation in the isotropic continuum of the lateral chains either by reducing the temperature or by increasing the molecular weight[181] (similar to the Col$_{hex}$ to N

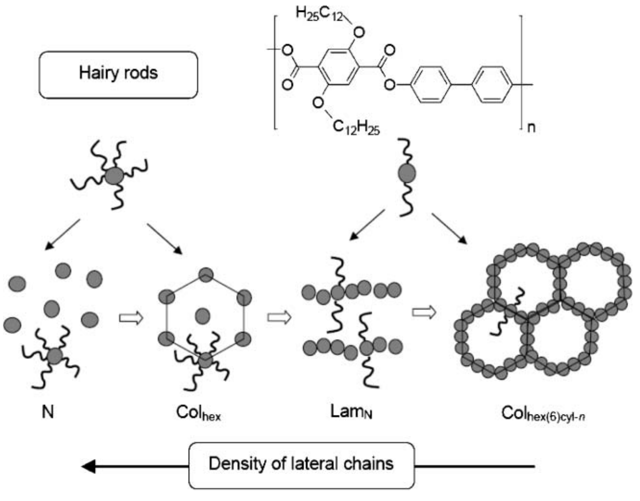

Fig. 54 Phase sequence of rigid main chain polymers with lateral chains depending on the size and density of lateral chains (views along the polymer backbones).

transition observed for Cu-soaps by changing the concentration of lipophilic solvents[182]). Decreasing the density of the lateral chains leads to contacts between the polymer backbones which give rise to a segregation of the backbones and the lateral chains which in turns leads to lamellar LC phases, composed of aromatic and aliphatic sublayers. In these lamellar phases, similarly to the $\mathrm{Lam_N}$ phases of the bolaamphiphiles, the rod-like cores are arranged parallel to the layer planes (see Fig. 54).[183–186] Also $\mathrm{Lam_{Sm}}$ and correlated layer structures ($\mathrm{Col_{rec}}$ phases) were observed if a regular sequence of different building blocks is incorporated in the polymer backbones.[184,187,188]

Further reducing the number of lateral chains or reducing their length leads to hexagonal honeycomb structures.[183,189] The major difference of these honeycomb phases to the hexagonal cylinder phases of the low molecular weight T-shaped amphiphiles is the orientation of the aromatic cores with respect to the columns inside the cylinders. Due to the extreme length of the polymer backbones their high tendency for parallel alignment is dominating and therefore these backbones are aligned parallel to the cylinder long axes. This orientation of the rigid cores and the absence of a segregation within the cylinder walls represent major differences to the polygonal cylinder phases formed by the low molecular weight T-shaped bolaamphiphiles. In the hexagonal honeycombs formed by the main chain polymers there is no restriction of the side length of the cylinders and hence, the size of the hexagons can be increased and reduced nearly continuously. Therefore, the hexagonal cylinder structure, which provides the minimum circumference-to-area ratio, is maintained if the size and density of the lateral chains is changed, *i.e.* no cylinders with other polygonal shapes than hexagonal were observed. New modes of organization can be expected for Janus type polymers with different and incompatible lateral chains[190] which should lead to double-layer structures for the lamellar phases and 2D super-lattice structures for the polygonal honeycombs, where the interior of adjacent cells is different. For such polymers also polygonal honeycombs with other shapes could be possible of the size of the distinct chains is different.

4.4 Filled mesh phases and channeled layer phases

As shown in Fig. 12 and Fig. 50 the transition between the two structurally different types of layer structures, from the smectic phases (Sm, rod-like cores perpendicular to the layer planes) to the laminated phases (Lam, rod-like cores parallel to the layer planes), takes place *via* different types of polygonal honeycomb structures. As explained earlier (Section 2.6), giant cylinders represent intermediate states of the last stage of this transition, the transition from simple honeycombs (length of the cylinder walls corresponds to one molecule) to the Lam phases. Here we will focus attention on the first steps of this transformation, the transition from smectic phases to the polygonal cylinder phases. In the series of bolaamphiphiles (see Fig. 6 and Fig. 15) the increasing size of the lateral chains at first distorts the layers by the randomly distributed lateral chains, which leads to a reduction of the mesophase stability. As segregation sets in, these lateral chains form larger domains which are randomly distributed in these smectic phases. The typical feature of these mesophases is a diffuse scattering in the small angle region of the XRD pattern which corresponds to the mean distance between these domains. Upon further elongation of the chains these domains grow and distort the layers to such extend that the sharp layer reflection in the XRD pattern cannot be detected. These smectic phases without distinct layer reflection are assigned as $\mathrm{SmA^+}$.[47] Further elongation of the lateral chains leads to a transition to the rhombic LC cylinder phase which is the first stable cylinder phase in the series of bolaamphiphiles (see Fig. 6 and Fig. 12).

For the facial amphiphiles a broader diversity of different molecular structures has been reported and hence different pathways for the transition from smectic to LC cylinder phases have been observed (Fig. 52).[46,53] As in these molecules longer terphenyl units are used as rod-like building blocks and as the lateral EO chains are more flexible, triangular cylinders become possible. Furthermore, the mode of molecular organization is strongly dependent on the size and polarity of the lateral chains as well as on the length of the terminal alkyl chains. If the polarity of the lateral chains is modest, as for polyether chains with terminal COOH groups, a direct transition from smectic phases to cylinder phases incorporating triangular cylinders (see Fig. 52(e)) takes place.[60] It seems that these cylinders are formed as soon as the segregation of these chains sets in, *i.e.* no distorted smectic phases were observed. If the lateral chains are more polar, as in the case of molecules with metal carboxylate ($\mathrm{COO^-\ M^+}$) terminated polyether chains segregation is stronger and new mesophases appear.[53] Due to the ionic groups these chains have a stronger segregation tendency and form relatively small randomly distributed polar domains located within the aromatic sublayers of the smectic phases. This is again indicated by a diffuse scattering in the small angle region of the XRD pattern, but in this case the layer reflection is retained, *i.e.* the smectic layers seem to be more robust. This might be due to the presence of longer terphenyl units. In this special type of smectic LC phase, assigned as *f*illed *r*andom *m*esh phase

(SmA_{frm}) there are randomly distributed holes in the aromatic layers which are filled by the polar lateral groups (see Fig. 52(b)).[53] Upon increasing the size of the lateral groups these polar domains expand. If there are relatively long terminal chains, so that the polar domains in adjacent layers cannot fuse, the polar domains within the aromatic sublayers organize into a hexagonal 2D lattice (filled hexagonal mesh layers) and at reduced temperature these layers adopt a long range positional correlation in an ABC fashion, leading to the 3D rhombohedral lattice (Rho/$R\bar{3}m$ phase, see Fig. 52(c)).[53,191] Hence, this mesophase belongs to the correlated layer structures.

If the length of the lateral chains is further increased, polar solvents or salts are added, or the length of the terminal alkyl chains is reduced, then polar domains of adjacent layers can fuse to infinite columns which penetrate the layers and organize into a hexagonal 2D lattice. This mesophase consists of alternating layers of aromatic cores and aliphatic chains (see Fig. 55, pink meshes) penetrated at right angle by columns (blue) with undulating profile containing the polar lateral groups (*ch*anelled *l*ayer phase, ChL_{hex} phase, Fig. 52(d) and 55). The terphenyls are standing perpendicular to the layer planes, *i.e.* parallel to the polar columns. This mesophase is unique as it combines two distinct types of LC organization in one structure, smectic and columnar. In contrast to the phase structures shown in Fig. 49 the columns are organized perpendicular to the layers, thus leading to mesophases with a hexagonal 3D lattice (*P6mmm*).[53] This mesophase can also be regarded as derived from a $Col_{hex}{}^2$ phase (Fig. 52(k)) if the rod-like units in the nematic continuum around the columns (with an orientation of the rods parallel to the columns) would adopt a long range positional order in layers.

With further increasing size of the polar lateral chains a transition from the Rho and ChL_{hex} phases to polygonal honeycombs takes place (see Fig. 52). Often a temperature dependent transition between the ChL_{hex} phase and these polygonal honeycomb structures is observed.[46] At this transition a complete reorganization of the aromatic cores with respect to the polar columns takes place. The ChL_{hex} phase is stabilized by the parallel alignment of the aromatic cores with respect to each other and with respect to the polar cylinders, *i.e.* the formation of this phase is more likely for terphenyl derivatives than for biphenyls, where the tendency for parallel alignment is less important. Therefore, this kind of mesophase is missing for the biphenyl derived bolaamphiphiles. In addition, as the aromatic cores are aligned parallel to the polar columns in the ChL_{hex} phase, there is no strict limitation for the expansion of these columns by the aromatic cores as it is found in the polygonal cylinders. Moreover, the columns can easily adopt a circular cross sectional area which also reduces the intermaterial interfaces. This is advantageous for the organization of molecules with highly incompatible lateral chains (*e.g.* alkali metal carboxylates). For these molecules with large interaction parameters (strong incompatibility) between the polar and the nonpolar parts the columns have a high tendency to minimize the interfacial areas with the nonpolar micro-domains by increasing the diameter of the polar columns. Because in triangular and square cylinders the diameter of the polar columns is strongly limited, cylinder phases incorporating such cylinders are replaced by the ChL_{hex} phase, which allows an easy expansion of these domains. On the other hand, for molecules with larger lateral chains the organization in square or pentagonal cylinders seems to be more favorable than in Chl_{hex} structures. The reason for the predominance of the cylinder structures is not completely clear, possibly unfavorable contacts between alkyl chains and polar groups can be minimized in these structures. Hence, there are several opposing tendencies which lead to a delicate balance between different complex mesophase architectures.

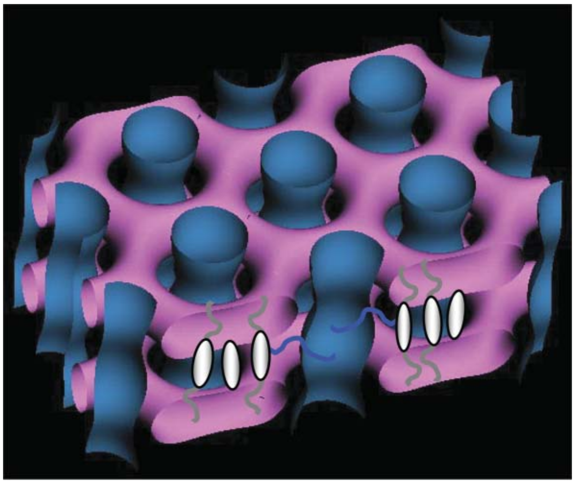

Fig. 55 Experimentally determined electron density map of the hexagonal channeled layer phase (ChL_{hex}) formed by facial amphiphiles;[53] the blue cylinders are filled with the polar lateral chains, the perforated layers of the alkyl chains are shown in pink; the rod-like cores are located between the pink layers and are arranged parallel to the blue columns.

4.5 Polymer morphologies related to filled mesh phases and channeled layer phases

Polymer morphologies analogous to the channeled layer phase were found for diblock copolymers[192–194] composed of a smectic LC side chain polymer block and an isotropic coil block. The coiled blocks form columns which pack in hexagonal symmetry with the lamellar interfaces of the smectic LC phase perpendicular to the column long axis, giving rise to an orthogonal orientation of the columns with respect to the layers, the same as seen in the ChL_{hex} phase.

Polymer morphologies related to the filled mesh phases were observed for a linear ABC triblock polymer[195] and very recently also for an ABC star shaped block copolymers.[196] Here the majority components form the uninterrupted layers, the second component forms the meshes and the minority component fills the holes. Within these mesh layers there is a hexagonal order. In contrast to the situation found for the low molecular weight systems where at the inset of hexagonal order these layers adopt a long range positional order (Rho-phase, see Fig. 52(c)), for the star polymer with a weaker coupling of the layers, there is no long range correlation between the hexagonal meshes. There are also similarities of the correlated and non-correlated Lam_{Sm} phases discussed in Section 4.1 with the hierarchical *Lamellae-in-Lamellae* structures formed by LC-coil block copolymers.[92]

5 Influence of solvents on the LC phase structures

As all molecules represent amphiphiles their mesophase morphologies can be influenced by solvents specifically interacting with one of the incompatible molecular parts.[197] Thus, these materials represent amphotropic LC, capable of forming LC phases as pure materials as well as in the presence of solvents.[198,199] As shown in Fig. 56 for a facial amphiphile with a carbohydrate unit the $\mathrm{Col_{hex}}$ phase of the pure compound (left side of the phase diagram in Fig. 56) is replaced by a $\mathrm{Lam_N}$ phase and a $\mathrm{Lam_{Iso}}$ phase by addition of polar solvents which swell the polar lateral groups.[46] As another example, in the series of facial amphiphiles with relatively small lateral chains the SmA phases of the pure compounds can be replaced by different types of cylinder phases and $\mathrm{ChL_{hex}}$ phases after addition of protonic solvents.[55,69] Also the nematic phases of facial amphiphiles with lateral crown ether units (see Chart 1), were replaced by columnar phases after addition of protonic solvents or alkali metal salt solutions.[42,54,200]

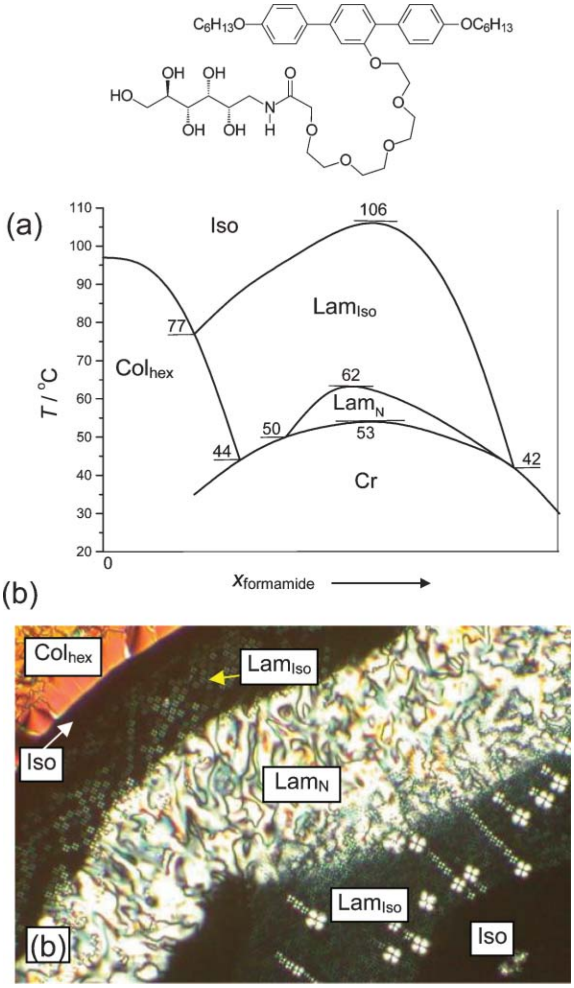

Fig. 56 Induction of lyotropic Lam phases in the binary system between a facial amphiphile and formamide: (a) sketch of the binary phase diagram; (b) contact region of the facial amphiphile (top left) with formamide (bottom right) as observed between crossed polarizers.[46] Reprinted with permission from *J. Am. Chem. Soc.*, 2005, **127**, 16578–16591. Copyright 2005, American Chemical Society.

Polar protonic solvents specifically coordinate to the polar groups and thus have three distinct functions. They increase the incompatibility of the lateral chains which leads to stronger interaction parameters, reinforcing segregation (N to SmA and polygonal cylinder to $\mathrm{ChL_{hex}}$ transitions). These solvents also provide additional attractive interactions by intermolecular H-bonding which stabilizes the mesophases, and the coordinated solvent molecules increase the effective volume of these lateral chains which modifies the mesophase morphology (SmA to Col transition, change of the cylinder shape and Col to Lam transition).

A systematic study was carried out with dendritic oligoamines (DAB dendrimers) in combination with facial amphiphiles incorporating COOH terminated oligo(oxyethylene) side chains.[201] With increasing dendrimer concentration the segregation of the lateral chains is reinforced by formation of ion pairs (ammonium salt formation) and the volume of the polar regions is increased. Depending on the concentration of the dendrimer a large section of the phase sequence shown in Fig. 52, ranging from a SmA phase for the pure amphiphile to the square cylinder phase for the highest dendrimer concentration was observed for this binary system (Fig. 57). These mixed systems represent a new type of supramolecular dendrimers[16] held together by ionic self assembly.[202–205]

Beside the organization of the T-shaped amphiphiles in thermotropic and lyotropic liquid crystalline phases these molecules have also a strong tendency to form well organized structures at surfaces, as for example at the air water interface.[206–208]

6 Summary

LC research is a rapidly developing field which is just at the beginning and has a significant and not yet fully realized potential with significant impact on other disciplines of science. A whole zoo of new and complex mesophase structures has become available by appropriate designed of relatively simple polyphilic molecules. It is amazing that these molecules can form such a wide variety of different phase structures only by slight modification of a successful fundamental molecular structure. The same approach is used by nature in biological systems where, for example, permutation of peptide sequences with only 20 different amino acids leads to a series of functional proteins optimized for a variety of quite different functions in living systems.

Further expansion of the concept of polyphilic molecules to four-, five- and higher multi-block molecules, changing the molecular topology and geometry, combination of these complex mesophase morphologies with larger structures provided by self-organization of dendrimers[16] and block-copolymers is expected to lead to hierarchical structures[192,193] with even higher complexity. Additional options are provided by the introduction of directed packing of bent units (banana molecules[15]), giving rise to polar order, and by combination with chirality[14] which should induce chiral superstructures.

The ultimate scientific goal of future work is to gain a detailed understanding of the fundamental rules of programmed self assembly at different length scales, ranging from low molecular weight molecular crystals and liquid crystals as

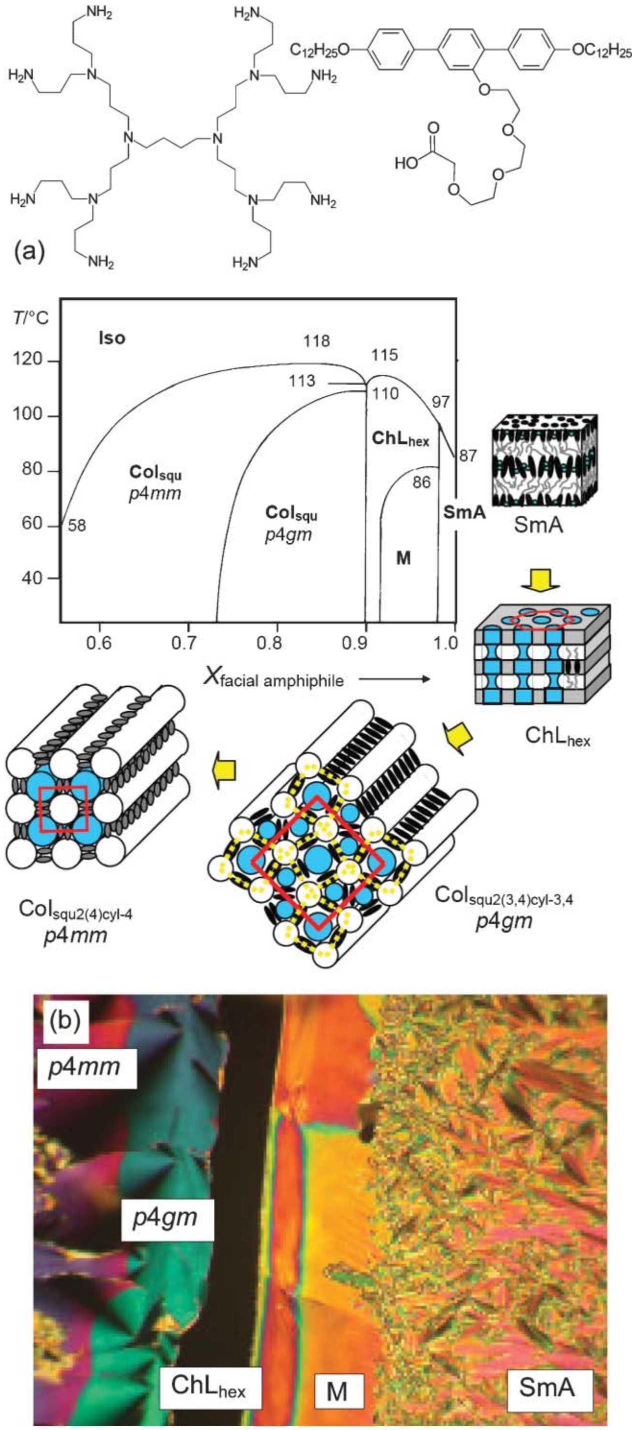

Fig. 57 (a) Binary phase diagram of the binary system of an facial amphiphile with terminal COOH group at the lateral chain with a third generation DAB dendrimer (b) textures of the distinct mesophases as observed between crossed polarizers in the contact region between the two components (M = unknown mesophase).[201]

the smallest units, *via* block copolymers to nanoparticles and macroscopic objects,[209] In addition, it should be possible to generalize the rules of self assembly in systems differing in the degree of mobility ranging from flexible amphiphiles and block copolymers *via* combinations of rigid and flexible units, described herein, to solid-state materials, as solid crystals and nanoparticle arrays. By increasing the complexity of such soft matter systems the number of interactions contributing to self assembly is enlarged and more detailed information could be gained. Therefore, the stepwise transition from simple to complex structures and from less ordered to more ordered structures in such systems might contribute to the fundamental understanding of self assembly in other complex systems, such as solid crystals[210] and living systems.

7 Definitions related to nets and tiling pattern

Some definitions, not explained in the text are summarized here; for a more detailed mathematical treatment of 2D tilings see the book of Grünbaum and Sheppard.[79] 3D-nets and polyhedra which are of relevance for metal–organic frameworks and coordination polymers were collected and analyzed by Wells.[78]

7.1 Net topologies

Uniform net. Network of points (nodes) that repeats regularly in space. The shortest circuit starting from any point and including any of the links, meeting at points in an *n*-gon.

Uninodal net. Net, in which the shortest circuits have all the same size (*n*-gons).

***p*-Connected net.** Net in which all points (nodes) have the same connectivity (*p*).

For nets incorporating identical circuits, but different types of nodes, the connectivity of each node (*p*,*q*) is given as $(n,{}^{\mathrm{p}}_{\mathrm{q}})$. For example, the *p*4*gm* or *p*2*gg* pentagonal cylinder phases can be described as $(5,{}^{3}_{4})$ nets, *i.e.* as nets composed of 3-fold and 4-fold nodes incorporated in 5-membered smallest circuits (see Fig. 20). As for any plane net the connectivity *p* corresponds to the number of *n*-gons meeting at a point, nets composed of different circuits (*n*,*m*), but identical nodes (*p*) can be described with the expression $({}^{\mathrm{n}}_{\mathrm{m}},p)$. For example, the *p*4*gm* phase formed by triangular and square cylinders (*n*,*m* = 3,4) and 5-fold nodes (*p* = 5) is assigned as $({}^{3}_{4},5)$ (see Fig. 20).

7.2 Classification and definitions of tiling pattern

Tiling. Tessellation of a Euclidean plane by *polygons*, herein only *edge-to-edge* tilings by convex polygons are considered.

Edge-to-edge tilings. All corners and sides of the polygons coincide with the vertices and edges of the tiling. For example, Fig. 19 (a), (b) and (d)–(f) are edge-to-edge tilings, whereas (c) is not. *Polygons* are described by corners and sides whereas *tiles* are described by vertices and edges. This is illustrated in Fig. 19(d), the points A, B, D and E are corners of the tile, but A, B, C, D, E and F are vertices of a tiling. The line segments AB, BD, DE and EA are sides of a tile, whereas AB, BC, CD, DE, EF and FA are edges of the tiling.

Regular polygon. Convex polygons with all side-length and angles are identical.

Congruent tiles. All tiles are the same size and shape.

Valence of vertex (v). Number of edges meeting at a vertex of a tiling.

Vertex-type. Number of polygons meeting at a vertex of a tiling, including the sequence of the polygons.

Regular vertex. A vertex is called regular if the angle between each consecutive pair of edges is $2\pi/v$, (v is the valence of the vertex).

Classification according to symmetry

Periodic tiling. A tiling which admits at least two translations in non-parallel direction (tiling pattern with 2D-lattice).

Symmetric tiling. A tiling which can be mapped to itself by at least one symmetry beside the identity (translation in one direction, rotation, reflection).

Classification according to the involved tiles and vertices

Archimedean tiling. Edge-to-edge tiling of a plane by regular polygons such that all vertices are of the same type = *Homogeneous tiling* = *uniform edge-to-edge tiling*. There are 11 Archimedean tilings shown in Fig. 21 at the right, 8 *semiregular tilings* + 3 *regular tilings*.

Regular tiling. Edge to edge tiling with one type of regular polygons that all vertices are of the same type. There are only three regular tilings by regular triangles (3^6), squares (4^4) and regular hexagons (6^3).

Semiregular tiling. Edge-to-edge tiling of a plane by (different) regular polygons such that all vertices are of the same type. There are 8 semiregular tilings, which belong to the *Archimedean tilings*.

Monohedral tiling. A tiling in which all tiles are *congruent*.

Laves tiling. Monohedral tiling with regular vertices. There are 11 Laves tilings shown in Fig. 21 at the left. The three *regular tilings* also belong to the Laves tilings.

Inhomogeneous tiling. Edge to edge tiling with regular polygons (no specific type of vertex is required). There is an infinite number of inhomogeneous tessellations.

Dihedral tiling. A tiling in which there are only two distinct sets of *congruent* prototiles.

Acknowledgements

The author is indebted to the students and collaborators whose names appear in the joint publications listed herein. This work was supported by the German Research Council (DFG) through several projects (TS 39/11, GRK 894), the government of Sachsen-Anhalt through the Cluster of Excellence "Nanostructured Materials", the Fonds der Chemischen Industrie (FCI) and the European Union (through the Marie-Curie Research Training Network, project "Supramolecular Liquid Crystal Dendrimers (LCDD)", contract HPRN-CT-2000-00016) and is presently supported by the ESF-EUROCORES-SONS project SCALES.

References

1 For reviews, see: J. W. Steed and J. L. Atwood, *Encyclopedia of Supramolecular Chemistry*, Marcel Dekker, New York, 2004; J. W. Steed and J. L. Atwood, *Supramolecular Chemistry*, Wiley, Chichester, 2000; H.-J. Schneider and A. Yatsimirsky, *Principles and Methods of Supramolecular Chemistry*, Wiley, Chichester, 2000; J.-M. Lehn, *Supramolecular Chemistry: Concepts and Perspectives*, VCH, New York, 1995.
2 A. P. H. J. Schenning and E. W. Meijer, *Chem. Commun.*, 2005, 3245.
3 J. E. Anthony, *Chem. Rev.*, 2006, **106**, 5028.
4 R. Ballardini, V. Balzani, A. Credi, M. T. Gandolfi and M. Venturi, *Acc. Chem. Res.*, 2001, **34**, 445.
5 Y. Shirai, J.-F. Morin, T. Sasaki, J. M. Guerrero and J. M. Tour, *Chem. Soc. Rev.*, 2006, **35**, 1043.
6 A. L. Sisson, M. R. Shah, S. Bhosalea and S. Matile, *Chem. Soc. Rev.*, 2006, **35**, 1269; S. Bhosale, A. L. Sisson, N. Sakai and S. Matile, *Org. Biomol. Chem.*, 2006, **4**, 3031.
7 D. Pauluth and K. Tarumi, *J. Mater. Chem.*, 2004, **14**, 1219.
8 *Handbook of Liquid Crystals*, ed. D. Demus, J. W. Goodby, G. W. Gray, H.-W. Spiess and V. Vill, Wiley-VCH, Weinheim, 1998.
9 C. Tschierske, *J. Mater. Chem.*, 1998, **8**, 1485.
10 C. Tschierske, *J. Mater. Chem.*, 2001, **11**, 2647.
11 C. Tschierske, *Annu. Rep. Prog. Chem., Sect. C: Phys. Chem.*, 2001, **97**, 191.
12 T. Kato, N. Mizoshita and K. Kishimoto, *Angew. Chem.*, 2006, **118**, 44.
13 Beside thermotropic LC phases, which are formed depending on the temperature, there are also lyotropic LC phases for which the properties are additionally influenced by a solvent (solvent-induced mesophases).
14 H.-S. Kitzerow and C. Bahr, *Chirality in Liquid Crystals*, Springer-Verlag, New York, 2001.
15 R. A. Reddy and C. Tschierske, *J. Mater. Chem.*, 2006, **16**, 907; M. B. Ros, J. L. Serrano, M. R. De La Fuente and C. L. Folcia, *J. Mater. Chem.*, 2005, **15**, 5093; H. Takezoe and Y. Takanishi, *Jpn. J. Appl. Phys., Part 1*, 2006, **45**, 597.
16 B. Donnio and D. Guillon, *Adv. Polym. Sci.*, 2006, **201**, 45.
17 J. W. Goodby, G. H. Mehl, I. M. Saez, R. P. Tuffin, G. Mackenzie, R. Auzély-Velty, T. Benvegnu and D. Plusquellec, *Chem. Commun.*, 1998, 2057.
18 K. Borisch, S. Diele, P. Göring, H. Kresse and C. Tschierske, *J. Mater. Chem.*, 1998, **8**, 529.
19 P. Fuchs, C. Tschierske, K. Raith, K. Das and S. Diele, *Angew. Chem., Int. Ed.*, 2002, **41**, 628.
20 X. H. Cheng, K. Das, S. Diele and C. Tschierske, *Langmuir*, 2002, **18**, 6521.
21 A. Kohlmeier and D. Janietz, *Chem. Mater.*, 2006, **18**, 1483.
22 S. Diele, *Curr. Opin. Colloid Interface Sci.*, 2002, **7**, 333; S. Kutsumizu, *Curr. Opin. Solid State Mater. Sci.*, 2002, **6**, 537; M. Imperor-Clerc, *Curr. Opin. Colloid Interface Sci.*, 2005, **9**, 370.
23 A. Pegenau, T. Hegmann, C. Tschierske and S. Diele, *Chem.–Eur. J.*, 1999, **5**, 1643.
24 A. Pegenau, X. H. Cheng, C. Tschierske, P. Göring and S. Diele, *New J. Chem.*, 1999, **23**, 465.
25 X. H. Cheng, S. Diele and C. Tschierske, *Angew. Chem., Int. Ed.*, 2000, **39**, 592.
26 V. Percec, C. M. Mitchell, W.-D. Cho, S. Uchida, M. Glodde, G. Ungar, X. Zeng, Y. Liu, V. S. K. Balagurusamy and P. A. Heiney, *J. Am. Chem. Soc.*, 2004, **126**, 6078.
27 S. Hassan, W. Rowe and G. J. T. Tiddy, in *Handbook of Applied Surface and Colloid Chemistry*, ed. K. Holmberg, Wiley, Chichester, 2002, vol. 1, p. 465.
28 I. W. Hamley, *The Physics of Block-Copolymers*, Oxford University Press, Oxford, 1998.
29 V. Abetz and P. F. W. Simon, *Adv. Polym. Sci.*, 2005, **189**, 125.
30 M. Lee, B.-K. Cho and W.-C. Zin, *Chem. Rev.*, 2001, **101**, 3869.
31 J.-H. Ryu, B.-K. Cho and M. Lee, *Bull. Korean Chem. Soc.*, 2006, **27**, 1270.

32 M.-H. Park, J.-H. Ryu, E. Lee, K.-H. Han, Y.-W. Chung, B.-K. Cho and M. Lee, *Macromol. Rapid Commun.*, 2006, **27**, 1684.

33 E. Nishikawa and E. T. Samulski, *Liq. Cryst.*, 2000, **27**, 1463.

34 M.-A. Guillevic and D. W. Bruce, *Liq. Cryst.*, 2000, **27**, 153.

35 D. Lose, S. Diele, G. Pelzl, E. Dietzmann and W. Weissflog, *Liq. Cryst.*, 1998, **24**, 707.

36 H.-T. Nguyen, C. Destrade and J. Malthete, in *Handbook of Liquid Crystals*, ed. D. Demus, J. Goodby, G. W. Gray, H.-W. Spiess and V. Vill, Wiley-VCH, Weinheim, 1998, vol. 2B, p. 865.

37 Molecular topology describes the connectivity of molecular graphs, *i.e.* linear, branched and cyclic molecules are topologically distinct arrangements whereas rings of different size or chains of different length are topologically equivalent: D. M. Walba, *Tetrahedron*, 1985, **41**, 3212.

38 W. Weissflog, in *Handbook of Liquid Crystals*, ed. D. Demus, J. W. Goodby, G. W. Gray, H.-W. Spiess and V. Vill, Wiley-VCH, Weinheim, 1998, vol. 2B, p. 835.

39 P. Judeinstein, P. Berdagué, J.-P. Bayle, N. Sinha and K. V. Ramanathan, *Liq. Cryst.*, 2001, **28**, 1691.

40 S. V. Arehart and C. Pugh, *J. Am. Chem. Soc.*, 1997, **119**, 3027; A. C. Small, D. K. Hunt and C. Pugh, *Liq. Cryst.*, 1999, **26**, 849.

41 F. Hildebrandt, J. A. Schröter, C. Tschierske, R. Festag, R. Kleppinger and J. H. Wendorff, *Angew. Chem., Int. Ed. Engl.*, 1995, **34**, 1631.

42 R. Plehnert, J. A. Schröter and C. Tschierske, *J. Mater. Chem.*, 1998, **8**, 2611.

43 F. Hildebrandt, J. A. Schröter, C. Tschierske, R. Festag, M. Wittenberg and J. H. Wendorff, *Adv. Mater.*, 1997, **9**, 564.

44 B. Chen, U. Baumeister, S. Diele, M. K. Das, X. Zeng, G. Ungar and C. Tschierske, *J. Am. Chem. Soc.*, 2004, **126**, 8608.

45 B. Chen, X. B. Zeng, U. Baumeister, G. Ungar and C. Tschierske, *Science*, 2005, **307**, 96.

46 B. Chen, U. Baumeister, G. Pelzl, M. K. Das, X. B. Zeng, G. Ungar and C. Tschierske, *J. Am. Chem. Soc.*, 2005, **127**, 16578.

47 M. Kölbel, T. Beyersdorff, X. H. Cheng, C. Tschierske, J. Kain and S. Diele, *J. Am. Chem. Soc.*, 2001, **123**, 6809.

48 X. H. Cheng, M. Prehm, M. K. Das, J. Kain, U. Baumeister, S. Diele, D. Leine, A. Blume and C. Tschierske, *J. Am. Chem. Soc.*, 2003, **125**, 10977.

49 X. H. Cheng, M. K. Das, U. Baumeister, S. Diele and C. Tschierske, *J. Am. Chem. Soc.*, 2004, **126**, 12930.

50 X. H. Cheng, M. K. Das, S. Diele and C. Tschierske, *Angew. Chem., Int. Ed.*, 2002, **41**, 4031.

51 M. Prehm, X. H. Cheng, S. Diele, M. K. Das and C. Tschierske, *J. Am. Chem. Soc.*, 2002, **124**, 12072.

52 M. Prehm, S. Diele, M. K. Das and C. Tschierske, *J. Am. Chem. Soc.*, 2003, **125**, 614.

53 B. Chen, X. B. Zeng, U. Baumeister, S. Diele, G. Ungar and C. Tschierske, *Angew. Chem., Int. Ed.*, 2004, **43**, 4621.

54 J. A. Schröter, C. Tschierske, M. Wittenberg and J. H. Wendorff, *Angew. Chem., Int. Ed. Engl.*, 1997, **36**, 1119.

55 J. A. Schröter, C. Tschierske, M. Wittenberg and J. H. Wendorff, *J. Am. Chem. Soc.*, 1998, **120**, 10669.

56 Bolaamphililes are amphiphiles where two polar groups are separated by a lipophilic chain. In a more general sense bolaamphiphiles represent a special type of linear ABA amphiphiles.

57 M. Kölbel, T. Beyersdorff, I. Sletvold, C. Tschierske, J. Kain and S. Diele, *Angew. Chem., Int. Ed.*, 1999, **38**, 1077.

58 http://mathworld.wolfram.com.

59 A cylinder can be formed from any closed plane curve. If the curve has straight sides and corners (mathematically there is nothing wrong with this) it is a generalized polygonal cylinder. Unfortunately the term cylinder (without qualification) is commonly used to refer to the solid bounded by the cylindrical surface (with any cross section) and the parallel top and bottom faces and even more specifically for the particular case of a cylindrical solid with circular cross section. In this manuscript cylinder is exclusively used in the sense of a generalized cylinder, *i.e.* as a cylindrical surface, see ref. 58.

60 F. Liu, B. Chen, U. Baumeister, X. Zeng, G. Ungar and C. Tschierske, *J. Am. Chem. Soc.*, 2007, **129**, 9578.

61 From the point of view of the molecules these cylinders are quasi-infinite, only restricted by boundaries in the experimental setup.

62 The polygonal cylinder surface together with the polygonal base and top is a *right prism*. (In a right prism the edges and faces are perpendicular to the base faces.) The prism itself consists only of the faces, edges and vertices, whereas the interior is not included. The region inside the enclosed figure is assigned as the ''solid'' or ''volume of the figure'', see ref. 58.

63 Moreover, the term *prismatic honeycomb* must not be used because it is already given to a 3D-honeycomb which is different from the structures reported herein, see ref. 58.

64 Often LC phases with a 2D square lattice are also assigned as tetragonal phases; however this is misleading, because there are distinct types of tetragonal figures, namely rectangular and square. Moreover, there is a tetragonal 3D lattice. Hence, tetragonal should only be used to describe a tetragonal 3D-lattice, whereas columnar phases should be assigned as rectangular or square columnar phases, respectively.

65 G. Ungar, Y. Liu, X. Zeng, V. Percec and W.-D. Cho, *Science*, 2003, **299**, 1208.

66 A. Takano, W. Kawashima, A. Noro, Y. Isono, N. Tanaka and Y. Matsushita, *J. Polym. Sci., Part B: Polym. Phys.*, 2005, **43**, 2427.

67 X. Zeng, G. Ungar, Y. Liu, V. Percec, A. E. Dulcey and J. K. Hobbs, *Nature*, 2004, **428**, 157.

68 G. Ungar and X. Zeng, *Soft Matter*, 2005, **1**, 95.

69 The proof of the pentagonal cylinder structure for the Col$_{squ}$/*p*4*gm* phases by electron density calculation[45] was the basis of the fundamental understanding of the self-organization in the liquid crystalline phases of T-shaped amphiphiles. Also the cylinder phases of the bolaamphiphiles have been confirmed by electron density calculations which will be reported in future papers. On the basis of these results, the earlier proposed models reported for the thermotropic and lyotropic organization of facial amphiphiles[42,43,54,55] and also for the Col$_{rec}$/*p*2*gg* phase of the T-shaped bolaamphiphiles[47,57] have been revised. The columnar mesophases of the diol based facial amphiphiles reported in ref. 42 and 43 are presently under reinvestigation. In fact these mesophases represent LC cylinder phases. Probably, these cylinders have a triangular or quadrilateral shape. All Col$_{rec}$/*p*2*gg* phases of the bolaamphiphiles, actually represent pentagonal cylinder phases.

70 T. C. Hales, *Discrete Comput. Geom.*, 2001, **25**, 1.

71 In these Col$_{hex}$ phases the hexagonal lattice parameter (a_{hex} = 3.4–3.7 nm) is nearly independent on the size of the lateral chain and only restricted by the length of the bolaamphiphilic core (L = 1.7–2.1 nm for all bolaamphiphiles with biphenyl cores) according to the equation $a_{hex,calc} = 3^{1/2}L$. The strict relations between molecular length and the size of the cylinder walls is a general feature of all LC cylinder phases.

72 M. Prehm, F. Liu, U. Baumeister, X. Zeng, G. Ungar and C. Tschierske, *Angew. Chem., Int. Ed.*, 2007, DOI: 10.1002/anie.200703171.

73 V. Percec, M. Glodde, M. Peterca, A. Rapp, I. Schnell, H. W. Spiess, T. K. Bera, Y. Miura, V. S. K. Balagurusamy, E. Aqad and P. A. Heiney, *Chem.–Eur. J.*, 2006, **12**, 6298.

74 L. Gehringer, C. Bourgogne, D. Guillon and B. Donnio, *J. Am. Chem. Soc.*, 2004, **126**, 3865.

75 S. Jiang, A. Göpfert and V. Abetz, *Macromol. Rapid Commun.*, 2003, **24**, 932.

76 *International Tables for X-Ray Crystallography*, ed. N. M. Henry and K. Lonsdale, Kynoch Press, Birmingham, 1952, vol. 1, Symmetry Groups.

77 K. E. Plass, A. L. Grzesiak and A. J. Matzger, *Acc. Chem. Res.*, 2007, **40**, 287.

78 A. F. Wells, *Three-Dimensional Nets and Polyhedra*, Wiley, New York, 1977.

79 B. Grünbaum and G. C. Shephard, *Tilings and Patterns*, W. H. Freeman, New York, 1987.

80 Though the T-shaped amphiphiles discussed herein and ABC star triblock copolymers represent ternary amphiphiles with a branched architecture, there are differences not only provided by the presence of a rigid segment, but also regarding the distribution of the incompatible units within the molecules. Whereas in ABC stars each arm is formed by a distinct polymer chain, in the T-shaped amphiphiles two of the arms are segmented, hence these molecules represent ternary four-block molecules.

81 S. Sioula, N. Hadjichristidis and E. L. Thomas, *Macromolecules*, 1998, **31**, 5272; S. Sioula, N. Hadjichristidis and E. L. Thomas, *Macromolecules*, 1998, **31**, 8429.

82 K. Yamauchi, K. Takahashi, H. Hasegawa, H. Iatrou, N. Hadjichristidis, T. Kaneko, Y. Nishikawa, H. Jinnai, T. Matsui, H. Nishioka, M. Shimizu and H. Furukawa, *Macromolecules*, 2003, **36**, 6962.

83 H. Hückstädt, A. Göpfert and V. Abetz, *Macromol. Chem. Phys.*, 2000, **201**, 296.

84 V. Abetz and S. Jiang, *e-Polymers*, 2004, 054.

85 A. Takano, S. Wada, S. Sato, T. Araki, K. Hirahara, T. Kazama, S. Kawahara, Y. Isono, A. Ohno, N. Tanaka and Y. Matsushita, *Macromolecules*, 2004, **37**, 9941.

86 K. Hayashida, W. Kawashima, A. Takano, Y. Shinohara, Y. Amemiya, Y. Nozue and Y. Matsushita, *Macromolecules*, 2006, **39**, 4869.

87 K. Hayashida, A. Takano, S. Arai, Y. Shinohara, Y. Amemiya and Y. Matsushita, *Macromolecules*, 2006, **39**, 9402.

88 V. Abetz, S. Jiang and A. Göpfert, *e-Polymers*, 2004, 040.

89 T. Gemma, A. Datano and T. Dotera, *Macromolecules*, 2002, **35**, 3225.

90 P. Tang, F. Qiu, H. Zhang and Y. Yang, *J. Phys. Chem. B*, 2004, **108**, 8434.

91 Monte-Carlo calculation with more rigid Janus particles could probably be used to predict the LC phases of the T-shaped low molecular weight amphiphiles: A. G. Vanakaras, *Langmuir*, 2006, **22**, 88.

92 S. Valkama, T. Ruotsalainen, A. Nykänen, A. Laiho, H. Kosonen, G. ten Brinke, O. Ikkala and J. Ruokolainen, *Macromolecules*, 2006, **39**, 9327.

93 T. Asari, S. Arai, A. Takano and Y. Matsushita, *Macromolecules*, 2006, **39**, 2232.

94 A similar morphology incorporating two distinct types of columns, but without cylinder structure was reported for a linear ABC triblock copolymer: V. Abetz, K. Markgraf and V. Rebizant, *Macromol. Symp.*, 2002, **177**, 139.

95 According to $\Delta G = \Delta H - T\Delta S$ the importance of the entropy of mixing increases with rising temperature and therefore formation of ordered fluids is only achieved below a distinct order–disorder transition temperature (assigned as clearing temperature in LC systems). Above this temperature long-range order is lost and isotropic liquids are formed.

96 A. J. Müller, V. Balsamo and M. L. Arnal, *Adv. Polym. Sci.*, 2005, **190**, 1.

97 Y.-L. Loo, R. A. Register and A. J. Ryan, *Macromolecules*, 2002, **35**, 2365.

98 Better alignment can often be achieved under oscillating shear fields.

99 C. Lin, Y. Liu, S. Rinker and H. Yan, *ChemPhysChem*, 2006, **7**, 1641.

100 U. Feldkamp and C. M. Niemeyer, *Angew. Chem., Int. Ed.*, 2006, **45**, 1856.

101 S. Pitchiaya and Y. Krishnan, *Chem. Soc. Rev.*, 2006, **35**, 1111.

102 N. C. Seeman, *Angew. Chem., Int. Ed.*, 1998, **37**, 3220.

103 Y. He, Y. Chen, H. Liu, E. Ribbe and C. Mao, *J. Am. Chem. Soc.*, 2005, **127**, 12202.

104 P. J. Paukstelis, J. Nowakowski, J. J. Birktoft and N. C. Seeman, *Chem. Biol.*, 2004, **11**, 1119.

105 P. J. Paukstelis, *J. Am. Chem. Soc.*, 2006, **128**, 6794.

106 J. L. Kadrmas, A. J. Ravin and N. B. Leontis, *Nucleic Acids Res.*, 1995, **23**, 2212.

107 Y. He, Y. Tian, A. E. Ribbe and C. Mao, *J. Am. Chem. Soc.*, 2006, **128**, 15978.

108 H. Yan, S. H. Park, G. Finkelstein, J. H. Reif and T. H. LaBean, *Science*, 2003, **301**, 1882.

109 Y. He, Y. Tian, Y. Chen, A. E. Ribbe and C. Mao, *Chem. Commun.*, 2007, 165.

110 N. Chelyapov, Y. Brun, M. Gopalkrishnan, D. Reishus, B. Shaw and L. Adleman, *J. Am. Chem. Soc.*, 2004, **126**, 13924.

111 B. Bing, R. Sha and N. C. Seeman, *J. Am. Chem. Soc.*, 2004, **126**, 10230.

112 L. Brammer, *Chem. Soc. Rev.*, 2004, **33**, 476.

113 S. Leiningen, B. Olenyuk and P. J. Stang, *Chem. Rev.*, 2000, **100**, 853.

114 D. Zhao and J. S. Moore, *Chem. Commun.*, 2003, 807.

115 S. R. Seidel and P. J. Stang, *Acc. Chem. Res.*, 2002, **35**, 972.

116 Examples of discrete supramolecular pentagons: B. Hasenknopf, J.-M. Lehn, N. Boumediene, A. Dupont-Gervais, A. V. Dorsselaer, B. O. Kneisel, G. Baum and D. Frenske, *J. Am. Chem. Soc.*, 1997, **119**, 10956; C. S. Campos-Fernandez, R. Clerac, J. M. Koomen, D. H. Russell and K. R. Dunbar, *J. Am. Chem. Soc.*, 2001, **123**, 773; A. Satake, H. Tanaka, F. Hajjaj, T. Kawai and Y. Kobuke, *Chem. Commun.*, 2006, 2542.

117 Coordination of polypyridine ligands by multiple metal ions is another way to discrete grid structures with defined size: E. Breuning, G. S. Hanan, F. J. Romero-Salguero, A. M. Garcia, P. N. W. Baxter, J.-M. Lehn, E. Wegelius, K. Rissanen, H. Nierengarten and A. van Dorsselaer, *Chem.–Eur. J.*, 2002, **8**, 3458.

118 B. Moulton and M. J. Zaworothko, *Chem. Rev.*, 2001, **101**, 1629.

119 In such frameworks, the topology of the interconnection of the nodes is of major importance and beside the plane nets also 3D nets are of importance. Hence, description of these materials is usually based on net topologies.[78].

120 K. Biradha, M. Sarkar and L. Rajput, *Chem. Commun.*, 2006, 4169.

121 C. N. R. Rao, S. Natarajan and R. Vaidhyanathan, *Angew. Chem., Int. Ed.*, 2004, **43**, 1466.

122 P.-K. Chen, Y.-X. Che, L. Xue and J.-M. Zheng, *Cryst. Growth Des.*, 2006, **6**, 2517.

123 M. J. Zaworotko, *Chem. Commun.*, 2001, 1.

124 P. Vishweshwar, D. A. Beauchamp and M. Zaworotko, *Cryst. Growth Des.*, 2006, **5**, 2429.

125 Discrete aggregates with a square shape were recently obtained for a laterally substituted azobenzene rod-like core with terminal COOH groups after photoisomerization of the azo-groups to the *cis*-configuration: F. Rakotondradany, M. A. Whitehead, A.-M. Lebuis and H. F. Sleiman, *Chem.–Eur. J.*, 2003, **9**, 4771.

126 J. J. Perry, G. J. McManus and M. J. Zaworotko, *Chem. Commun.*, 2004, 2534.

127 T. Nyui, T. Nogami and T. Ishida, *CrystEngComm*, 2005, **7**, 612.

128 X.-Y. Wang, L. Wang, Z.-M. Wang and S. Gao, *J. Am. Chem. Soc.*, 2006, **128**, 674.

129 B. Moulton, J. Lu and M. J. Zaworotko, *J. Am. Chem. Soc.*, 2001, **123**, 9224.

130 S. R. Batten and R. Robson, *Angew. Chem., Int. Ed.*, 1998, **37**, 1460.

131 S. Subramanian and M. J. Zaworotko, *Angew. Chem., Int. Ed. Engl.*, 1995, **34**, 2127; S. Noro, S. Kitagawa, M. Kondo and K. Seki, *Angew. Chem., Int. Ed.*, 2000, **39**, 2082.

132 K. Biradha, M. Sakar and L. Rajput, *Chem. Commun.*, 2006, 4169.

133 D. N. Dybtsev, H. Chun and K. Kim, *Angew. Chem., Int. Ed.*, 2004, **43**, 5033.

134 K. Takaoka, M. Kawano, M. Tominaga and M. Fujita, *Angew. Chem., Int. Ed.*, 2005, **44**, 2151.

135 S. Lee, A. B. Mallik, Z. Xu, E. B. Lobkovsky and L. Tran, *Acc. Chem. Res.*, 2005, **38**, 251.

136 Y.-H. Kiang, G. B. Gardner, S. Lee and Z. Xu, *J. Am. Chem. Soc.*, 2000, **122**, 6871.

137 Y.-H. Kiang, S. Lee, Z. Xu, W. Choe and G. B. Gardner, *Adv. Mater.*, 2000, **12**, 767.

138 S. Stepanow, N. Lin, D. Payer, U. Schlickum, F. Klappenberger, G. Zoppellaro, M. Ruben, H. Brune, J. V. Barth and K. Kern, *Angew. Chem., Int. Ed.*, 2007, **46**, 710, and references cited therein.

139 For example, a chiral Kagome was formed by 1,4′′′′-dicyanopentaphenyl on Ag(111): U. Schlickum, R. Decker, F. Klappenberger, G. Zoppellaro, S. Klyatskaya, M. Ruben, K. Kern, H. Brune and J. V. Barth, *EUROCORES Workshop on Self-Organised NanoStructures*, Strasbourg, France, 31st May–1st June 2007, Book of Abstracts, p. 17.

140 S. Stepanow, N. Lin, J. V. Barth and K. Kern, *J. Phys. Chem.*, 2006, **110**, 23472.

141 Reviews: S. De Feyter and F. De Schryver, *Top. Curr. Chem.*, 2005, **258**, 205; S. De Feyter and F. De Schryver, *J. Phys. Chem. B*, 2005, **109**, 4290.

142 M. Ruben, D. Payer, A. Landa, A. Comisso, C. Gattinoni, N. Lin, J.-P. Collin, J.-P. Sauvage, A. De Vita and K. Kern, *J. Am. Chem. Soc.*, 2006, **128**, 15644.

143 M. Lackinger, S. Griessl, W. M. Heckl, M. Hietschold and G. W. Flynn, *Langmuir*, 2005, **21**, 4984.
144 J. Lu, Q.-D. Zeng, C. Wang, Q.-Y. Zheng, L. Wana and C. Bai, *J. Mater. Chem.*, 2002, **12**, 2856.
145 L. Kampschulte, S. Griessl, W. M. Heckl and M. Lackinger, *J. Phys. Chem. B*, 2005, **109**, 14074.
146 M. Stöhr, M. Wahl, C. H. Galka, T. Riehm, T. A. Jung and L. H. Gade, *Angew. Chem., Int. Ed.*, 2005, **45**, 7394.
147 L. Kampschulte, M. Lackinger, A.-K. Maier, R. S. K. Kishore, S. Griessl, M. Schmittel and W. M. Heckl, *J. Phys. Chem. B*, 2006, **110**, 10829.
148 S. Furukawa, H. Uji-i, K. Tahara, T. Ichikawa, M. Sonoda, F. C. De Schryver, Y. Tobe and S. De Feyter, *J. Am. Chem. Soc.*, 2006, **128**, 3502.
149 K. Tahara, S. Furukawa, H. Uji-i, T. Uchino, T. Ichikawa, J. Zhang, W. Mamdouh, M. Sonoda, F. C. De Schryver, S. De Feyter and Y. Tobe, *J. Am. Chem. Soc.*, 2006, **128**, 16613.
150 Moreover, this relation is not restricted to 2D nets, it can also be applied to 3D-nets and polygon-honeycombs (foams).[78].
151 D. T. Bong, T. D. Clark, J. R. Granja and M. R. Ghadiri, *Angew. Chem., Int. Ed.*, 2001, **40**, 988.
152 C. H. Görbitz, *Chem.–Eur. J.*, 2007, **13**, 1022.
153 V. Percec, A. E. Dulcey, V. S. K. Balagurusamy, Y. Miura, J. Smidrkal, M. Peterca, S. Nummelin, U. Edlund, S. D. Hudson, P. A. Heiney, H. Duan, S. N. Magonov and S. A. Vinogradov, *Nature*, 2004, **430**, 764.
154 A. P. Cote, A. I. Benin, N. W. Ockwig, M. O'Keeffe, A. J. Matzger and O. M. Yaghi, *Science*, 2005, **310**, 1166.
155 P. R. Ashton, C. G. Claessens, W. Hayes, S. Menzer, J. F. Stoddart, A. J. P. White and D. J. Williams, *Angew. Chem., Int. Ed. Engl.*, 1995, **34**, 1862.
156 D. Venkataraman, S. Lee, J. Zhang and J. S. Moore, *Nature*, 1994, **371**, 591.
157 S. Höger, V. Enkelmann, K. Bonrad and C. Tschierske, *Angew. Chem., Int. Ed.*, 2000, **39**, 2267.
158 S. Burghardt, A. Hirsch, B. Schade, K. Ludwig and C. Böttcher, *Angew. Chem., Int. Ed.*, 2005, **44**, 2976.
159 N. Kellermann, W. Bauer, A. Hirsch, B. Schade, K. Ludwig and C. Böttcher, *Angew. Chem., Int. Ed.*, 2004, **43**, 2959.
160 Interestingly, very recently also isolated polyhedral vesicles were observed if the vesicle walls are rigidified by perfluorinated chains: A. G. Gonzalez-Perez, M. Schmutz, G. Waton, M. J. Romero and M. P. Krafft, *J. Am. Chem. Soc.*, 2007, **129**, 756.
161 For recent progress in multi-compartment micelles composed of fluorinated and hydrocarbon compartments, see: Z. Li, M. A. Hillmyer and T. P. Lodge, *Macromolecules*, 2006, **39**, 765; Z. Li, M. A. Hillmyer and T. P. Lodge, *Langmuir*, 2006, **22**, 9409; J.-F. Lutz and A. Laschewsky, *Macromol. Chem. Phys.*, 2005, **206**, 813.
162 S.-W. Lee, C. Mao, C. E. Flynn and A. M. Belcher, *Science*, 2002, **296**, 892.
163 F. M. van der Kooij and H. N. W. Lekkerkerker, *Langmuir*, 2000, **16**, 10144.
164 E. V. Shevchenko, D. V. Talapin, C. B. Murray and S. O'Brien, *J. Am. Chem. Soc.*, 2006, **128**, 3620.
165 T. Mokari, E. Rothenberg, I. Popov, R. Costi and U. Banin, *Science*, 2004, **304**, 1787.
166 N. B. Bowden, M. Weck, I. S. Choi and G. M. Whitesides, *Acc. Chem. Res.*, 2001, **34**, 231.
167 M. J. Ecuti and G. P. Crawford, *Opt. Eng.*, 2004, **43**, 1973.
168 D. L. D. Caspar and E. Fontano, *Proc. Natl. Acad. Sci. USA*, 1996, **93**, 14271.
169 T. Dotera and T. Gemma, *Philos. Mag.*, 2006, **86**, 1085.
170 K. Hayashida, T. Dotera, A. Takano and Y. Matsushita, *Phys. Rev. Lett.*, 2007, **98**, 195502.
171 D. Levine and P. J. Steinhardt, *Phys. Rev. B*, 1986, **34**, 596.
172 N. M. Patel, M. R. Dodge, M. H. Zhu, R. G. Petschek, C. Rosenblatt, M. Prehm and C. Tschierske, *Phys. Rev. Lett.*, 2004, **92**, 015501.
173 N. M. Patel, I. M. Syed, C. Rosenblatt, M. Prehm and C. Tschierske, *Liq. Cryst.*, 2005, **32**, 55.
174 Also 45° tilted SmC phases and SmC phases with even larger tilt angles are known: S. Lagerwall, A. Dahlgren, P. Jägemalm, P. Rudquist, K. D'have, H. Pauwels, R. Dabrowski and W. Drzewinski, *Adv. Funct. Mater.*, 2001, **11**, 87.
175 A. De Vries, *Mol. Cryst. Liq. Cryst.*, 1970, **10**, 219.
176 C. Neumann, D. R. Loveday, V. Abetz and R. Stadler, *Macromolecules*, 1998, **31**, 2493.
177 A cylinder-in-lamellae morphology was also suggested for a Col_{hex} LC phase formed by a perfluoroalkyl-substituted benzoic acid: A. Schaz and G. Lattermann, *Liq. Cryst.*, 2005, **32**, 407.
178 The hexagonal lattice parameter is much smaller than expected for a cylinder structure and also the electron density maps indicate a uniform electron density around the polar columns.[46].
179 I. M. Saez and J. W. Goodby, *J. Mater. Chem.*, 2005, **15**, 26.
180 P. K. Karahaliou, P. H. J. Kouwer, T. Meyer, G. H. Mehl and D. J. Photinos, *Soft Matter*, 2007, **3**, 857.
181 M. Knaapila, R. Stepanyan, B. P. Lyons, M. Torkkeli and A. P. Monkam, *Adv. Funct. Mater.*, 2006, **16**, 599.
182 R. Seghrouchni and A. Skoulios, *J. Phys. II Fr.*, 1995, **5**, 1385.
183 K. Fu, N. Sekine, M. Sone, M. Tokita and J. Watanabe, *Polym. J.*, 2002, **34**, 291.
184 B. Carbonnier, T. Pakula and D. A. M. Egbe, *J. Mater. Chem.*, 2005, **15**, 880.
185 T. Kim, L. Arnt, E. Atkins and G. N. Tew, *Chem.–Eur. J.*, 2006, **12**, 2423.
186 P. Riala, A. Andreopoulou, J. Kallitsis, A. Gitsas and G. Floudas, *Polymer*, 2006, **47**, 7241.
187 B. Carbonnier, A. K. Andreopoulou, T. Pakula and J. K. Kallitis, *Macromolecules*, 2004, **37**, 3576.
188 B. Carbonnier, A. K. Andreopoulou, T. Pakula and J. K. Kallitis, *Macromol. Chem. Phys.*, 2005, **206**, 66.
189 J. Watanabe, N. Sekine, T. Nematsu, M. Sone and H. R. Kricheldorf, *Macromolecules*, 1996, **29**, 4816.
190 L. Li and D. M. Collard, *Macromolecules*, 2006, **39**, 6092.
191 Non-filled mesh phases, where the holes within one type of sublayers are filled by excess material from adjacent sublayers were observed for block copolymers,[28] rod–coil molecules[30] and lyotropic systems: Y. Wang, M. C. Holmes, M. S. Leaver and A. Fogden, *Langmuir*, 2006, **22**, 10951.
192 J. Ruokolainen, G. ten Brinke and O. Ikkala, *Adv. Mater.*, 1999, **11**, 777.
193 O. Ikkala and G. ten Brinke, *Chem. Commun.*, 2004, 2131.
194 E. Verploegen, L. R. C. McAfee, L. Tian, D. Verploegen and P. T. Hammond, *Macromolecules*, 2007, **40**, 777.
195 K. Markgraf and V. Abetz, *e-Polymers*, 2001, 015.
196 K. Hayashida, N. Saito, S. Arai, A. Takano, N. Tanaka and Y. Matsushita, *Macromolecules*, 2007, **40**, 3695.
197 C. Tschierske, *Curr. Opin. Colloid Interface Sci.*, 2002, **7**, 355.
198 H. Ringsdorf, B. Schlarb and J. Venzmer, *Angew. Chem., Int. Ed.*, 1998, **27**, 113.
199 C. Tschierske, *Prog. Polym. Sci.*, 1996, **21**, 775.
200 In the case of crown ether derivatives it was shown that alkali metal ions giving stable complexes with the crown ether units lead to higher stabilities if the induced LC phases than those with lower binding constants, indicating a specific recognition process.
201 A. G. Cook, U. Baumeister and C. Tschierske, *J. Mater. Chem.*, 2005, **15**, 1708.
202 C. F. J. Faul and M. Antonietti, *Adv. Mater.*, 2003, **15**, 673.
203 R. Martın-Rapun, M. Marcos, A. Omenat, J. Barbera, P. Romero and J. L. Serrano, *J. Am. Chem. Soc.*, 2005, **127**, 7397; M. Marcos, R. Martın-Rapun, A. Omenat, J. Barbera and J. L. Serrano, *Chem. Mater.*, 2006, **18**, 1206.
204 I. Koltover, T. Salditt, J. O. Radler and C. R. Safinya, *Science*, 1998, **281**, 78.
205 D. Tsiourvas, T. Felekis, Z. Sideratou and C. M. Paleos, *Liq. Cryst.*, 2004, **31**, 739.
206 J. A. Schröter, R. Plehnert, C. Tschierske, S. Katholy, D. Janietz, F. Penacorada and L. Brehmer, *Langmuir*, 1997, **13**, 796.
207 R. Plehnert, J. A. Schröter and C. Tschierske, *Langmuir*, 1999, **15**, 3773.
208 R. Plehnert, J. A. Schröter and C. Tschierske, *Langmuir*, 1998, **14**, 5245.
209 N. B. Bowden, M. Weck, I. S. Choi and G. M. Whitesides, *Acc. Chem. Res.*, 2001, **34**, 231.
210 J. A. R. P. Sarma and G. R. Desiraju, *Cryst. Growth Des.*, 2002, **2**, 93.